International Journal of Innovation Engineering and Science Research

Editorial Board

International Journal of Innovation Engineering and Science Research

Volume 3 ISSUE 5 November-December 2019

EVALUATION OF EXTRACTS FROM DRY FRUITS OF BLACK BLUEBERRY (VACCINIUM MYRTILLUS L.) THROUGH ONE-DIMENSIONAL AND MULTI-DIMENSIONAL REGRESSION ANALYSIS FOR FLAVONOID PHENOLIC COMPOUNDS

Krasimir Krastev
PhD, Associate professor, Thrakia University, faculty of Technics and technologies, 8602, Yambol, Bulgaria,

Radostina Stefanova
Assistant professor, Thrakia University, faculty of Technics and technologies, 38 Yambol, Bulgaria

Antoaneta Georgieva
PhD, Associate professor, Thrakia University, faculty of Technics and technologies, Yambol, Bulgaria

ABSTRACT

The aim of the study is to develop a technology for obtaining extracts of dried fruits of black blueberry. The basic extraction parameters have been established. The influence of the technological parameters of the extraction process on the content of the flavonoidphenoliccompounds in the extracts is analyzed. Mathematical data processing was performed by one-dimensional and multi-dimensional regression analysis. Estimates were made on the degree of influence of the factors as well as on their level of significance. Fischer's criterion is assessed, as well as its probability. Residue assessment and analysis was performed by normal probability plot of residues, the scatter plot of the predicted residual values and the residual histogram. The extracts obtained were determined by the amount of flavonoid phenolic compounds to enrich the fruit juices with BAV. The effect of the extractant type, the duration and temperature of the extraction and the hydromodule on the color parameters were investigated. The results of the planned experiment are statistically processed with the Statistica program. Residue assessment and analysis was performed by normal probability plot of residues, the scatter plot of the predicted residual values and the residual histogram. The results obtained suggest that 70% ethyl alcohol, temperature 65 ° C, duration 3-4 h and 1:30 hydromodule are technologically reasonable choices for obtaining extracts with a maximum content of common flavonoid phenolic compounds. Adequate mathematical models were described describing the dependencies of the individual parameters in the extraction of the common flavonoid phenolic compounds. Technology for obtaining extracts with maximum content of common Adequate mathematical models were described describing the dependencies of the individual parameters in the extraction of the common flavonoid phenolic compounds has been developed.

Keywords: *extracts, black blueberry fruits, flavonoid phenolic compounds, regression analysis.*

I. INTRODUCTION

Studies conducted in different countries confirm that one of the main causes of pathological changes in the human body leading to premature aging and development of cardiovascular diseases,

oncological diseases and diabetes is the excessive accumulation of free radicals and active forms of oxygen in the biological fluid of the organism.
Increasing the content of free radicals in the cells creates conditions for the so- oxidative stress in which free radicals oxidize vessel walls, protein molecules, DNA and lipids.These radicals actively interact with membranes of lipids containing unsaturated bonds and alter the properties of cell membranes [1].
Berries contain powerful antioxidants and a proper balance of bioactive compounds. They are considered to be a good source of phenolic compounds, especially flavonoids and phenolic acids, which mostly contribute to their high antioxidant activity. Berries have recently received much attention for their health benefits, including antimutagenesis and anticarcinogenic activity for the prevention of various cancers and age-related diseases [2].
Beverages are anoptimal form of food that can be used to enrich the nutritional portion of irreplaceable nutrients and biologically active substances that have a beneficial effect on metabolism and immune resistance of the body [3].
In order to increase the nutritional value and antioxidant properties of juice-containing beverages, extracts of wild-growing raw materials having a prophylactic and functional effect can be introduced into the production technologies.
The aim of the study is to develop a technology for obtaining extracts of dried fruits of black bilberries. The basic extraction parameters have been established. The resulting extracts are analyzed for the purpose of enriching fruit juices with flavonoid phenolic compounds.

II. MATERIAL AND METHODS

A. Material. The object of the study is the fruits of *Vaccinium myrtillus* L. In wild plants, there are a number of BAV that can affect the life processes of the human body.
Forest fruits are rich in phenolic compounds and have great antioxidant activity. This makes them a potential raw material for producing extracts that can be used to develop functional beverages.Various variants of water and ethanol extracts from dried berries and black currant have been developed. The aqueous and ethanol extracts of the fruits are respectively 1:10, 1:20 and 1:30 fruit / extract ant hydromodul; at an extraction temperature of 35° -80° C and 1, 2, 3 and 4 hours.The physicochemical analyzes were conducted using standardized methods approved by good manufacturing practice.For each of the test quantities the mean values of three independent experiments are presented. Flavonoid phenolic compounds - spectrophotometric as a rutin,% by pharmacopoeial method [Pharmacopeia Russia]. General method of analysis [4].

B. Mathematical methods. Mathematical data processing was performed by one-dimensional and multi-dimensional regression analysis. By which were studied and evaluated the possible functional dependencies between two or more random variables.The main questions are whether there is a functional dependence between two dependent random variables and if so - to find a function that describes it sufficiently accurately. Various models have been studied, with the best-described dependencies being selected. Estimates were made on the degree of influence of the factors as well as on their level of significance. Fischer's criterion is assessed, as well as its probability.Residue assessment and analysis was performed by normal probability plot of residues, the scatter plot of the predicted residual values and the residual histogram. All results are presented analytically and graphically.
The processing was done through the statistical program STATISTICA (Stat Soft, Inc.).
All data are processed at level of significance α=0,05.

III. RESULTS AND DISCUSSION

The experimental results obtained for the effect of the type and concentration of the extractant were used to obtain a regression model as well as to study its suitability. After studying the polynomials of the first and second degrees, a model of the following appears to be the best:

$$y = b_0 + b_1 x + b_2 x^2 \quad (1)$$

where x is the percentage of ethyl alcohol as a percentage and y is the concentration of flavonoid phenolic compounds, mg%.

After statistical processing of the data, it is evident that the coefficient of determination $R^2 = 0,999$, which means that 99% of the change in parameter Y is due to the control factor x and is described with the model used. Of all the models studied, the coefficient of certainty is the highest. All the coefficients of the model are statistically significant, since $p - level << 0,05$ they are as follows:

$$b_0 = 59,95932 \; , \; b_1 = 2,16229 \; b_2 = -0,01665 \quad (2)$$

Fisher's criterion, F (2,9) = 9886,7, and its corresponding probability indicate that the model describes a significant part of the change in Y. The model performs better than the so-called naive average forecasts.

The regression equation is:

$$y = 59,95932 + 2,16229\,x - 0,01665\,x^2 \quad (3)$$

The resulting regression model describes the rights $y = f(x)$, that we can depict in R^2 .

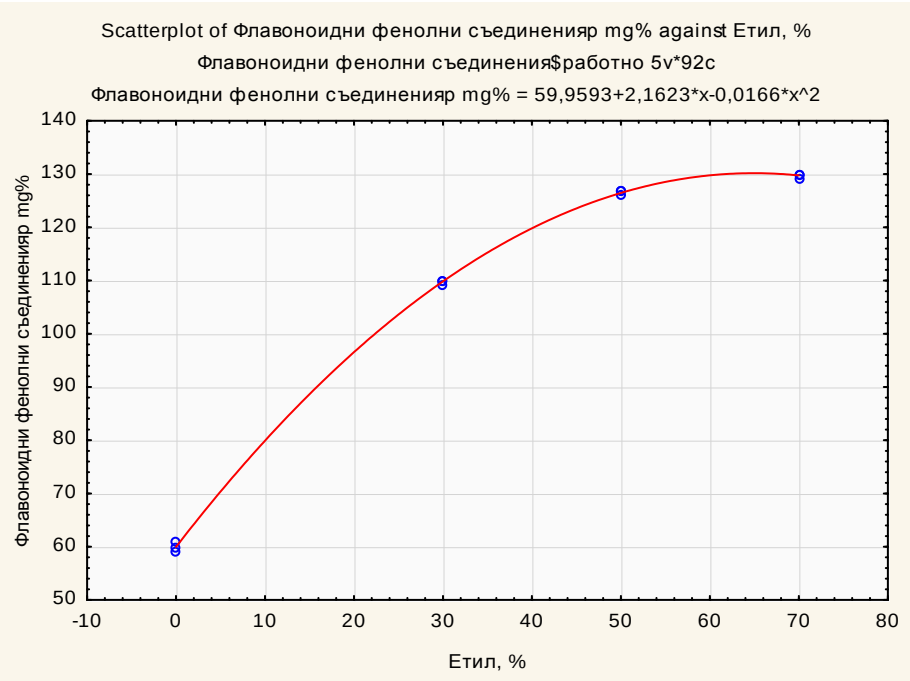

Fig.1. Model response line

The analysis of residues and their graphical representations are shown in Figure 2 in the so-called normal probability graph.

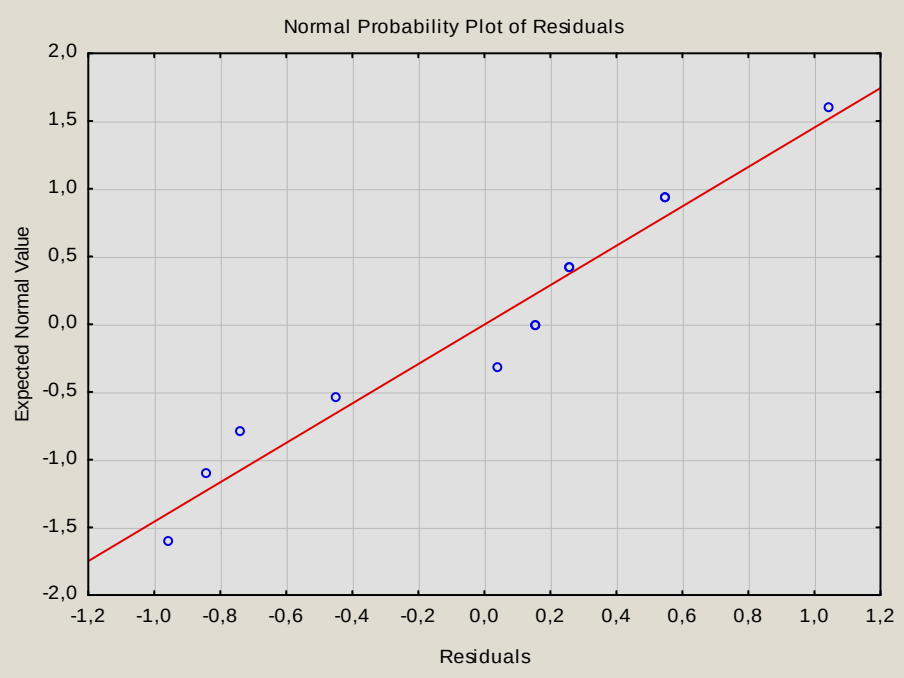

Fig.2. Normal probability plot of residuals

The analysis shows a lack of systematic deviation of the actual data from the theoretical curve, which indicates a normal distribution of residues.

We will check for residual dependence on predicted values from the model. For this purpose, we will analyze the scatterplot of the residuals from the predicted values - FIG. 3.

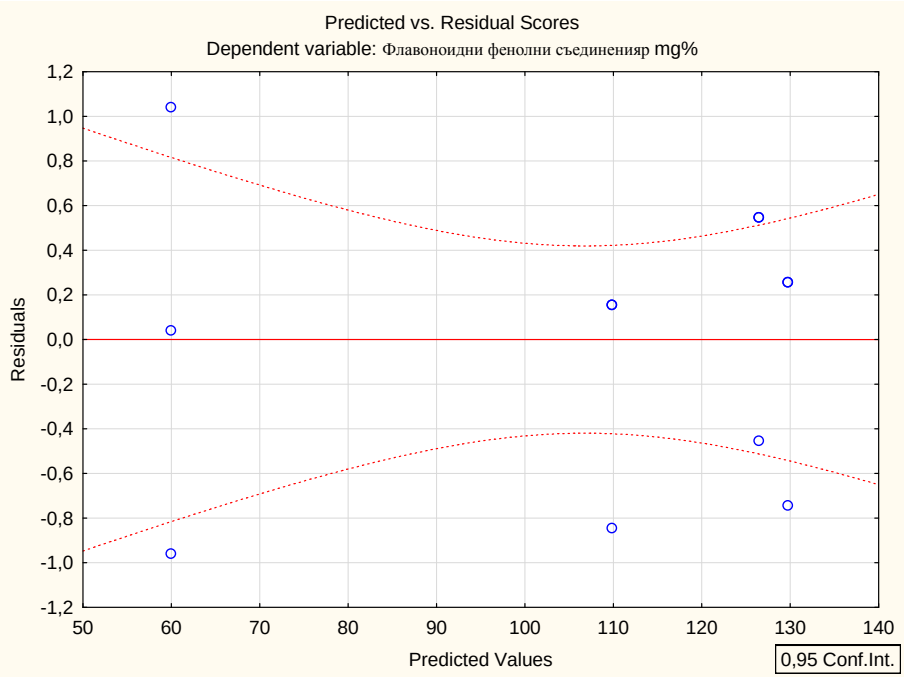

Fig. 3. Scatterplot of residual values from predicted values

The obtained graph shows that the systematic residuals are lacking and are sufficiently chaotic. We can conclude that the residuals do not depend on the predicted values.

To Conclude. From the obtained results we can draw the following conclusions:

1. From the analysis of residuals we can conclude that the obtained model is adequate.
2. The resulting model is linear and describes with great precision the experimental data obtained.

The experimental results obtained for the effect of the extraction temperature were used to obtain a regression model as well as to study its suitability. After studying the polynomials of the first and second degrees, a model of the following appears to be the best:

$$y = b_0 + b_1 x \quad (4)$$

Where **x** is the temperature in degrees Celsius and **y** is the concentration of flavonoid phenolic compounds, mg%.

After the statistical processing of the data it can be seen that the coefficient of determination $R^2 = 0,86$, which means that 86% of the change in parameter **Y** is due to the control factor x and is described with the model used. Of all the models studied, the coefficient of certainty is the highest. All the coefficients of the model are statistically significant, since $p - level << 0,05$ they are as follows:

$$b_0 = 70,10556,\ b_1 = 0,61889 \quad (5)$$

Fischer's criterion, **F** (1,10) = 56,145 p <, 00002, as well as its corresponding probability, show that the model describes a significant part of the change in **Y**. The model performs better than the so-called naive estimates of the averages .

The regression equation is:

$$y = 70,10556 + 0,61889\,x \quad (6)$$

The resulting regression model describes the rights $y = f(x)$, that we can depict in R^2 .

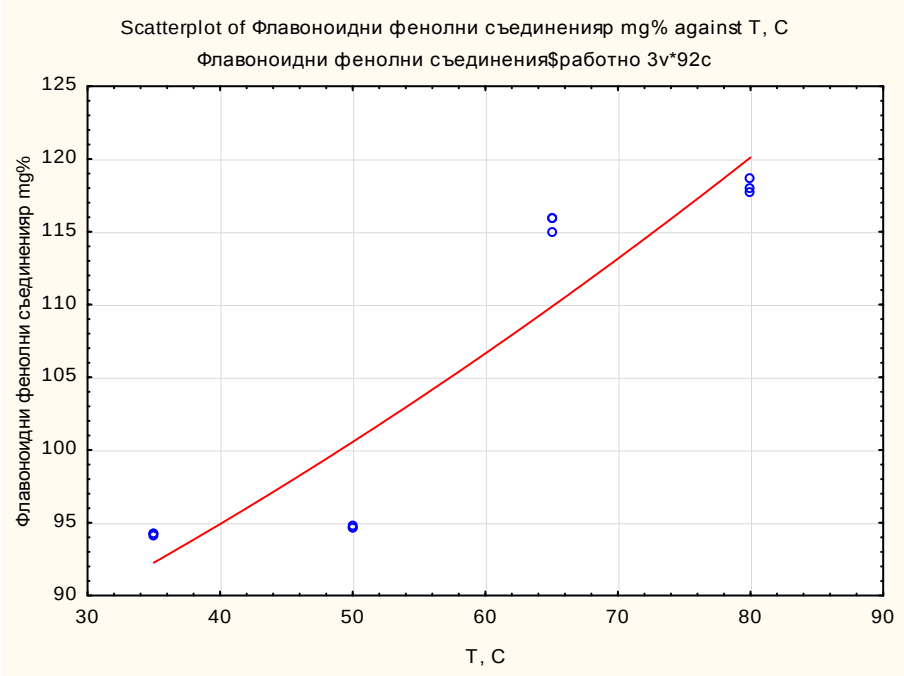

Fig.4. Model response line

The analysis of residues and their graphical representations are shown in Figure 5 in the so-called normal probability graph.

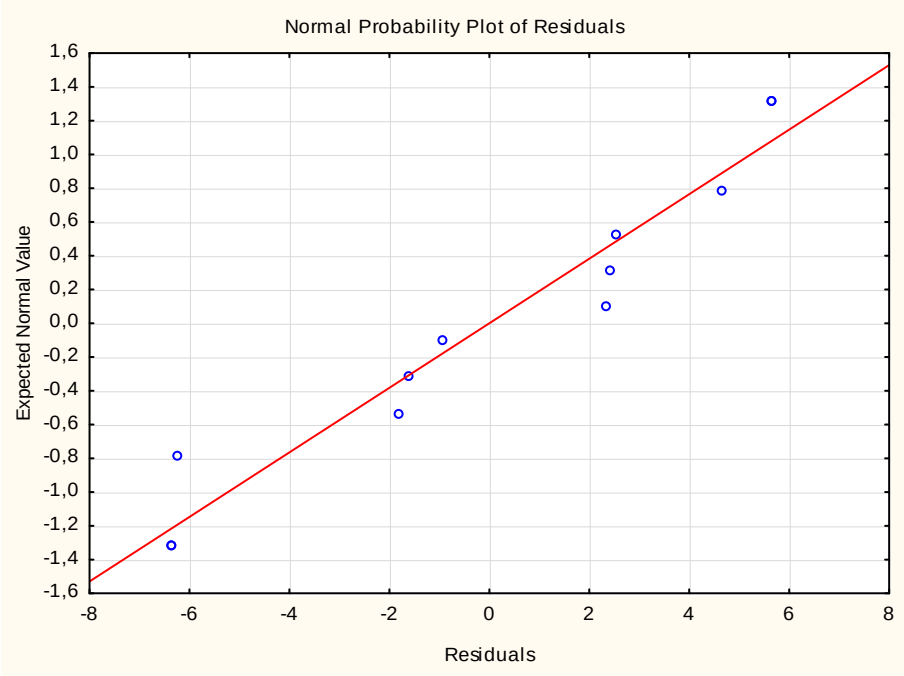

Fig.5. Normal probability plot of residuals

The analysis shows a lack of systematic deviation of the actual data from the theoretical curve, which indicates a normal distribution of residues.

We will check for residual dependence on predicted values from the model. For this purpose, we will analyze the scatterplot of the residuals from the predicted values - FIG. 6.

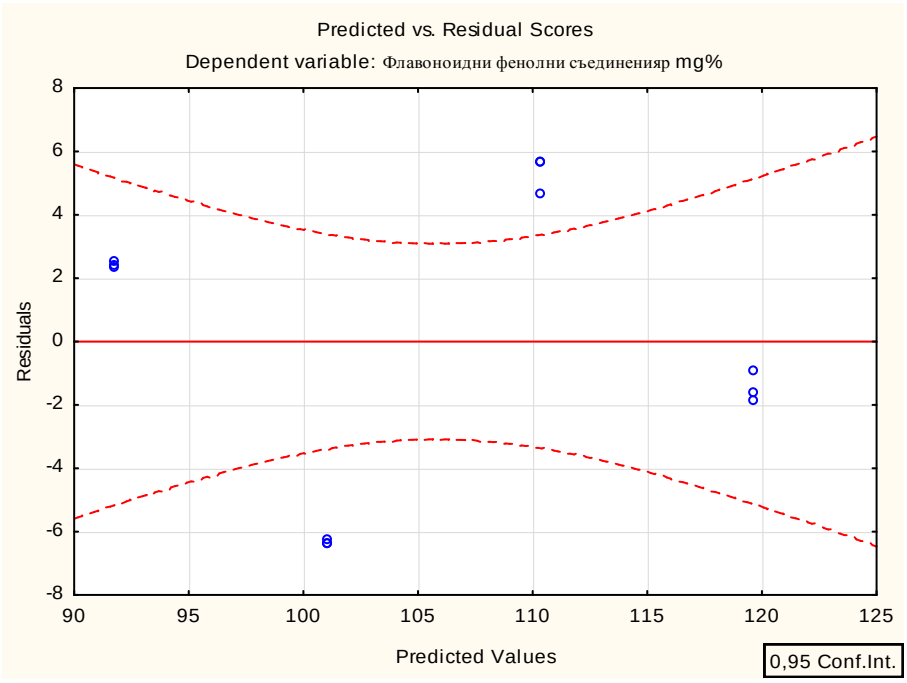

Fig. 6. Scatterplot of residual values from predicted values

The obtained graph shows that the systematic residuals are lacking and are sufficiently chaotic. We can conclude that the residuals do not depend on the predicted values.

To conclude. From the obtained results we can draw the following conclusions:

3. From the residue analysis, we can conclude that the model obtained is adequate.
4. The resulting model is linear and describes with great precision the experimental data obtained.

The experimental results obtained for the effect of extraction time were used to obtain a regression model as well as to study its suitability. After studying the polynomials of the first and second degrees, a model of the following appears to be the best:

$$y = b_0 + b_1 x \quad (7)$$

Where **x** is the time in minutes and **y** is the concentration of Flavonoid phenolic compounds, mg%.
After the statistical processing of the data it is seen that the coefficient of determination $R^2 = 0,98$, which means that 98% of the change in parameter **Y** is due to the control factor x and is described with the model used. Of all the models studied, the coefficient of certainty is the highest. All the coefficients of the model are statistically significant, since $p - level << 0,05$ they are as follows:

$$b_0 = 103,8333, \quad b_1 = 0,1978$$

Fisher's criterion, **F** (2,9) = 9886,7 F (1,10) = 433,43 p <, 00000, and its corresponding probability indicate that the model describes a significant part of the change in **Y**. The model performs better than the so-called naive average forecasts.
The regression equation is:

$$y = 103,8333 + 0,1978\,x \quad (8)$$

The resulting regression model describes the rights $y = f(x)$, that we can depict in R^2.

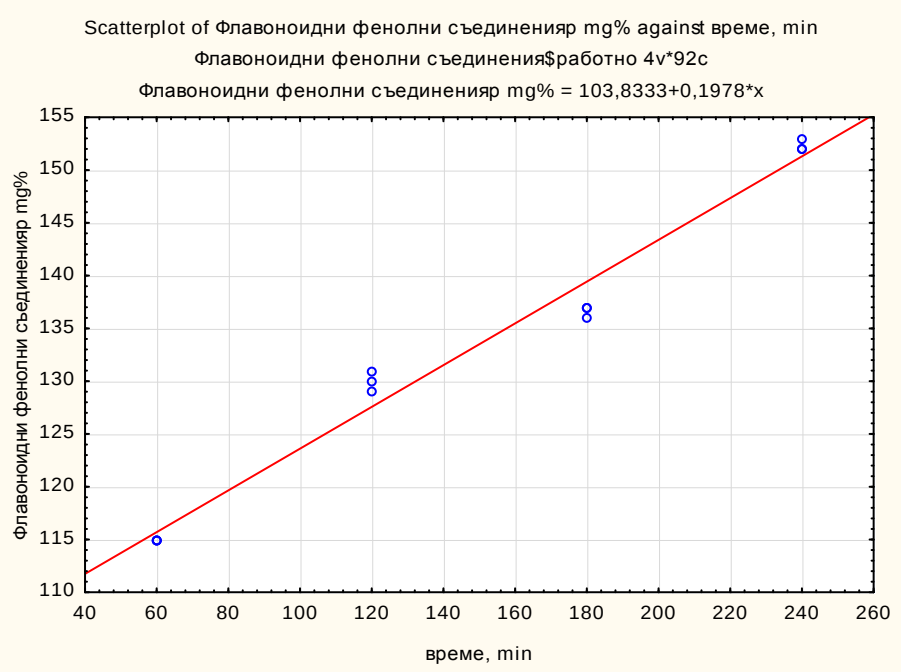

Fig.7. Model response line

The analysis of the residuals and their graphical representations are shown in Fig. 8 in the so-called normal probability graph.

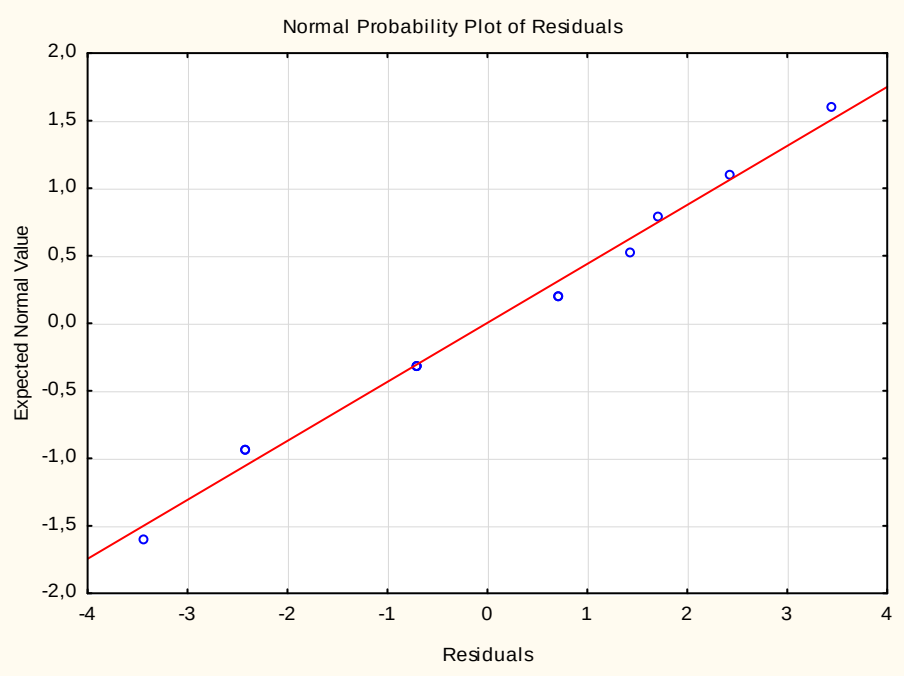

Fig.8. Normal probability plot of residuals

The analysis shows a lack of systematic deviation of the actual data from the theoretical curve, which indicates a normal distribution of residues.

We will check for residual dependence on predicted values from the model. For this purpose, we will analyze the scatterplot of the residuals from the predicted values - FIG. 9.

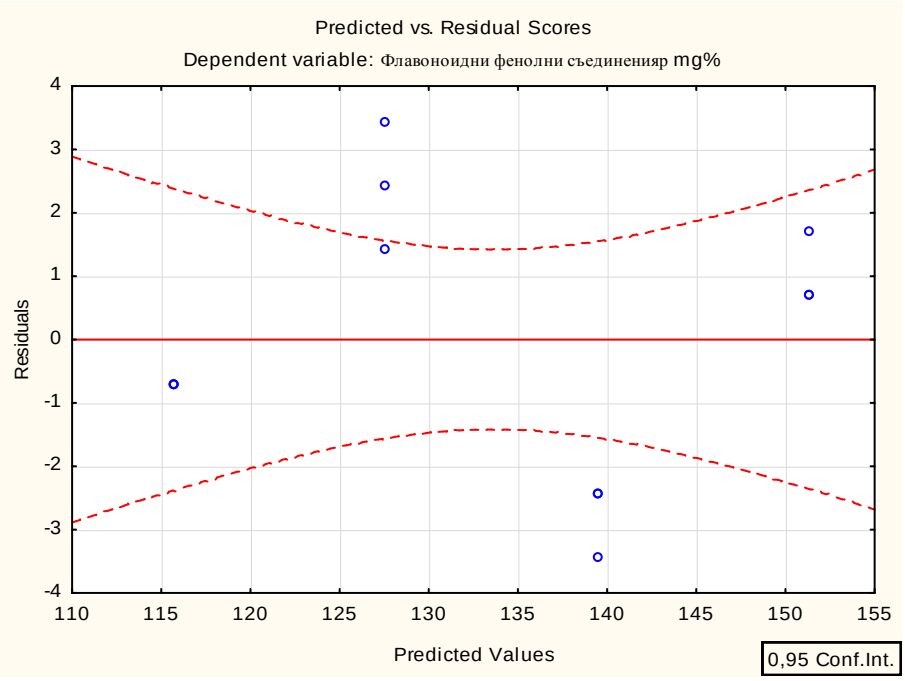

Fig.9. Scatterplot of residual values from predicted values

The obtained graph shows that the systematic residuals are lacking and are sufficiently chaotic. We can conclude that the residuals do not depend on the predicted values.

To conclude. From the obtained results we can draw the following conclusions:

5. From the analysis of residuals we can conclude that the model obtained is adequate.
6. The resulting model is linear and describes with great precision the experimental data obtained.

The experimental results obtained for the influence of the extraction hydromodule were used to obtain a regression model as well as to study its suitability. After studying the polynomials of the first and second degrees, a model of the following appears to be the best:

$$y = b_0 + b_1 x + b_2 x^2 \quad (9)$$

Where **x** is the hydromodule and **y** is the concentration of Flavonoid phenolic compounds, mg%.
After statistical processing of the data, it is evident that the coefficient of determination $R^2 = 0,999$, which means that 99% of the change in parameter **Y** is due to the control factor x and is described with the model used. Of all the models studied, the coefficient of certainty is the highest. All the coefficients of the model are statistically significant, since $p - level << 0,05$ they are as follows:

$$b_0 = 73,00000 \text{ , } b_1 = 7,48333 \; b_2 = -0,11500$$

Fisher's criterion, **F** (2,6) = 4727.4 p <, 00000, and its corresponding probability indicate that the model describes a significant part of the change in **Y**. The model performs better than the so-called naive forecasts average values.
The regression equation is:

$$y = 73,00000 + 7,48333\,x - 0,11500\,x^2 \quad (10)$$

The resulting regression model $y = f(x)$, describes the rights that we can depict in R^2 .

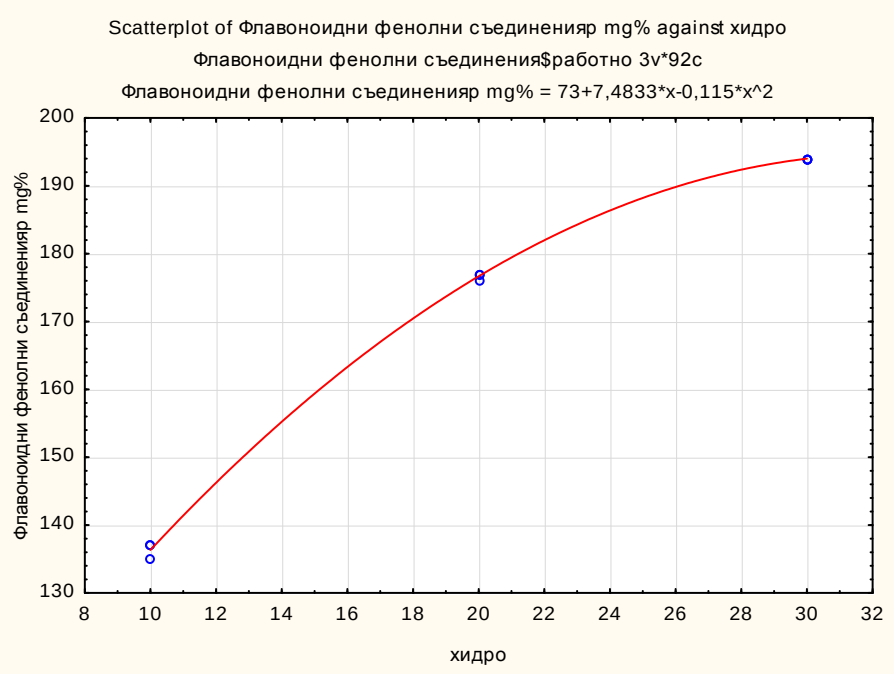

Fig.10. Model response line

The analysis of residuals and their graphical representations are shown in Figure 11 in the so-called normal probability graph.

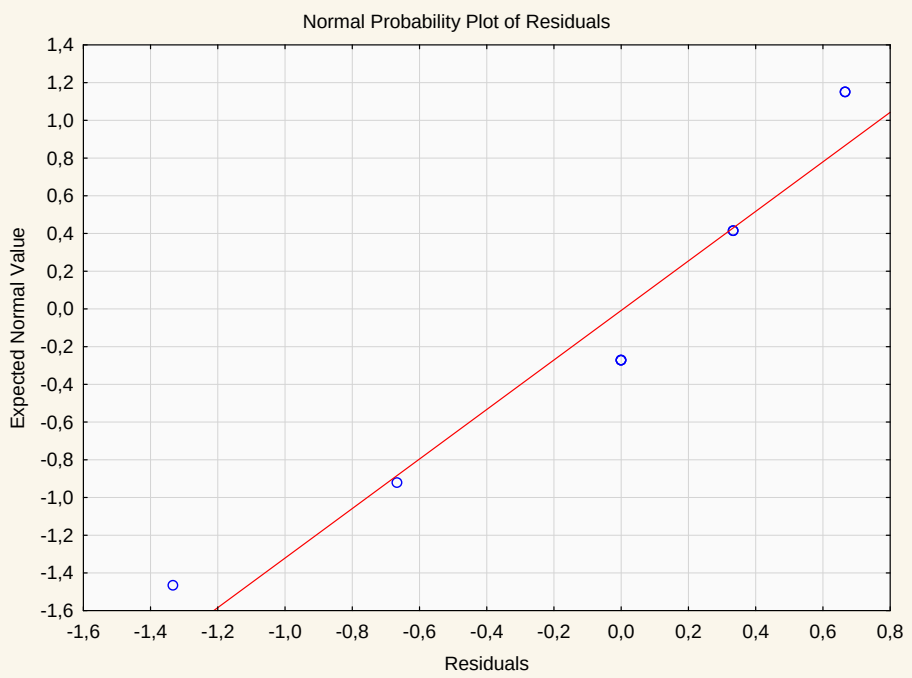

Fig.11. Normal probability plot of residuals

The analysis shows a lack of systematic deviation of the actual data from the theoretical curve, which indicates a normal distribution of residues.

We will check for residual dependence on predicted values from the model. For this purpose, we will analyze the scatterplot of the residuals from the predicted values - FIG. 12.

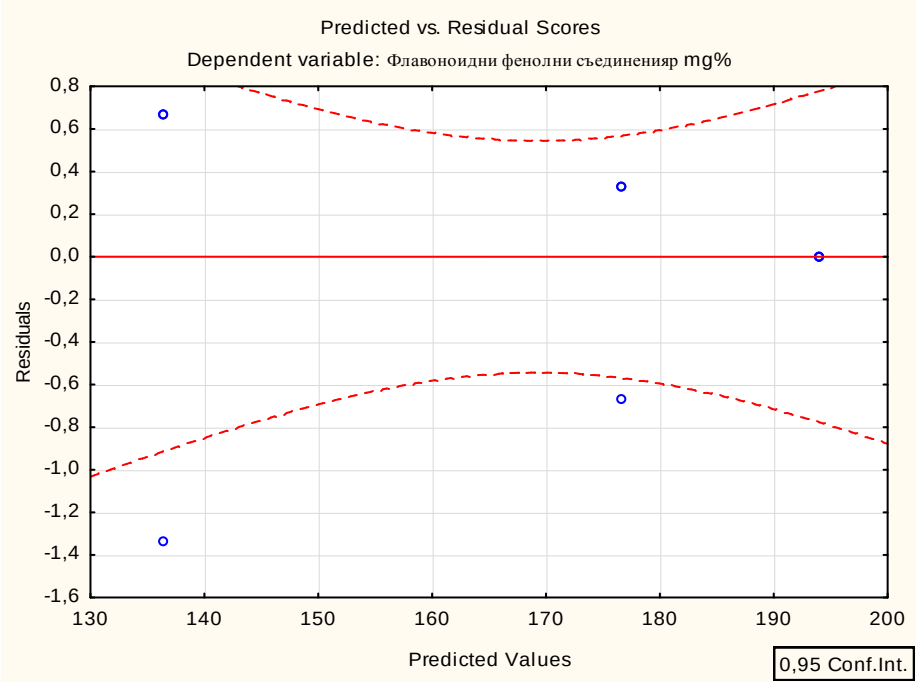

Fig.12. Scatterplot of residual values from predicted values

The obtained graph shows that the systematic residuals are lacking and are sufficiently chaotic. We can conclude that the residuals do not depend on the predicted values.

To conclude. From the obtained results we can draw the following conclusions:

7. From the analysis of residuals we can conclude that the model obtained is adequate.
8. The resulting model is linear and describes with great precision the experimental data obtained.

The experimental results obtained for the effect of ethyl alcohol concentration and extraction temperature on the concentration of flavonoid phenolic compounds were used to obtain a regression model as well as to study its suitability. We will look for multiple regressions between flavonoid phenolic compounds mg% - as a function of response and concentration of ethyl alcohol in percent and temperature in degrees Celsius. The best model turns out to be:

$$z = b_0 + b_1 x + b_2 T + b_3 x^2 + b_4 T^2$$

(11)

Where **x** is the percentage of ethyl alcohol in percent, T is the temperature and **z** is the concentration of Flavonoid phenolic compounds in mg%.

After the statistical processing of the data, it can be seen that the coefficient of determination $R^2 = 0,92$, which means that 92% of the change in parameter **Z** is due to the control factors **x** and **T** is described with the model used. Of all the models studied, the coefficient of certainty is the highest. The statistically significant coefficients of the model are as follows:

$$b_0 = 109,4582 \; b_1 = 2,2710 \; b_2 = -3,1015 \; b_3 = -0,0191$$

$$b_4 = 0,0309$$

Fisher's criterion, F (4,19) = 51,097 p <, 00000, as well as its corresponding probability indicate that the model describes a significant part of the change in **Z**. The model performs better than the so-called naive estimates of the averages.

The regression equation is:

$$z = 109,4582 + 2,2710\,x - 3,1015\,t - 0,0191\,x^2 + 0,0309\,T^2$$

(12)

The resulting regression model $z = f(x, y)$ describes the surface that we can depict in R^3.

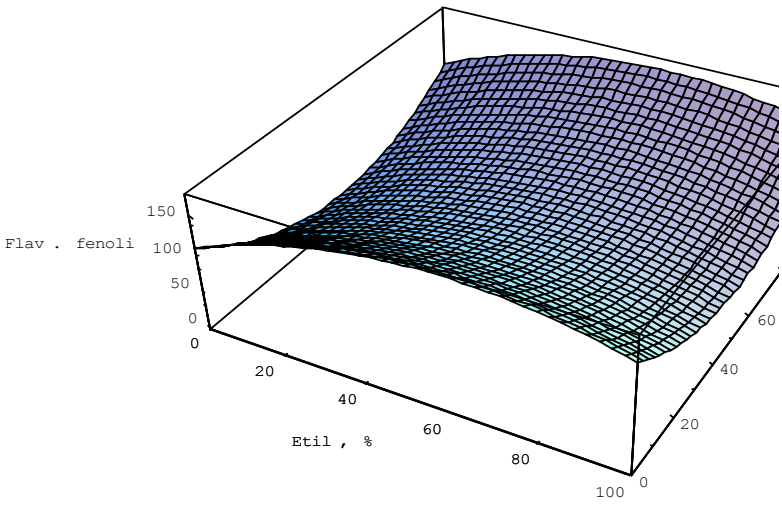

Fig.13. Model response line

The analysis of residuals and their graphical representations are depicted in Fig. 14 in the so-called normal probability graph.

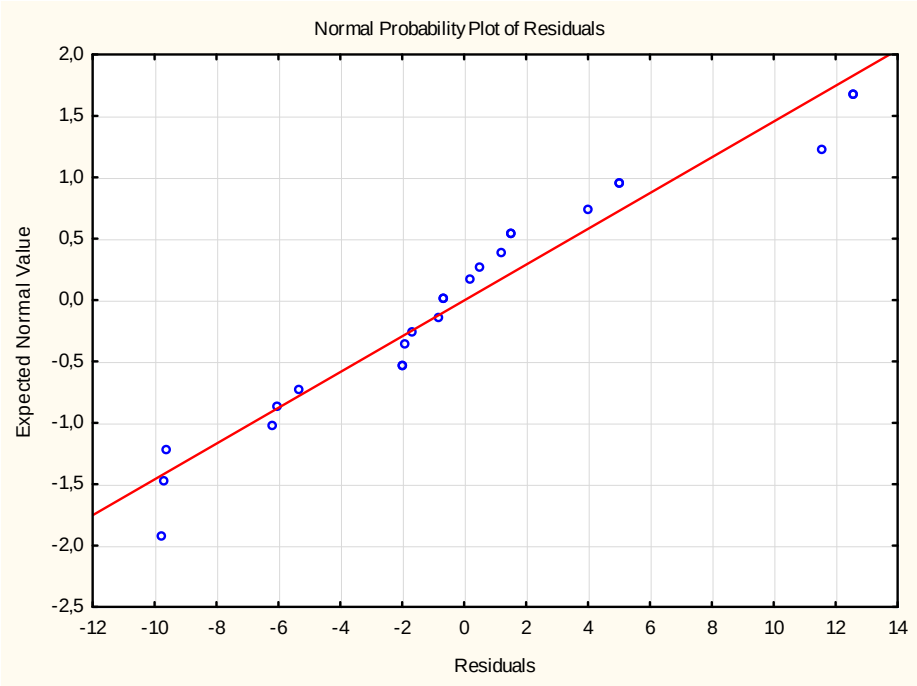

Fig.14. Normal probability plot of residuals

We will check for residual dependence on predicted values from the model. For this purpose, we will analyze the scatterplot of the residuals from the predicted values - FIG. 15.

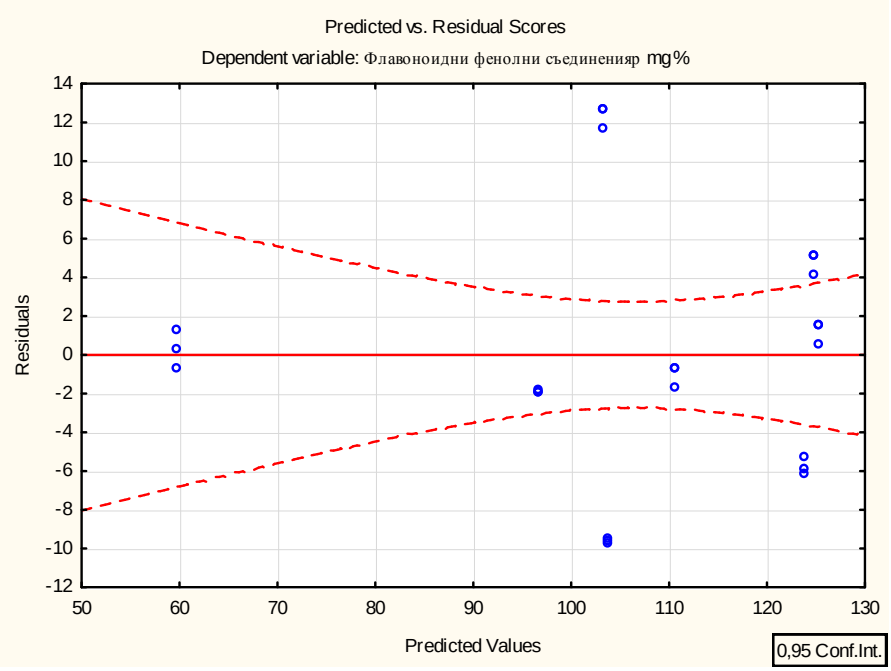

Fig.15. Scatterplot of residual values from predicted values.

The obtained graph shows that the systematic residuals are lacking and are sufficiently chaotic. We can conclude that the residuals do not depend on the predicted values.

To conclude. From the obtained results we can draw the following conclusions:

9. The resulting model is quadratic and describes with great precision the experimental data obtained.
10. From the residue analysis, we can conclude that our model is adequate.
11. From the standardized coefficients, it can be seen that the two factors - temperature and concentration have approximately the same effect, with a slight preference for the temperature by about 20%.

The experimental results obtained for the effect of the concentration of ethyl alcohol and the duration of extraction on the concentration of flavonoid phenolic compounds were used to obtain a regression model as well as to study its suitability. We will look for multiple regressions between flavonoid phenolic compounds mg% as a function of response and ethyl alcohol concentration in percent and time in minutes. The best model turns out to be:

$$z = b_0 + b_1 x + b_2 t + b_3 x^2 + b_4 t^2 \quad (13)$$

Where **x** is the percentage of ethyl alcohol in percent, t is the time in minutes, and **z** is the concentration of Flavonoid phenolic compounds in mg%.

After the statistical processing of the data it can be seen that the coefficient of determination $R^2 = 0,96$, which means that 96% of the change in parameter **Z** is due to the control factors **x** and **t** is described with the model used. Of all the models studied, the coefficient of certainty is the highest. The statistically significant coefficients of the model are as follows:

$$b_0 = 23,03852 \; b_1 = 2,16249 \; b_2 = 0,29188 \; b_3 = -0,01665$$

$$b_4 = -0,00018$$

Fisher's criterion, **F** (4,22) = 123,61 p <, 00000, and its corresponding probability indicate that the model describes a significant part of the change in **Z**. The model performs better than the so-called naive forecasts average values.

The regression equation is:

$$z = 23,03852 + 2,16249\,x + 0,29188\,t - 0,01665\,x^2 - 0,00018\,t^2 \quad (14)$$

The resulting regression model $z = f(x, y)$, describes the surface that we can depict in R^3.

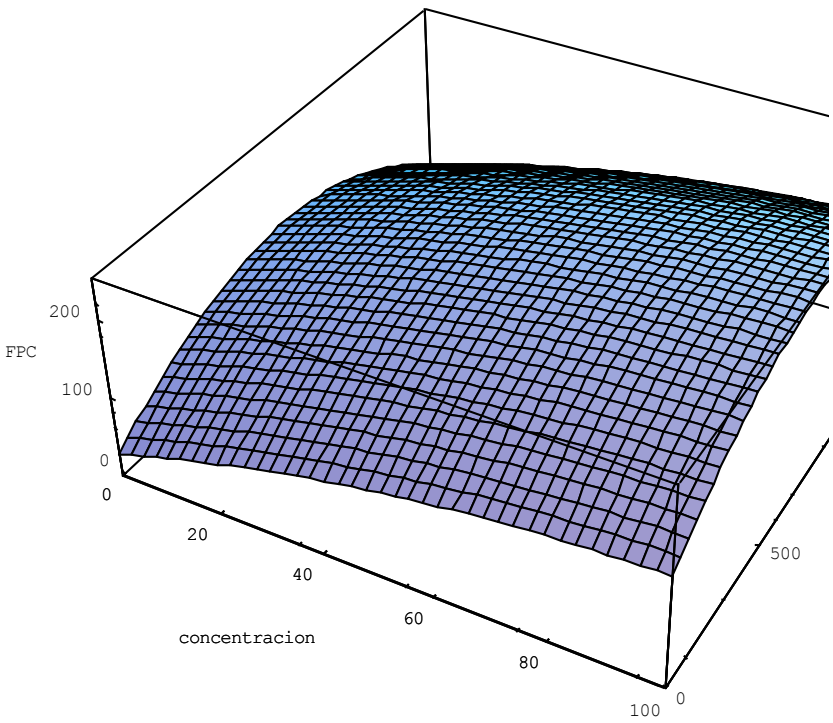

Fig.16. Model response line

The analysis of the residuals and their graphical representations are shown in Figure 17 in the so-called normal probability graph.

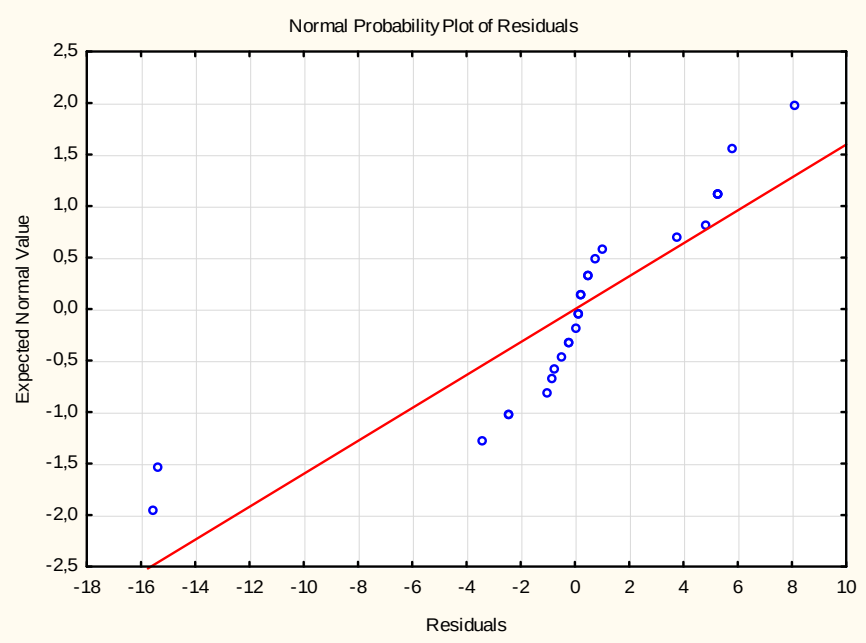

Fig. 17. Normal probability plot of residuals

We will check for residual dependence on predicted values from the model. For this purpose, we will analyze the scatterplot of the residuals from the predicted values - FIG. 18.

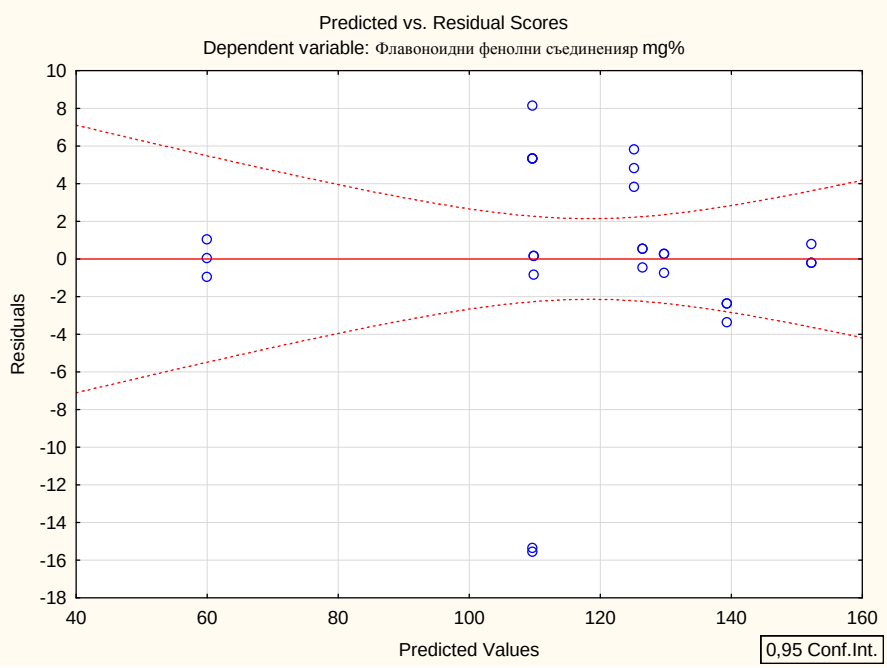

Fig.18. Scatterplot of residual values from predicted values

The obtained graph shows that the systematic residuals are lacking and are sufficiently chaotic. We can conclude that the residuals do not depend on the predicted values.

To conclude. From the obtained results we can draw the following conclusions:

12. The resulting model is quadratic and describes with great precision the experimental data obtained.
13. From the residue analysis, we can conclude that our model is adequate.

14. From the standardized coefficients it can be seen that the time factor exerts a threefold increase in the response function of the concentration.

REFERENCES

[1] Yashin, Y.NaturalAntioxidants. ContentinFoodProductsandImpact, HealthandAging,ed. TransLat,2009, p.212. (in Russian)

[2] Vesna, T.; Jasna, Č.B.; Lars, G.; Sonja, D.; Gordana, Ć. Superoxide anion radical scavenging activity of bilberry (*Vacciniummyrtillus*L.). *J. Berry Res.* 2010, *1*, 13–23.

[3] Akulinina, V. Enricheddrinks - a newnicheinthejuicemarket. Taraandopakovka, 2007, vol. 4, p.16,. (in Russian)

[4] StatePharmacopoeia of Russia. General methods of analysis - II ed., Medicine. 1987

Investigation of the Influence of the Parameters of the Process Extraction on the Content of the Phenolic Complex in the Extracts of the Dried Fruits of Blackcurrant

Antoaneta Georgieva
PhD, Associate professor, Thrakia University, faculty of Technics and technologies, Yambol, Bulgaria

Radostina Stefanova
Assistant professor, Thrakia University, faculty of Technics and technologies, 38 Yambol, Bulgaria,

Krasimir Krastev
PhD, Associate professor, Thrakia University, faculty of Technics and technologies, 8602, Yambol, Bulgaria

ABSTRACT

The optimal parameters of the extraction process for the extraction of biologically active substances from the dried fruits of blackcurrant have been established and experimentally confirmed. The phenolic complex of the extracts obtained at different parameters of the extraction process was investigated - selection of the extractant; extraction temperature; extraction time and hydromodule. Studied are the extracts obtained at the optimals extraction parameters for total phenols 1,023 g gallic acid / 100 g CB, phenolcarboxylic acids 0, 12%, flavonoid phenolic compounds 53,4 mg%, sum anthocyanins 238 mg% and tannins 2,47 g catechin / 100g CB. On the basis of the experimental data, the technological regimes of the extraction process were selected. The use of 70% C2H5OH as an extractant is technologically warranted to produce extracts of dried fruits blackcurrants with maximum content of phenols, flavonoids, anthocyanins and tannins. Technologically justified extraction temperature is 65-80oC. By increasing the extraction temperature to 80°C, the quantity of anthocyanins in the extracts increases, which positively affects the organoleptic evaluation of the final products. The optimum extraction time is 3-4 hours. During this extraction period, a maximum content of the phenolic complex is obtained. The results obtained suggest that the most advantageous hydromodul for extraction is 1:30.

Keywords: *extraction parameters, extracts, biologically active substances, dried fruit blackcurrants.*

I. INTRODUCTION

.

In today's context, the problem of rational nutrition is one of the main factors determining the state of human health, its working capacity and the sustainability of the influence of various adverse environmental factors. Reduced consumption of natural plant products has caused the development of functional disorders of the gastrointestinal tract and diseases related to metabolic disorders.
An analysis of the modern nutrition structure shows that further improvement and development of technologies for the production of biologically complete products with high content of biologically active substances is needed to improve nutritional status.
In this context, it is important to develop a technology for extracting biologically active substances from the fruits of wild raw materials, in particular from blackcurrants, and to include them in the development of new assortments of beverages.

In order to increase the nutritional value and antioxidant properties of the juice-containing beverages, extracts of wild raw materials having prophylactic and functional action can be introduced into production technologies.

The healing potential of wild shrub plants lies in their antioxidant, anti-allergic, anti-inflammatory and antiviral properties, which depend on polyphenolic complexes. Particular attention is given to the content of flavonoid phenolic compounds and anthocyanin pigments.

Beverages are an optimal form of food that can be used to enrich the nutritional portion with irreplaceable nutrients and biologically active substances that have a beneficial effect on metabolism and immune resistance of the body [1].

Studies conducted in different countries confirm that one of the main causes of pathological changes in the human body leading to premature aging and development of cardiovascular diseases, oncological diseases and diabetes is the excessive accumulation of free radicals and active forms of oxygen in the biological fluid of the organism . In order to increase the nutritional value and antioxidant properties of the juice-containing beverages, extracts of wild raw materials having prophylactic and functional action can be introduced into production technologies. The healing potential of wild shrub plants lies in their antioxidant, anti-allergic, anti-inflammatory and antiviral properties, which depend on polyphenolic complexes. Particular attention is given to the content of flavonoid phenolic compounds and anthocyanin pigments.

Blueberries and blackcurrant extracts serve as natural antioxidants. Berries contain powerful antioxidants and a proper balance of bioactive compounds. They are considered to be a good source of phenolic compounds, especially flavonoids and phenolic acids, which mostly contribute to their high antioxidant activity [2].

It fruits are a rich source of vitamin C and other health beneficial substances such as: routine, organic acids,pectins, micro-and macro nutrients and essential oils [3].

Blackcurrant fruits contain polyphenolic substances with antioxidant, antimicrobial, antiviral, and antibacterial properties [4, 5, 6, 7, 8]. In order to increase the nutritional value and antioxidant properties of juice-containing beverages, extracts of wild-growing raw materials having a prophylactic and functional effect can be introduced into the production technologies.

The purpose of this work is to determine, through research, the technologically sound parameters of the extraction process and to obtain extracts with a maximum BAV content.

The following tasks have been set to achieve this goal:

- establishment of the basic parameters of the process of extraction and development of technology for the extraction of BAV from the dried fruits of blackcurrant with the highest content of the phenolic complex.
- study of total phenolic compounds, phenolcarboxylic acids, flavonoid phenolic compounds, the sum of anthocyanins and tannins from the extracts obtained at different parameters of the extraction process.

II. Material and Methods

Object of study are the fruits of Ribesnigrum. In fruits contain a number of BAV that can affect the vital processes occurring in the human body.

The physicochemical and sensory analyzes were conducted using standardized methods approved by good manufacturing practice.

- General Phenol Compounds (AFS) spectrophotometric method with Folin-Denisa reagent,% as gallic acid [9].
- Phenol Carbonic Acid – Spectrophotometric [9].
- Flavonoid phenolic compounds – spectrophotometric [9].
- Anthocyanins - spectrophotometric such as cyanidine-3,5-diglucoside [9].
- Tanning substances - titrated with 0.02M potassium permanganate [9].

For the extraction of the vegetable raw material, various extractants are used: water and ethyl alcohol of various concentrations 30%, 50% and 70%. Concentration of the ethanol has a significant effect on the extraction of the various groups of compounds. To determine the optimum solvent, extractant is

added to a raw material. The feedstock / extractant ratio was 1:10 by weight of feedstock at 20°C for 24 hours. The change in concentration of the different groups of compounds in the extracts is due to their different solubility in ethanol and water and to the fact that they are extracted from dry plant material. Processes in plant raw materials are going on into the aquatic environment. Most of the compounds are found mainly in the vacuoles of the cells. To improve the extractability of substances contained in dry plant tissue, the raw material needs to absorb a certain amount of water. Water-alcohol solutions at a concentration close to absolute ethanol do not provide the necessary water to rehydrate the cells.
The effect of the hydromodule (1:10, 1:20 and 1:30), the temperature (35°C-80°C) and the duration of the extraction (1-4 hours) on the type and quantity of the extracted substances were investigated. Developed various variants of water and ethanol extracts from dried berries blackcurrant have been. The aqueous and ethanol extracts of the fruits are respectively athydromodul 1:10, 1:20 and 1:30 - fruit / extractant; at an extraction temperature of 35°, 50°, 65° and 80°C and extraction time 1, 2, 3 and 4 hours. The extracts are stored in tightly closed packages at 25°C in the dark. Each variant is developed in triple repeatability. The resulting extracts were subjected to physico-chemical analyzes. As a result of the research the process of extraction of phenolic compounds from dried fruit blackcurrant was optimized.

III. RESULTS AND DISCUSSION

The concentration of the total phenolic compounds is higher by extraction with ethyl alcohol compared to the water extraction. It grows with increasing the concentration of ethyl alcohol in the extracts, reaching its maximum in the extract with 70 % ethyl alcohol - Fig. 1.
When extracting to dried fruits blackcurrant with an increase in ethyl alcohol concentration from 30 % to 50 %, the amount of common phenolic compounds increased by 20 % and by extraction with 70 % ethyl alcohol the common phenolic compounds increased by 41% - Fig. 1.

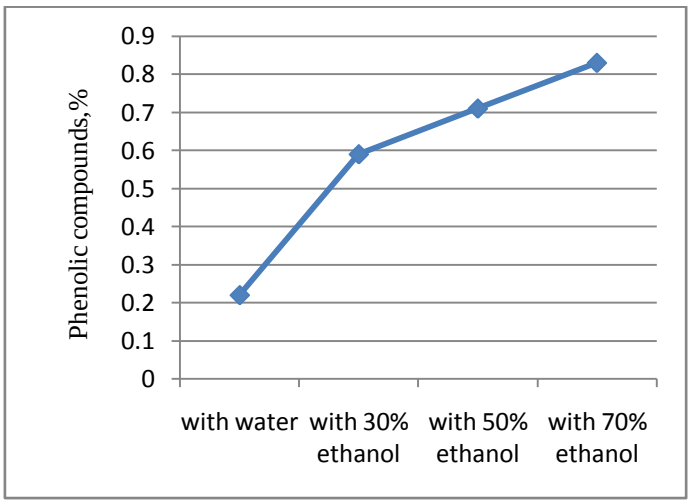

Fig. 1. Effect of the extractant concentration on the the total phenolic compounds content in extracts of dried fruits blackcurrant

The trend in the content of phenolic acids and flavonoid phenolic compounds is similar to that of the total phenolic compounds - Fig. 1, 2. Concentration of the phenolic acids by extraction with 30 %, 50 % and 70 % ethanol is higher, respectively, of 2.2; 3.6 and 3.9 times compared to their concentration in the aqueous extracts - Fig. 2.

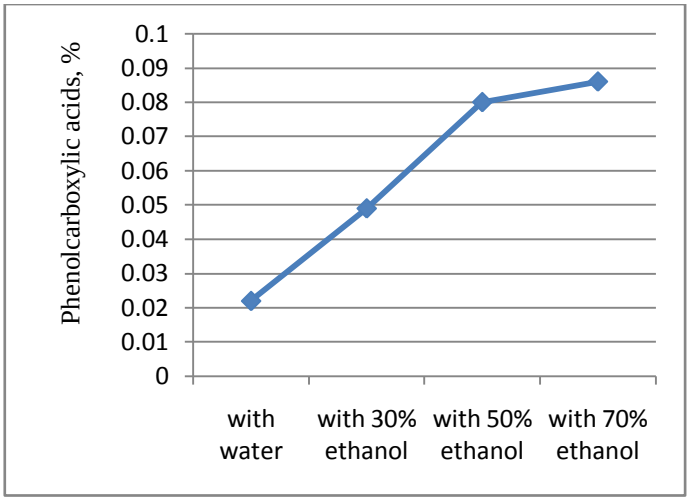

Fig. 2. Effect of extractant concentration on phenolcarboxylic acids content in extracts of dried fruits blackcurrant

For flavonoid phenolic compounds the increase in the concentration is 2,1; 3.3 and 3.5 times higher - Fig. 3.

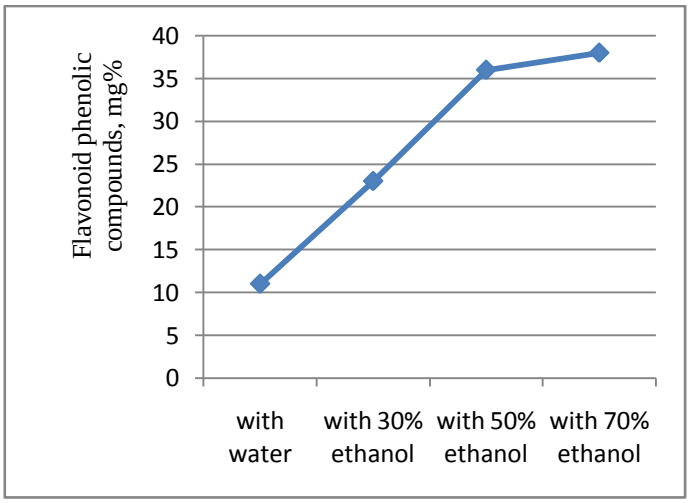

Fig. 3. Effect of extractant concentration on flavonoid phenolic compounds content in extracts of dried fruits blackcurrant

The amount of anthocyanins increases, with the highest being at 70% extractant and varying from 31 mg% when extracted with water to 189 mg% - Fig. 4.

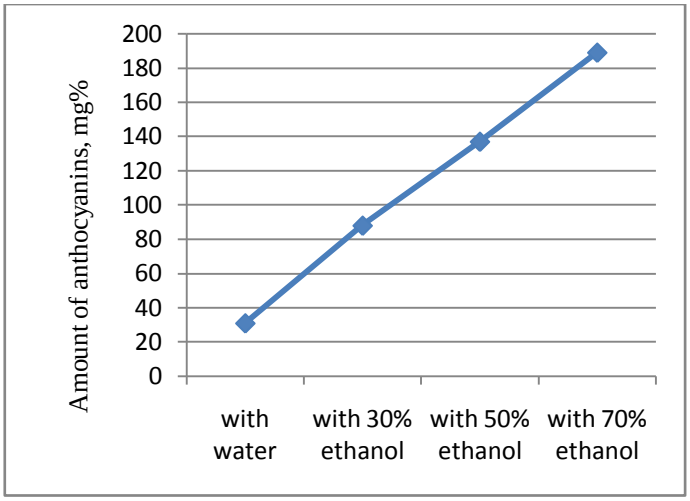

Fig. 4. Effect of extractant concentration on anthocyanins content in extracts of dried fruits blackcurrant

The change in the concentration of tanning substances follows the trend observed with other phenolic compound compounds. Tannins are most in the 70 % ethanol extract. The concentration of tannins in the extract is 19.2% higher than the extract with 30% ethanol - Fig. 5.

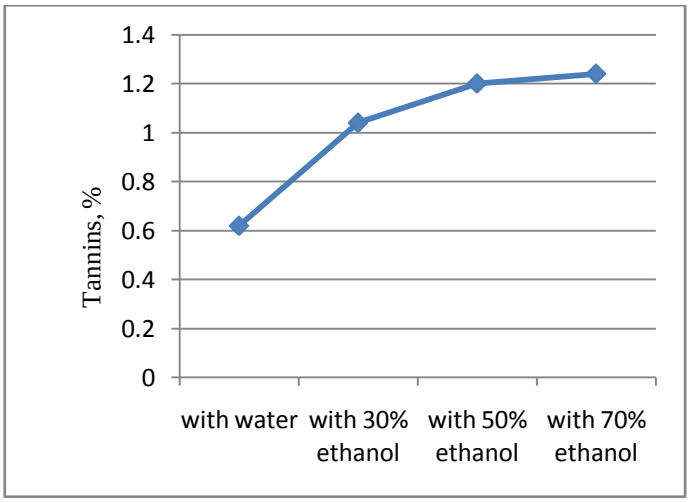

Fig. 5. Effect of extractant concentration on the content of tanning substances in extracts of dried fruits blackcurrant

In order to determine the optimal extraction temperature, four temperature variants were examined: 35 ° C, 50 ° C, 65 ° C and 80 ° C and 70 % C2 H5 OH as the solvent.

The results of studies on the effect of the extraction temperature on the chemical composition of blackcurrant extracts are given in Fig. 6-10.

The content of tanning substances extracted from dried currant berries ranges from 0.90 % to 1.33 % at an extraction temperature of 35°C, 50°C, 65°C and 80°C. The data show that with the increase of the temperature the quantity of tannins increases, their maximum value being at 80oC - Fig. 6.

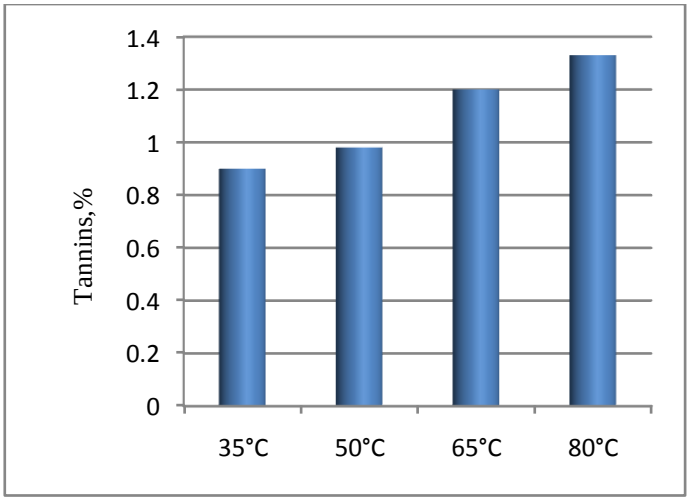

Fig. 6. Effect of extractant concentration on the content of tanning substances in extracts of dried fruits blackcurrant

The content of the total phenolic compounds in the extracts varies with different temperature regimes of 0.40 % at 50°C to 0.71 % at 65°C. The results obtained show that, by total phenol content of 0.71 g gallic acid / 100 g CB, the optimum extraction temperature for dried fruit blackcurrants is 65°C - Fig. 7.

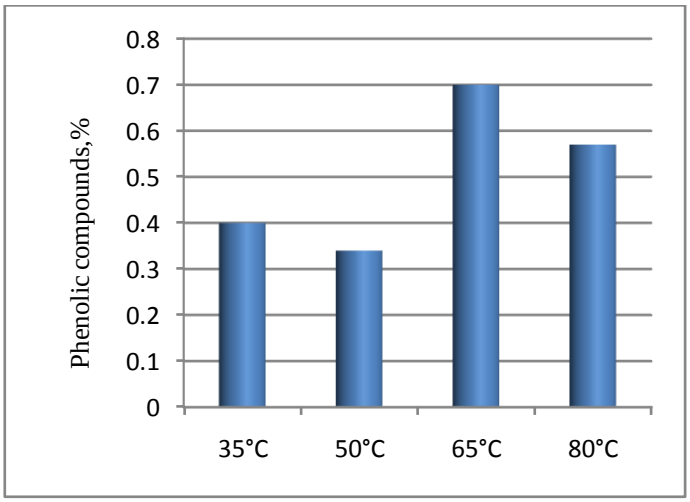

Fig. 7. Influence of the extraction temperature on the total phenolic compounds content in extracts of dried fruits blackcurrant

For the total content of flavonoid phenolic compounds, a favorable extraction temperature is 65°C - Fig. 8. Probably at higher temperatures some of them break down.

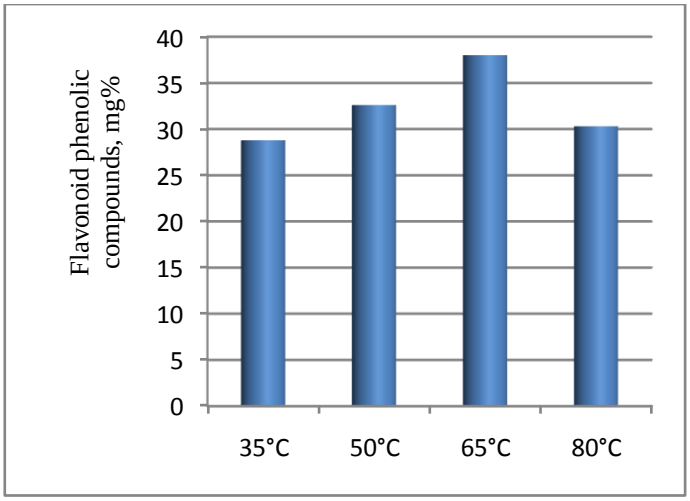

Fig. 8. Influence of the extraction temperature on flavonoid phenolic compounds content in extracts of dried fruits blackcurrant

By chemical structure and action, anthocyanin glycosides are close to flavonoids. By increasing the extraction temperature from 65°C to 80°C, the amount of anthocyanins in the dried fruit blackcurrant extract also increases. Therefore, for the sum of the anthocyanins, respectively 241 mg%, the optimum extraction temperature for the currant dried fruit is 80°C- Fig. 9.

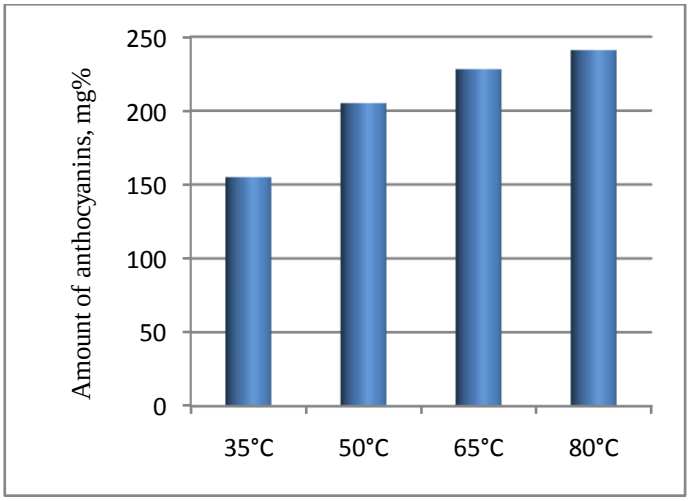

Fig. 9. Influence of the extraction temperature on anthocyanins content in extracts of dried fruits blackcurrant

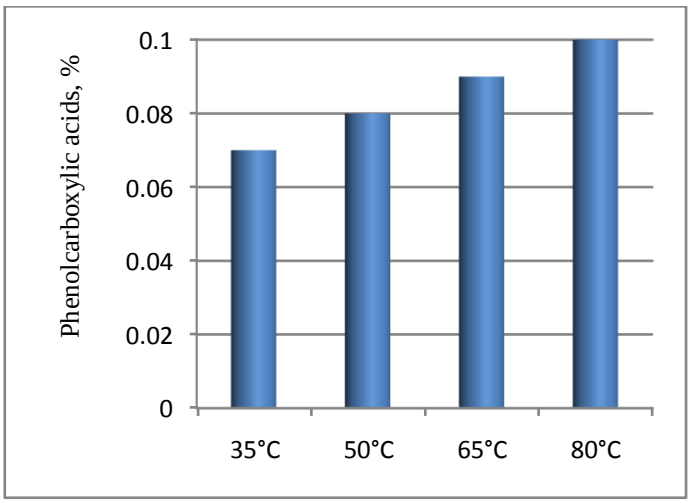

Fig. 10. Influence of the extraction temperature on phenolcarboxylic acids content in extracts of dried fruits blackcurrant

By total content of phenolic carbonic acids 0,1 % favorable temperature is 80°C - Fig. 10. Based on the results obtained, it can be concluded that the technologically justified extraction temperature is 65^{o} - 80^{o}C.

Based on the results obtained, it can be concluded that the technologically justified extraction temperature is 65o - 80oC. When high temperature is applied to the plant cells, their destruction occurs and the extraction of phenolic substances and flavonoids is facilitated. As a rule, phenolic substances are contained in natural sites not in the free but in the sugar-related state in the form of glucosides. In the heat treatment the bonds are destroyed and the phenolic substances are released from the cells.

The further increase in temperature does not help to increase full extraction and leads to the destruction of biologically active substances (polyphenols, vitamins). Therefore, raising the temperature in this case above 80 ° C is inappropriate.

In order to determine the process process life, extraction is carried out at optimal solvent values and an optimal extraction temperature for 1, 2, 3 and 4 hours. Results of studies on the influence of extraction duration on the physicochemical composition of the extracts are shown in Fig. 11-15. The concentration of the total phenolic compounds in extracts of dried fruit blackcurrant increased from 0.68 % in 1 hour to 0.95 % in 4 hours with 39.7 % - Fig. 11.

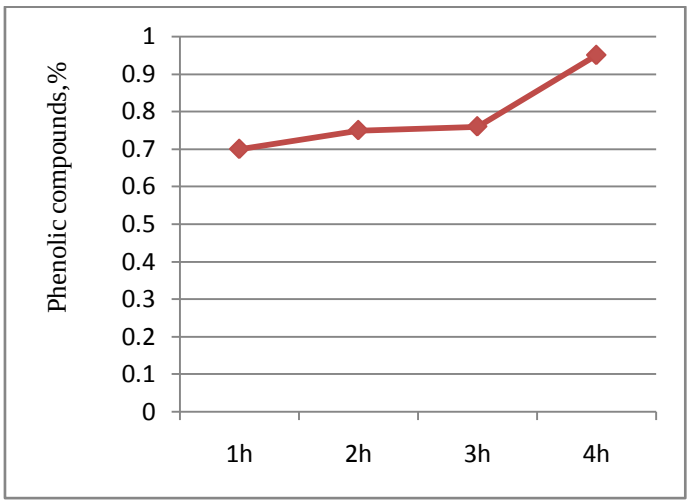

Fig. 11. Influence of the duration of extraction on the content of the total phenolic compounds in extracts of dried fruits blackcurrant

The amount of phenolcarboxylic acids extracted from the dried fruits of the blackcurrant by extraction with a different duration from 1 to 4 hours increases by 22% - Fig. 12.

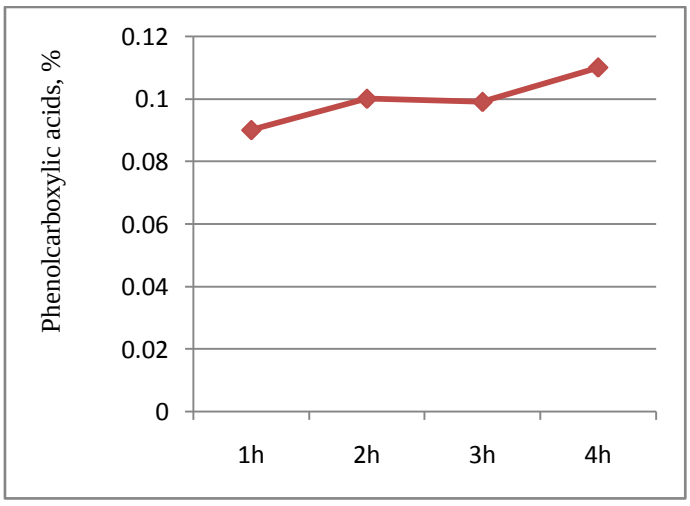

Fig. 12. Influence of duration of extraction on the phenolcarboxylic acids content in extracts of dried fruits blackcurrant

The content of the flavonoid phenolic compounds increased by 31.6 % with an extraction time of 1 to 4 hours - Fig. 13.

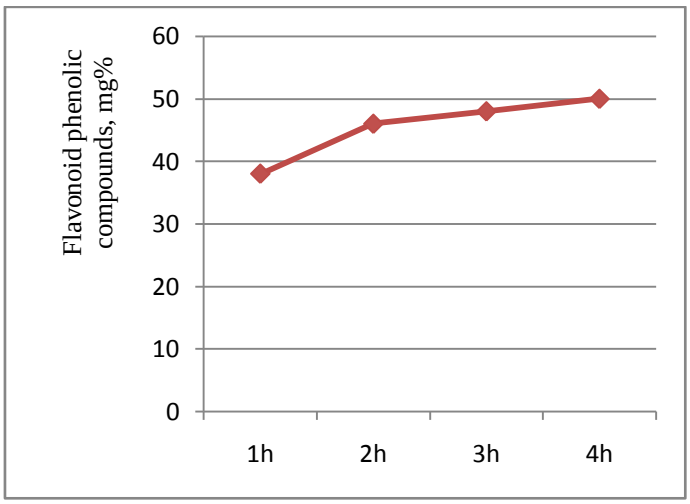

Fig. 13. Influence of the duration of extraction on the content of flavonoid phenolic compounds in extracts of dried fruits blackcurrant

Similar to flavonoid phenolic compounds, the amount of anthocyanins in blackcurrant extracts is also increasing. With different extraction times vary they range from 228 mg% to 243 mg%. The increase in the amount of anthocyanins in blackcurrant extracts with an increase in the duration of extraction is negligible by 6.6 % - Fig. 14.

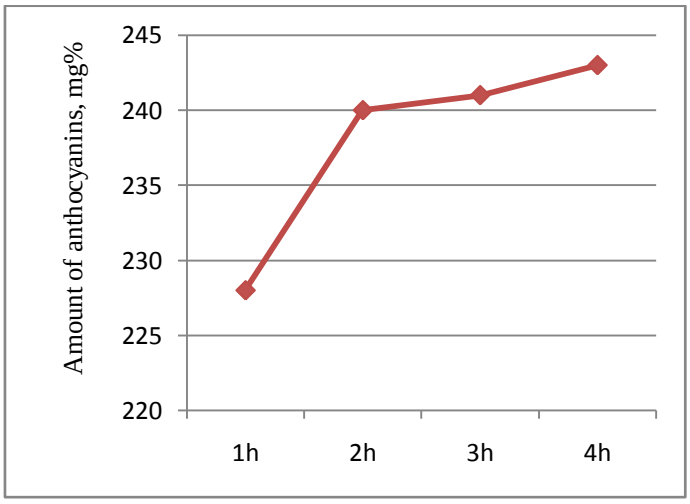

Fig. 14. Influence of the duration of extraction on the amount of anthocyanins in extracts of dried fruits blackcurrant

The content of tanning substances extracted from the blackcurrant at different extraction times ranges from 1.20 % to 1.41 %. The increase is 17.5 % respectively - Fig. 15.

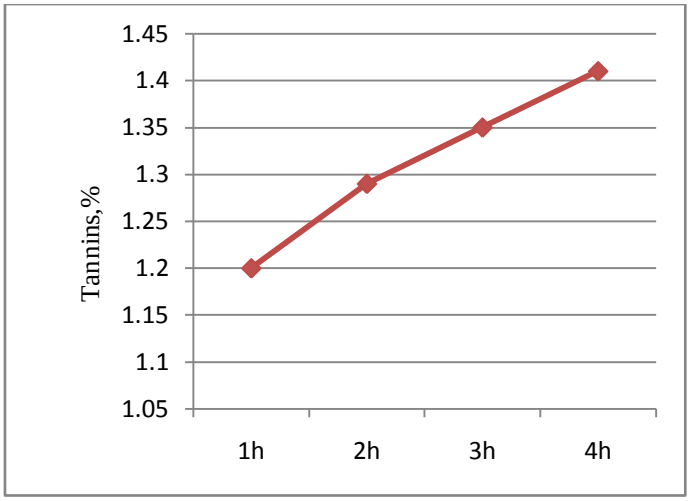

Fig. 15. Influence of the duration of extraction on the content of tanning substances in extracts of dried fruits blackcurrant

The results obtained from the studies allow us to conclude that about total phenolic complex content, the most advantageous extraction time is 3-4 hours.

The effect of the extraction hydromodule on the content of the phenolic complex in the extracts of the blackcurrant fruit is investigated.

The content of the total phenolic compounds in the blackcurrant fruit extracts varies with the different hydromodules, respectively, from 0.76 % at 1:10 to 1.02 % in the hydromodel 1:30. Technologically justified hydromolecule of extraction is 1:30 - Fig. 16.

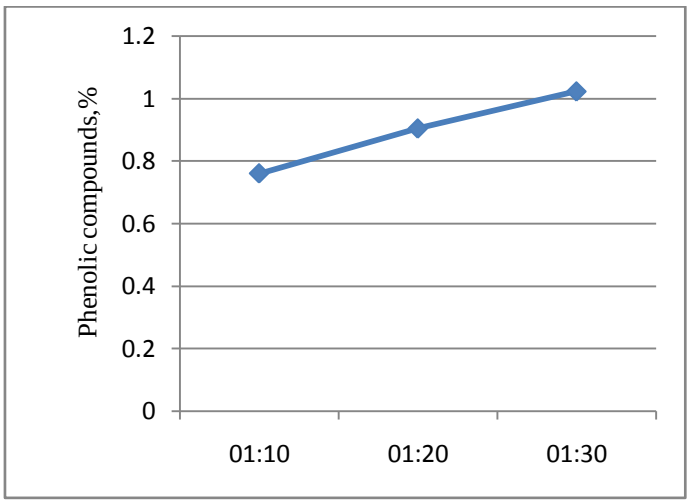

Fig. 16. Influence of the extraction hydromodul on the content of the total phenolic compounds in extracts of dried fruits blackcurrant

The amount of phenolcarboxylic acids extracted from the dried fruits of the blackcurrant by extraction with a different hydromodule increases and is highest at the hydromodule 1:30 - Fig. 17.

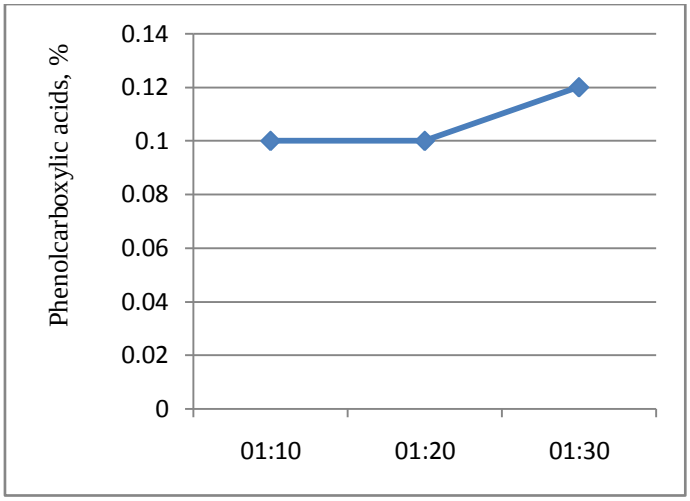

Fig. 17. Influence of the extraction hydromodul on the phenolcarboxylic acid content in extracts of dried fruits blackcurrant

The content of flavonoid phenolic compounds increased by 25.2 % at hydromodul 1:20. In hydromodul 1:30 the content of flavonoid phenolic compounds decreases by 11.2 % - Fig. 18.

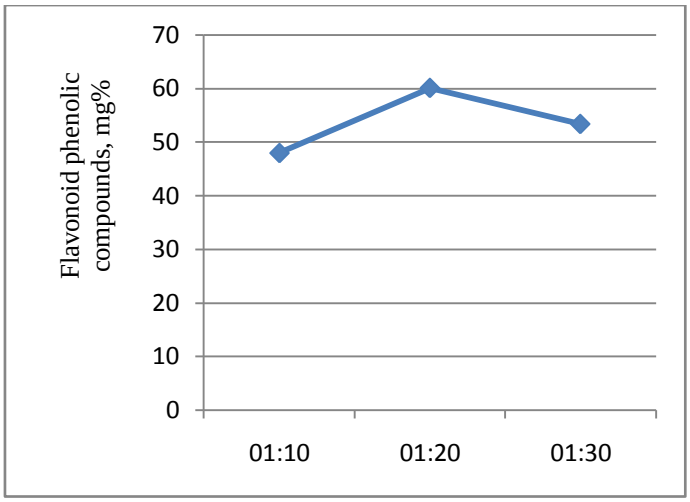

Fig. 18. Effect of extraction hydromodul on the content of flavonoid phenolic compounds in extracts of dried fruits blackcurrant

Studies of the amount of anthocyanins in the blackcurrant extract obtained in three different hydromodules show that the anthocyanin content ranges from 243 mg%, 233 mg% to 238 mg% - Fig. 19. The higher ratio of raw material to the extract ant does not significantly affect the amount of anthocyanins in blackcurrant extracts.

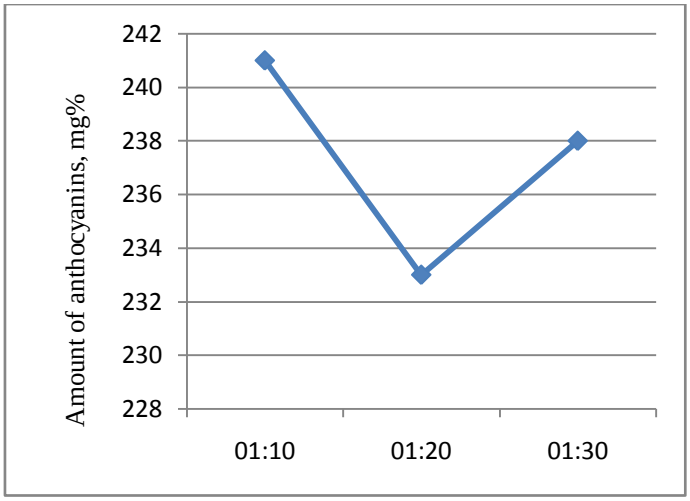

Fig. 19. Influence of the extraction hydromodul on the sum of anthocyanins in extracts of dried fruits blackcurrant

The content of tannins extracted from dried fruit blackcurrant ranges from 1.35 % to 2.47 % at the hydromodul 1:10 to 1:30. The data show that the hydromodule affects the amount of tannins, their maximum value being at a ratio between material and extractant 1:30 - Fig. 20.

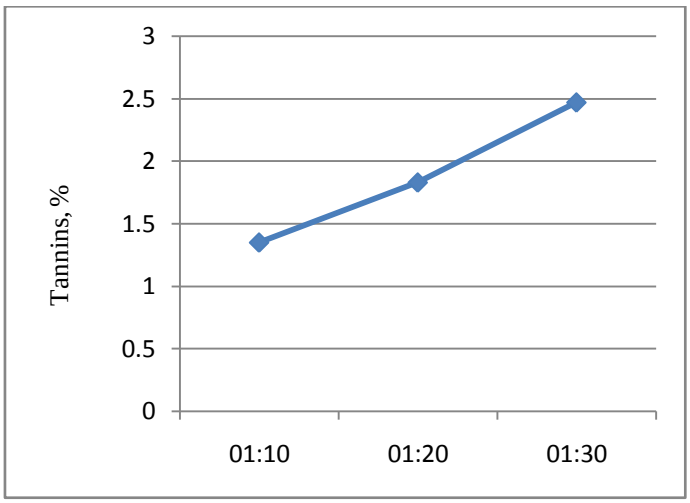

Fig. 20. Influence of the extraction hydromodul on the content of tanning substances in extracts of dried fruits blackcurrant

The results obtained suggest that the most advantageous hydromodul for extraction is 1:30 to obtain the extracts with the highest content of phenolic complex. To improve the extractability of substances contained in dry plant tissue, the raw material needs to absorb a certain amount of water, to provide the water needed to rehydrate the cells.

For the normal functioning of the body's complex antioxidant system, a wide range of biooxidants is required. Particularly effective is a systems in combination with the phenolic compounds contained in blackcurrant extracts, which themselves function as active antioxidants.

As a result of the research carried out, a technology was developed for the production of black currant extracts, the exemplary block diagram of which is shown in fig.21.On the basis of the experimental data, the technological regimes of the extraction process were selected.

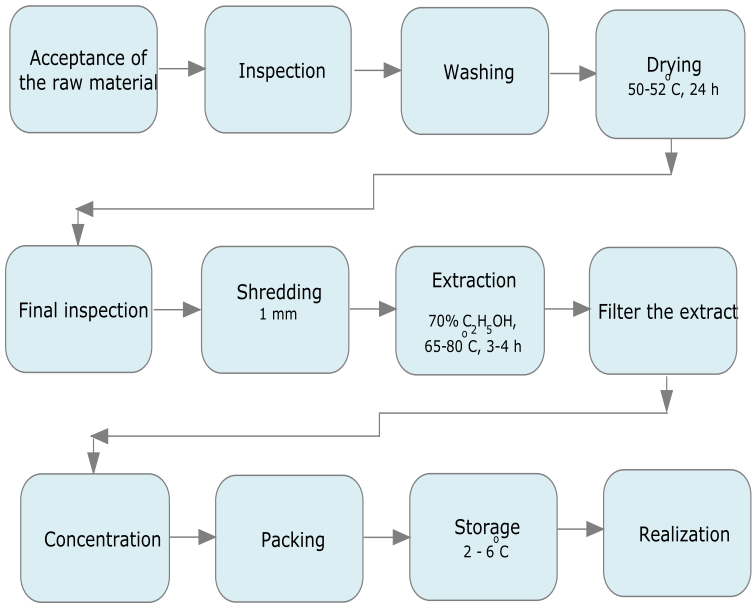

Fig. 21. Block scheme for obtaining extracts of dried fruits currants

A technology for the production of dried fruits currant extracts with a high content of biologically active substances used for the production of functional drinks is scientifically substantiated and developed.

IV. CONCLUSIONS

As a result of the research, the following conclusions can be drawn:

1. In the production of plant extracts, the choice of raw material is important for the physicochemical properties of the extract.
2. In the preparation of the extracts from the dried fruits of black currant, the technology of drying the raw material influences the physicochemical properties of the extract. Proper drying increases the shelf life and increases the phenolic complex content.
3. The use of 70% C_2H_5OH as an extractant is technologically warranted to produce extracts of dried fruits currants with maximum content of phenols, flavonoids, anthocyanins and tannins.
4. Technologically justified extraction temperature is 65°-80°C. Increasing the temperature above 80 °C does not lead to more complete extraction and destroys the biologically active substances. Therefore, raising the temperature in this case is inappropriate.
5. By increasing the extraction temperature to 80 °C, the quantity of anthocyanins in the extracts increases, which positively affects the organoleptic evaluation of the final products.
6. The optimum extraction time is 3-4 hours. During this extraction period, a maximum content of the phenolic complex is obtained.
7. On the basis of the experimental data, the technological regimes of the extraction process were selected.

REFERENCES

[1] Akulina, V. "Enriched drinks - a new niche in the juice market" Tare and packaging, vol. 4, 2007, pp.16

[2] Vesna, T.; Jasna, Č.B.; Lars, G.; Sonja, D.; Gordana, Ć. Superoxide anion radical scavenging activity of bilberry (Vaccinium myrtillus L.). J. Berry Res., 1, 2010, pp.13–23.

[3] Mattila P.H., Hellstom J.com, G.McDougalletal "Polyphenol and vitamin C contents in European commercial black currant juice products,"Food Chemistry, vol.127, no.3, 2011, pp.1216–1223.

[4] Krisch J., Ordogh L., Galgoczy L., Papp T. and Vagvolgyi C. "Anticandidal effect of berry juices and extracts from Ribes species," Central European Journal of Biology, vol. 4, no. 1, 2009, pp. 86–89.

[5] Molan A.L., Liu Z. and Kruger M."The ability ofblackcurrant extracts to positively modulate key markers of gastrointestinal functioninrats," World Journal of Microbiology and Biotechnology,vol.26,no.10,pp.2010, pp.1735–1743

[6] TABART J., FRANCK T., KEVERS C. ET AL."ANTIOXIDANT AND ANTIINFLAMMATORY ACTIVITIES OF RIBES NIGRUM EXTRACTS," FOOD CHEMISTRY,VOL.131,NO.4,2012, PP.1116–1122.

[7] Brangoulo H. L. and Molan P. C. "Assay of the antioxidant capacityoffoodsusingiron(II)-catalysed lipidperoxidation model for greater nutritional relevance," Food Chemistry, vol. 125,no.3,2011, pp.1126–1130.

[8] Szachowicz-Petelska B., Dobrzynska I., Skrzydlewska E. and Figaszewski Z. "Protective effect of blackcurrant on liver cell membrane of rats intoxicated with ethanol," Journal of Membrane Biology, vol. 245, 2012, pp. 191–200.

[9] State Pharmacopoeia of Russia General methods of analysis - II ed., Medicine, 1987.

.

International Journal of Innovation Engineering and Science Research
(ISSN: 2581-4591)
www.ijiesr.com

Engineering Properties of crude Oil contaminated clay Soil in Niger Delta Region of Nigeria

Nwachukwu A. N., Dike B. U., Njoku K. O., Ukachukwu. O. C.
Department of Civil Engineering, Federal University of Technology, PMB 1526, Owerri, Imo State Nigeria

ABSTRACT

Rivers state is one of the major oil producing states in the Niger-Delta region that has experienced oil pollution due to constant oil spills. The degradation has attracted the attention of both local and international organization like UNESCO, UNEP, WHO. E.t.c. The impact has become so serious that made British Broadcasting Co-Operation after visiting Rivers and Bayelsa State in 2009 declared Nigeria as oil pollution capital of the world. This research paper investigated the effect of crude oil pollution on selected geotechnical properties of clay soil in Akiogbologbo located in Engeni Ahoada L.G.A of Rivers state. The geotechnical parameters investigated are California bearing ratio (CBR), Coefficient of Permeability (K), consolidation parameters (Coefficient of consolidation Cv, Coefficient of volume compressibility av and Settlement S), Shear Strength Î, Cohesion C, and angle of internal friction Ø. The soils were collected at a depth of 2m. The collected samples were mixed with crude oil at different percentages between (0% - 14%) of the dry weight of the samples at 2% interval. Laboratory tests were conducted on both the contaminated and uncontaminated samples, Variations in the properties of the contaminated as well as uncontaminated samples were obtained at each level of contamination. The results show that CBR, and Coefficient of permeability (K) decreased from 12.6% and 3.28 × 10^{-4} cm/s at 0% contamination to 0.6% and 2.0 × 10^{-4} cm/s at 14% contamination, consolidation parameters Cv, av, and S increased from 6.46 × 10^{-7} KN/m^2 , 1.1 × 10^{-2} Kn/m^2 and 2.98mm at 0% to 9.65 × 10^{-7} KN/m^2, 1.23 × 10^{-2} KN/m^2 and 3.3mm at 14% contamination respectively. Angle of internal friction increased from 11^o at 0% to 13^o at 14%, Shear strength decreased from 125.11 KN/m^2 at 0% to 87.96 KN/m^2 at 14% cohesion decreased from to 81.93KN/m^2 at 0% to 58.87 KN/m^2 at 14% contamination. Changes on the value of the geotechnical parameters shows crude oil has negative impact on geotechnical properties of clay soil.

Keywords—Crude oil, Clay soil geotechnical parameters contamination, Niger-Delta.

I. INTRODUCTION

Soil contamination by crude oil and its product is one of the most widespread and serious geo-environmental problems confronting many oil producing nations in the world. Different contaminants have different chemical properties which influences geochemical reactions induced in the soil. Thus the level of contamination is affected by the chemical characteristics of the contaminants and to some extent physio-chemical properties of the soil concerned [4]. It is a well-known fact that petroleum products constitute one of the most prevalent sources of environmental pollution in the world today. Nigeria which is rated as the 6th largest oil producing nation is not left out in partaking of the negative effect of pollution [6]. It's Niger-Delta where most of the oil activities take place has experienced huge oil spills as a result of oil exploration refining and transportation. It is however very difficult to access oil spills in the Niger Delta region of Nigeria, owing to insincerity on the part of the operators of oil sector to give accurate report of occurrence of spillages in the region [10]. The amount of spillages in the Niger Delta region ecosystem over the past 50yrs is estimated to be more than 9million tons [11]. Again according to the Federal Government of Nigeria about 7000 oil spills may have occurred between 1970 and 2000[1]. Also the federal government documents a total of 2405 oil spills

accidents between 2000 and 2006 which represent an alarming rate of approximately 300 spills per annum. The rate of spill incident has escalated to such an unacceptable level in Niger Delta region leading to social and political issues like corruption, youth restiveness e.t.c. [2]. There are several reasons for the huge number of spills, these include lack of maintenance of oil pipelines. Most of the pipelines which convey oil are obsolete. According to international standards, oil pipelines supposed to be replaced after every 20years. Some of the pipes are laid above the ground exposing them to wear and tear [9]. Others are sabotage transportation, production and drilling process. Regardless of the source whenever these spills occur they impact negatively on the lives of the people in the area where they occur. It wipes out aquatic life and crops, fills the air with hazardous gases leaving its victims unable to find the life nature originally provided.

In general oil contamination causes massive environmental degradation, it is a serious geo-environmental problem as it impacts negatively on both Agricultural and geotechnical properties of soil.as well as groundwater. It percolates steadily into subsurface environment and water system. These hydrocarbons when they penetrates soil, affects the quality of the soil and changes the physical properties of the contaminated soil. In previous researches, it has been shown that oil contamination reduces the permeability strength and Atterberg limits of the soil[6]. Therefore it is pertinent to study geotechnical properties of oil contaminated soils for Engineering and Environmental purposes.

The objective of this paper therefore is to present changes on geotechnical properties of clay soil when clay soil samples were mixed with varying percentages of crude and subjected to laboratory testing. The geotechnical properties investigated are California bearing ratio (CBR), consolidation parameters (coefficient of consolidation Cv, compressibility coefficient Av and Settlement S), others are shear strength, angle of internal friction and cohesion C.

II. Materials and Method

The materials for this study are clay soil and crude oil. The clay soil was obtained from Akiogbologbo in Engenni Ahoada L.G.A. of Rivers State. The crude oil was obtained from a nearby Agip drilling rig location. Disturbed soil samples were collected at approximately 2.0m depth. The samples were air dried and mixed with water equivalent of natural moisture content. The clay soil samples were divided into eight equal parts with one sample as control (0% contamination).

The level of contamination was calculated as percentage by weight of uncontaminated prepared samples. Each sample was mixed with crude oil at 2%, 4%, 6%, 8%, 10%, 12%, and 14% level of contamination. The samples were placed in a closed container and kept in the laboratory for 14days for proper reaction between the samples and the oil. About 14 samples were prepared for each parameter standard and comprehensive laboratory investigation based on ASTM standard method of soil testing was conducted on the samples to determine the effect of crude oil the on geotechnical parameters. The following Geotechnical properties were investigated ; Shear strength, angle of internal friction and cohesion using unconsolidated undrained triaxial test (ASTM D 2850), Coefficient of permeability using constant head permeameter (ASTM D 2434), consolidation parameter (Cv, av, and S) using consolidometer (ASTM 2435), California bearing ratio CBR (ASTM 2434).

III. RESULTS AND DISCUSSION

Fig. 1 shows the result of variation of CBR of polluted clay soil with different concentration of crude oil

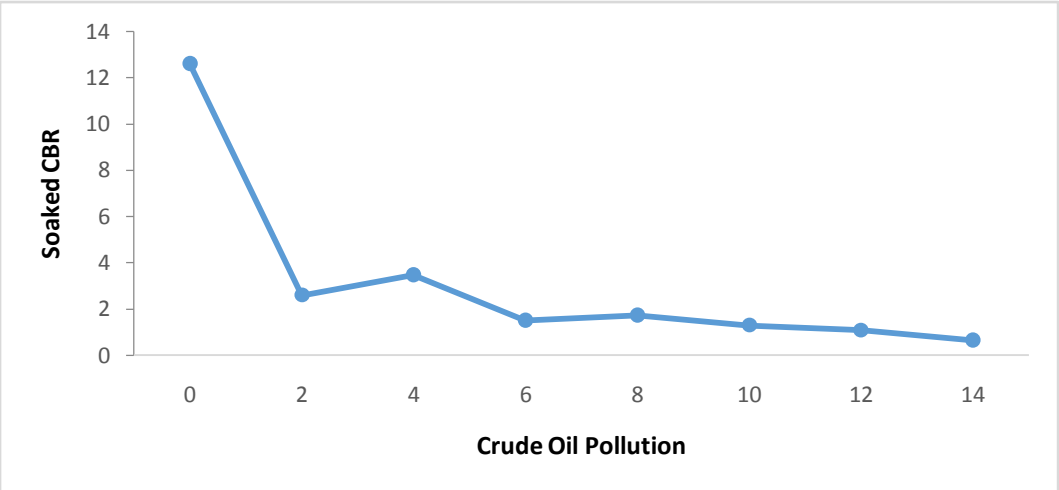

Fig 1: Variation of Soaked *CBR* of polluted clay soil with different concentration of crude oil

For crude oil contamination, the *CBR* decreased from 12.61% at 0% contamination to 0.66% at 14% contamination. The decrease in the *CBR* is as a result of lubricating effect of oil which caused the soil particles to slide over each other accounting for the decrease in the *CBR* values.

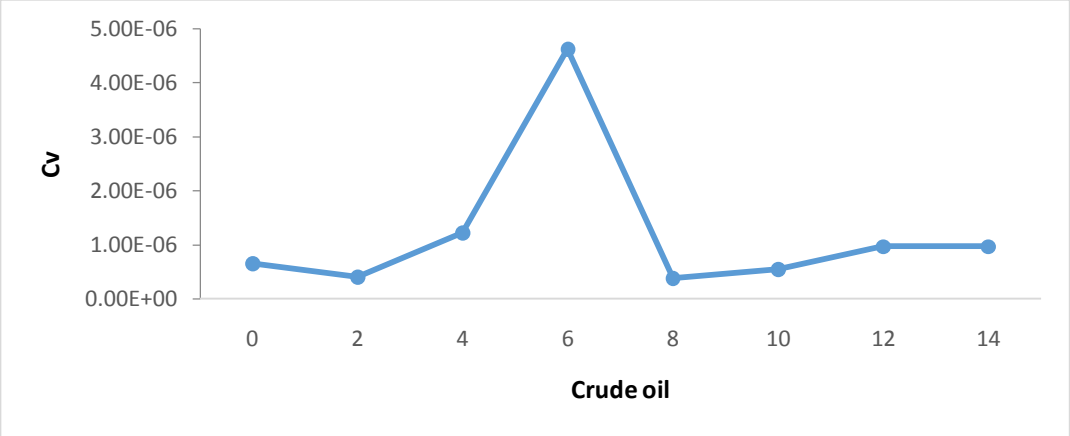

Fig. 2 Variation of Coefficient of Consolidation (C_v) of polluted clay soil with different concentration of crude oil

For clay contaminated with crude oil, the coefficient of consolidation increased from $6.46x10^{-7}$ m^2/s at 0% to $9.65 \times 10^{-7} m^2/s$ at 14%. The increase in the coefficient of consolidation Cv is as a result of increased oil contamination. This could be due to initial settlement and extrusion of oil from the soil material with increasing loading through the process of compressibility and consolidation which is time dependent. This result is in agreement with [3] but disagrees with earlier works by [8]. The increment in consolidation may also be as a result of reduction in void ratio as a result of the presence of oil, therefore the viscous properties of crude oil greatly influenced the rate at which the compressibility of the soil under applied pressure is behaving.

Fig. 3 shows the result of Variation of Coefficient of Compressibility (a_v) of polluted clay soil with different concentration of crude oil.

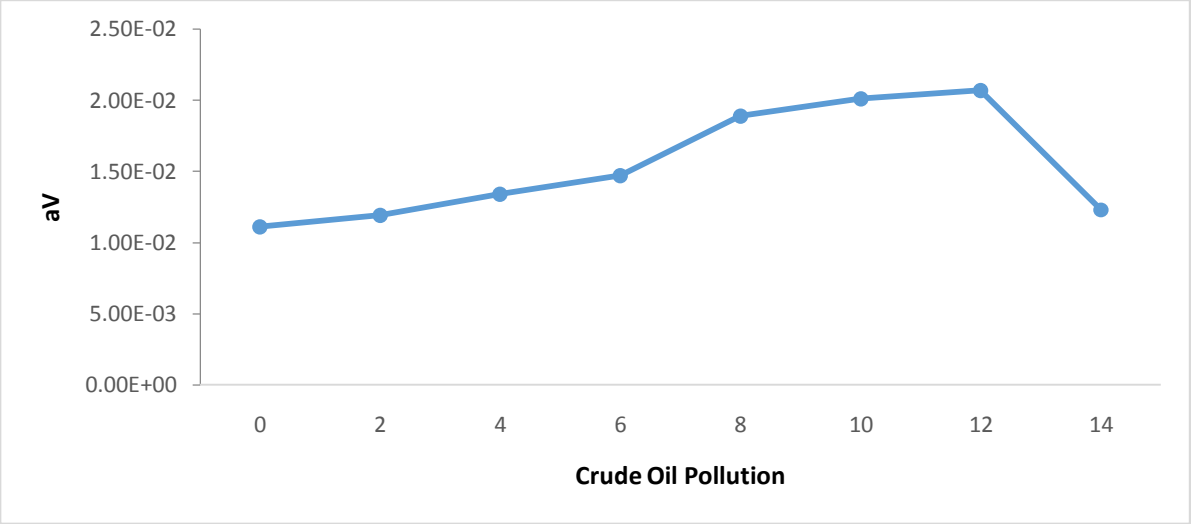

Fig.3 Variation of Coefficient of Compressibility of polluted clay soil with different concentration of crude oil

The volume compressibility (av) increased progressively from 11 x 10^{-2} m^2KN at 0% to 2.6 x 10^{-2}at 12% contamination before decreasing to 1.25 x 10x $10^{-2}m^2KN$at 14%. This could be due to initial settlement and extrusion of oil from the soil material with increasing loading through the process of compressibility and consolidation which is time dependent. This result is in agreement with [3] but disagrees with earlier works by [8].

Fig. 4 shows the result of Settlement of polluted clay soil with different concentration of crude oil

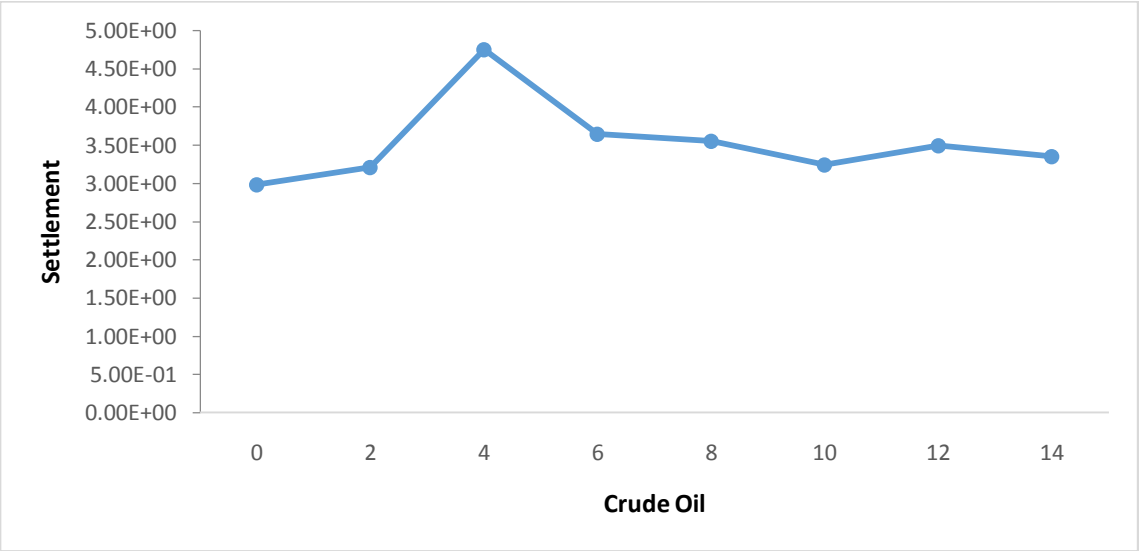

Fig. 4 Variation of settlement test of polluted clay soil with different concentration of crude oil

The settlement increased from 2.98mm at 0% to 4.75mm at 4% and decreased steadily to 3.35 mm at 14% contamination level.

Fig.5 shows the result of Permeability test of polluted clay soil with different concentration of crude oil.

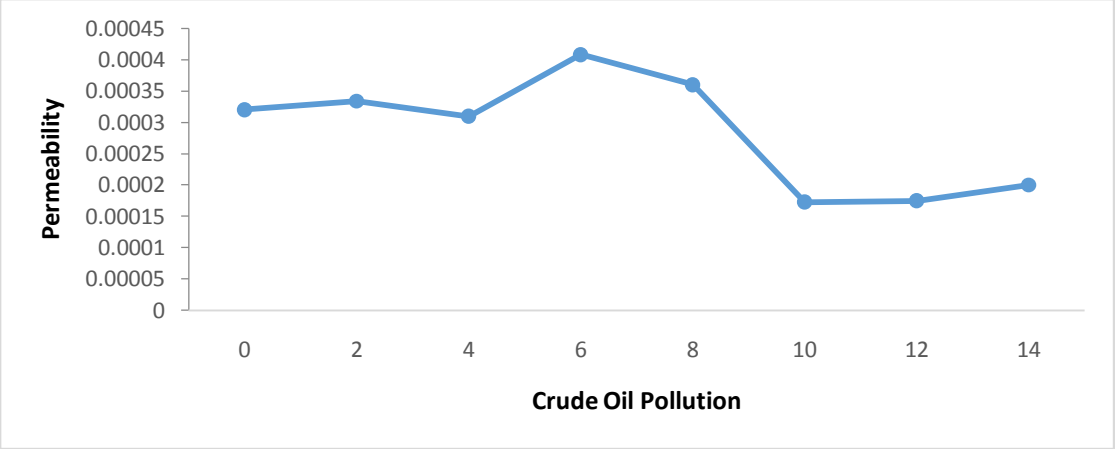

Fig. 5 Variation of permeability coefficient of polluted clay soil with different concentration of crude oil

The value of the coefficient of permeability (k) first increased to 4.1 X 10^{-} 4 cm/s at 6% contamination before decreasing to 2.0 x 10^{-4}cm/s at 14% contamination (about 12%) reduction. The decreased may have been caused by crude oil which were entrapped in the pore spaces thereby blocking the free flow of water through the soil mass.

Fig.6 shows the result of Variation of Friction Angle of polluted clay soil with different concentration of crude oil

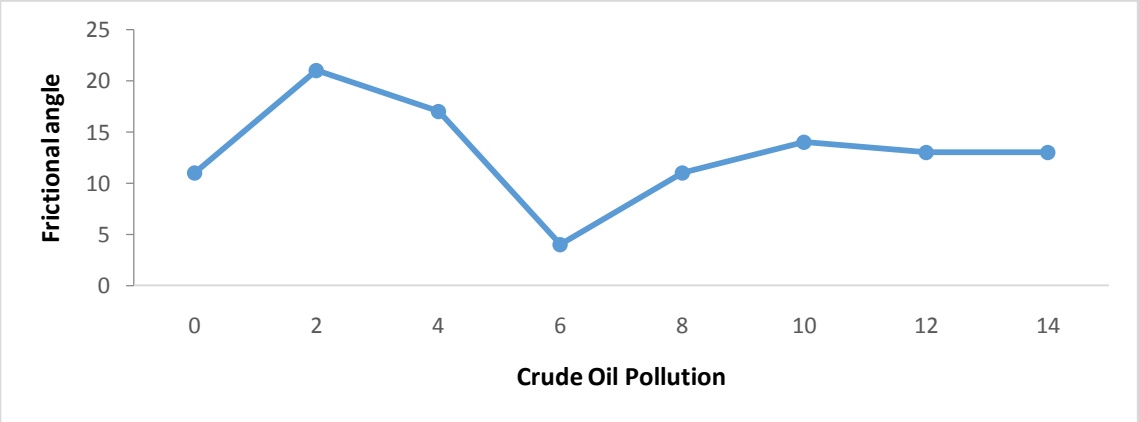

Fig.6 Variation of Friction Angle of polluted clay soil with different concentration of crude oil

The angle of internal friction increased from 11° at 0% to 21° at 2% contamination after which it showed an inconsistent decrease. It decreased from 21^0 to 4^0 at 4% contamination before increasing to 13^0 at 14%

Fig.7 shows the result of Variation of Shear Strength Parameters of polluted clay soil with different concentration of Crude oil

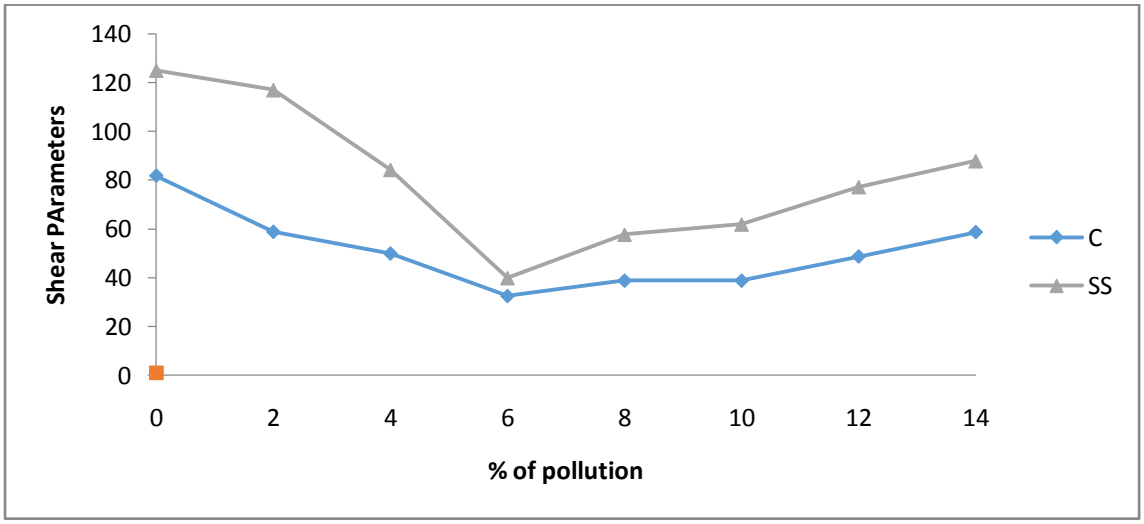

Fig.7 Variation of Shear Strength Parameters of polluted clay soil with different concentration of Crude oil

For clay contaminated with crude oil, the cohesion decreased from 81.93KN/m² at 0% contamination to 48.87KN/m² at 12% and increased again to 58.87KN/m² at 14% contamination. The angle of internal friction increased from 11° at 0% to 21° at 2% contamination after which it showed an inconsistent decrease. The shear strength showed progressiveon decrease from 125.11 KN/m² at 0% contamination to 87.96 KN/m² at 14% contamination. The decrease is a result of lubricating effect of the crude oil. Test specimen used in this study were prepared by mixing soils with contaminants which however forms a different soil structure [4]. Long term contamination showed a reduction in shear strength with decrease in pore dielectric constant. The crude oil decreased the pore fluid viscosity which eventually led to reduction of soil shear strength. The results however are in agreement with the work of [4].

IV. CONCLUSION

Laboratory investigation was carried on both uncontaminated at contaminated samples at different level of contamination 0%, 2%, 4%, 6%, 8%, 10%, 12% and 14%.
CBR, Coefficient of Permeability decreased. Cv, av and S increased as a result of contamination. Shear strength î, Cohesion C decreased while Ø increased.
From the result of this investigation it is not advisable to erect buildings and other Civil Engineering structures on soil contaminated with crude oil without proper geotechnical investigation. This is necessary to establish the level of contamination and carry out necessary remedial measures before such structures can be erected in the site.

REFRENCES

[1] E. Ayanova (2012). Oil pollution and international marine environmental law. Journal of Information Technology. 12(8):29-40.

[2] S.A. Egwu, (2012). "Oil spill control and management": Petroleum Technology Development Journal. Vol 1 pp 1-6

[3] T. S. Ijimdiya, (2010) "The Effect of Compactive Effort on the Compaction Characteristics of oil Contaminated Lateritic Soils. International Journals for Engineering (IJE). Vol. 4, No. 4. Pp. 549-554.

[4] M.Khamehchiyan, , A.H. Charkhabi and M. Tajik (2007). Effect of crude oil contamination on geotechnical properties of clayey and sandy soils. Eng. Geology Vol. 180 pp 220-224

[5] Laboratory soils testing (1970) Engineer Manual EM-1110-2-1906, U.S. Army Corps of Engineers, Dept. of the Army, Washington, D.C.

[6] Mashala, K., Charkhabi, A.M. and Tajik, M. (2006) "The effects of crude oil contamination on Geotechnical properties of *Bushe* in coastal soils in Iran": *Journal of the Geotechnical Society* London vol 214

[7] C. P. Nwilo and Badejo, T, O. (2009). "Laboratory studies on the influence of crude oil spillage on lateritic soil shear strength, a case study of Niger Delta area of Nigeria." Journal of Earth Science and Geotechnical Engineering 3 .vol. 2, pp 73-83.

[8] D.K. Talukda, and Saika, B.D (2013). "Effect of crude oil on some consolidation properties of clay soil. International Journal of EngineeringTechnology and advanced Engineering. vol 3 pp 117-120

[9] A. O. Tolulope (2004). "Oil exploration and environmental degradation, The Nigerian experience". International information archives, International Information Society for Environmental Information Science EIA 04-039, 2: 387-393

[10] Steiner, R. (2008). Double standards international standards to prevent and control pipeline oil spills compared with shell practice in Nigeria. A report submitted to friends of the Earth (2008).

[11] Kadafa, A.Y (2012). "Oil exploration and spillage in the Niger Delta of Nigeria": Journal of Oil and environmental research. Vol 2 No. 3 pp 38-49.

International Journal of Innovation Engineering and Science Research
(ISSN: 2581-4591)
www.ijiesr.com

Evaluation of Temperature-Humidity Changes in Closed Type Water Buffalo Barns in Terms of Animal Welfare

IsrafilKocaman[1] Can BurakSisman[1]

[1]*Namik Kemal University Agricultural Faculty*
Biosystems Engineering Department, Tekirdag, Turkey

ABSTRACT

The aim of this study was to evaluate temperature and relative humidity changes in closed type buffalo barns for different seasons in terms of animal welfare. In this study, two Anatolian Water Buffaloes group, which were assumed to have the same genetic similarities were formed based on their age and lactation number. One of this groups was housed in the Barn-I, where the climatic environment was controlled at an optimum level, and the other was housed in the Barn-II under current farming conditions. The amount of area and internal volume per buffalo in the barns were kept equal. As a result of the research, it was determined that the indoor temperature and relative humidity values were not a problem in terms of animal welfare in the Barn-I. For Barn-II, the increase in the relative humidity of the indoor environment during the winter months and the fact that the temperature was above 25 ° C in the summer had a negative effect on animal welfare. It is suggested that a good ventilation and misting system should be planned together in closed buffalo barns especially in winter and summer months in order to control the climatic environment at an optimum level.

Keywords—*Anatolian Water Buffalo, Closed type barn, Animal welfare, temperature, relativehumidity*

I. INTRODUCTION

In order to increase animal production, it is essential to improve and optimize the indoor climatic environment conditions while trying to increase the yield potential of animals by feeding and genetic improvements [1]. Because many scientific studies have shown that the effect of genetic structure on yield is around 30% and feeding and housing conditions are around 70% [2, 3]. There are very few places in the world that will consistently provide optimum climatic conditions for livestock all year round. Therefore, the effects of climatic conditions deviating from the optimum situation on animals are investigated and suitable climatic conditions for optimum production are continuously investigated.

Temperature is the most important environmental factor affecting the physiological activities of animals. Because temperature is an important index to affect the health and comfort of animals. The temperature range in which animals can perform and produce their productive functions in the best way is defined as the 'Comfort Zone ve and covers a narrow temperature range [4]. As you move away from the comfort zone, cold stress starts at low temperatures and temperature stress starts at high temperatures. Both stress conditions can adversely affect the meat and milk yield of livestock. It is recommended that the indoor temperature of the comfort zone and the thermo-neutral zone for water buffaloes is between 2-21 ° C and the upper limit value for physiological thermo regulator mechanism is 27 ° C [5].

One of the important environmental conditions for animal welfare is relative humidity. The effect of relative humidity on animals, which varies within certain limits at certain temperatures, is related to indoor temperature. Generally, high temperatures and relative humidity create anorexia in animals, reducing the consumption of feed required by animals for maximum productivity [6]. In optimum conditions, the relative humidity should be between 60-80%. The relative humidity should never be less than 30% and more than 90% [7].

The aim of this study was to evaluate temperature and relative humidity changes in closed type buffalo barns for different seasons in terms of animal welfare

II. Material and Method

This study was conducted in a water buffalo farm which is located in Thrace Part of Istanbul Province. The study area is located at 41° 12' northern latitude and 28° 44' east longitude and average altitude from sea level is 119 m. [8]

In the selected farm, two water buffalo groups which were assumed to have genetic similarities were formed. One of this groups was housed in the Barn-I, where the climatic environment was controlled at an optimum level, and the other was housed in the Barn-II under current farming conditions. The amount of area and internal volume per buffalo in the barns were kept equal., The temperature and relative humidity values of the indoor and outdoor air were measured for 24 hours along a year with thermo-hygrometer at 10minute intervals in the both barns. In order to prevent heat stress in controlled barn conditions (Barn-I), a misting system was installed and the indoor temperature was kept around 25 ^{o}C. The obtained data were compared with literature values for different seasons and evaluated in terms of animal welfare.

III. Result and discussion

The amount of heat and water vapor produced by the animals in the barns varies depending on the temperature and humidity values of indoor environment. For this reason, when the thermal environment control is not sufficient in the barn, animal welfare is adversely affected as a result of the negative impact of heat stress, effective utilization of the genotypic potential decreases and results in yield losses [9]. Considering the climatic conditions of the region where the research was carried out, indoor temperature of 13 ° C and indoor relative humidity of 75% were suitable for the winter season in closed buffalo barns. Daily changes of avrege temperature and relative humidity values of Barn-I, Barn-II and outdoor air in the winter season were given graphically in Figure 1 and Figure 2.

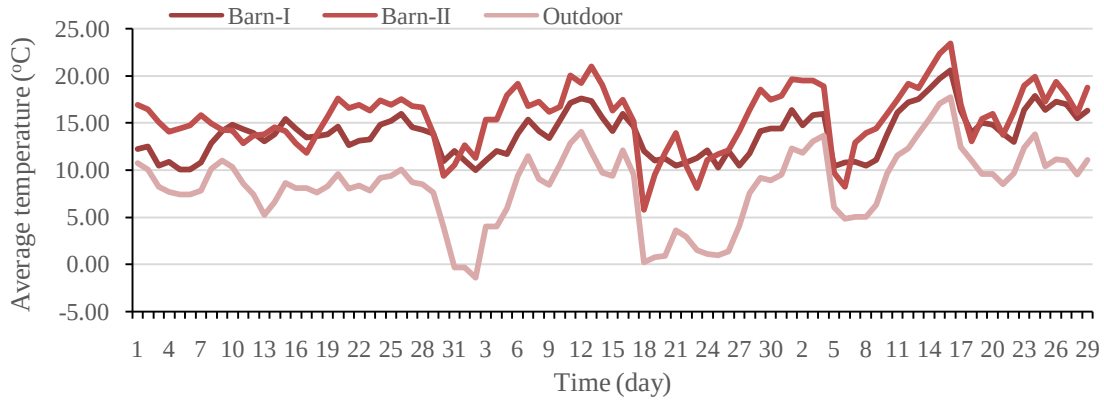

Fig.1. Average temperature valuesof the indoor and outdoor air in winter months

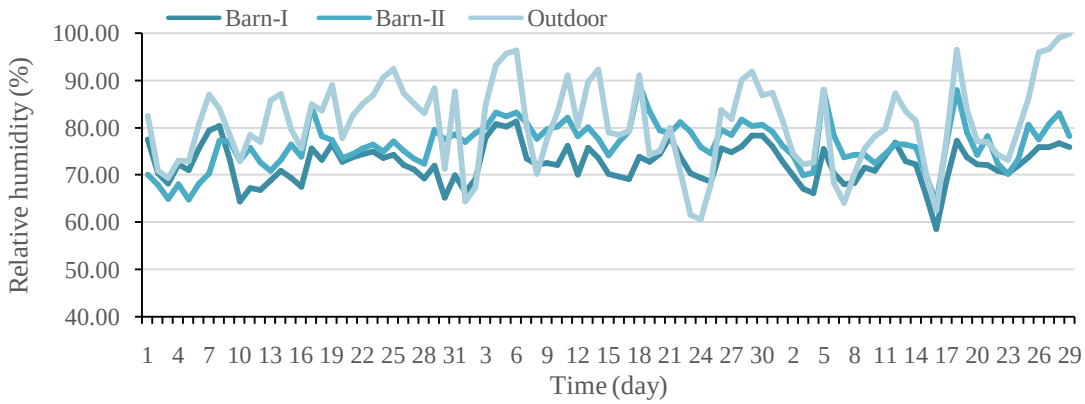

Fig. 2. Average relative humidity values of the indoor and outdoor air in winter months

In Figure 1, the lowest and highest average temperature values were 10 ^{o}C and 20.5 ^{o}C in Barn-I, 5.4 ^{o}C and 23.4 ^{o}C in Barn-II, respectively. Indoor temperatures for both barns were at suitable levels. However, while the average temperatures of Barn-I varied among narrower limits, this values changed among the wider limits in Barn-II. The lack of ventilation chimneys in the Barn-II and the use of windows for ventilation caused difficulty to control indoor temperature and deviations from the optimum temperature of 13 ° C that we accept for water buffaloes. The average temperature values of outdoor varied between -0.34 ^{o}C and 17.7^{o}C.

When the indoor relative humidity values were examined in Figure 2, it varied between 64.5% and 81.4% in the Barn-I, while these values varied between 64.8% and 89.2% in the Barn-II. The indoor relative humidity values of Barn-I had not any problem for water buffalo welfare for the winter season. However, it has seen that these values were above the acceptable limits in Barn-II. Too high or too low relative humidity may adversely affect the thermoregulatory ability of animals and consequently deteriorate animal health [10]. The outdoor relative varied between 60.5% and 99.8% during the winter months.

Daily changes of avrege temperature and relative humidity values of Barn-I, Barn-II and outdoor air in the spring season were given graphically in Figure 3 and Figure 4.

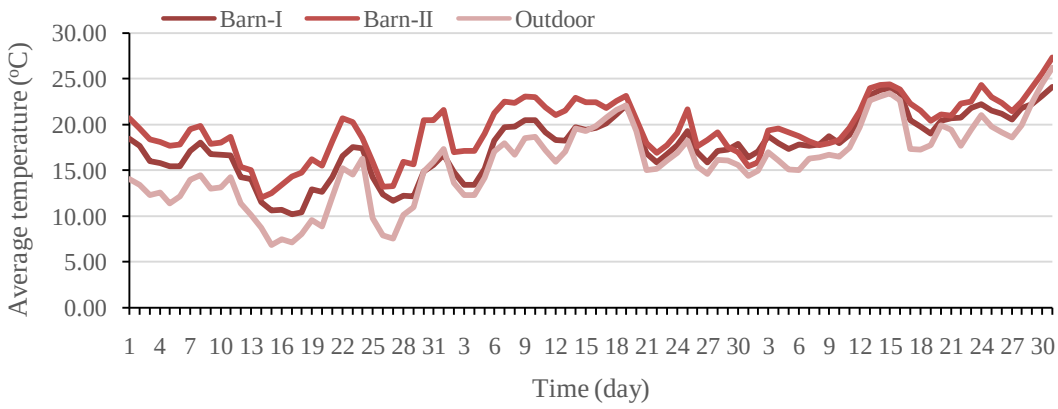

Fig. 3**.** Average temperature values of the indoor and outdoor air in spring months

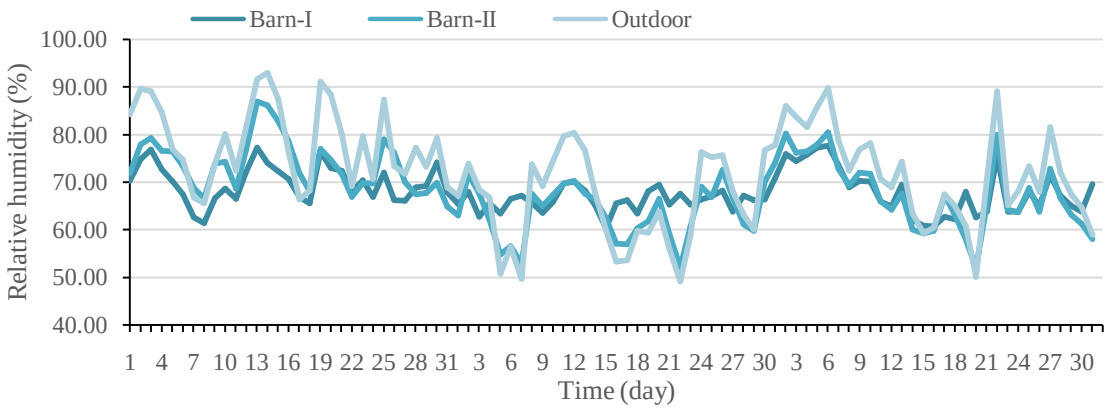

Fig. 4. Average relative humidity values of the indoor and outdoor air in spring months

In Figure 3, the lowest and highest average indoor temperatures were 10.2 ^{o}C and 23.1 ^{o}C in Barn-I, 10.7 ^{o}C and 27.4 ^{o}C in Barn-II, respectively. According to the suggested indoor temperature value of 18 ^{o}C, the average temperature values in Barn-I were not at a level that cause a stress for the water buffaloes. The recorded values for Barn-II were sometimes above the optimum temperature. When the relative relative humidity values were examined in Figure 4, it varied between 60.7% and 77.6% in Barn-I, while it varied between 52.1% and 86.9% in Barn-II. When the relative humidity values were compared with 75%, it could be said that the relative humidity values of Barn-I had not any problem for water buffalo welfare. It has seen that these values were above the acceptable limits for Barn-II.

Daily changes of average temperature and relative humidity values of Barn-I, Barn-II and outdoor air in the summer season were given graphically in Figure 5 and Figure 6.

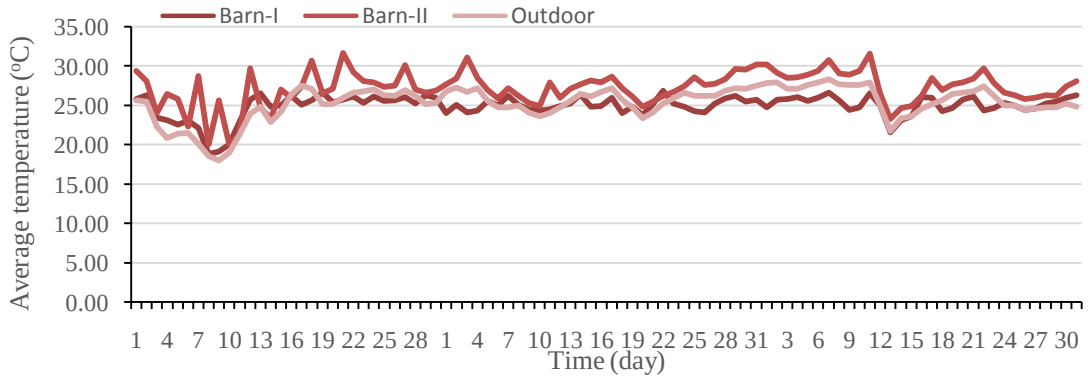

Fig. 5.Average temperature values of the indoor and outdoor air in summer months

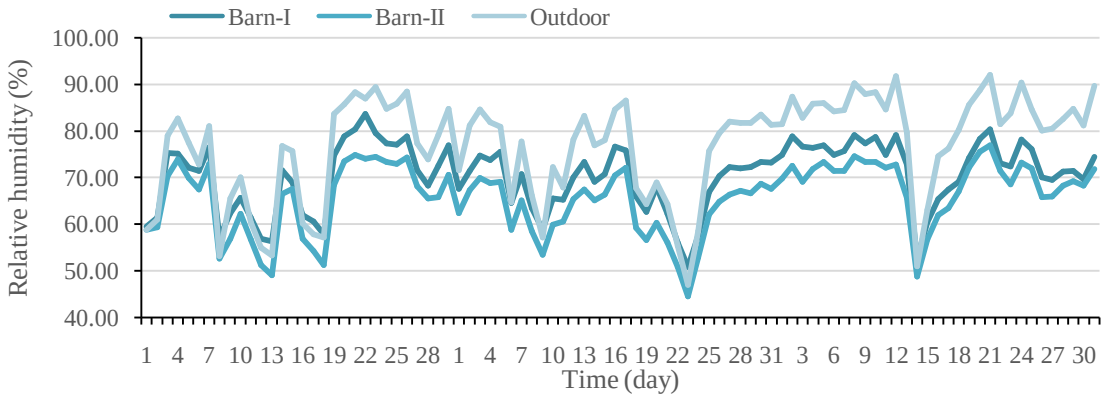

Fig. 6. Average relative humidity values of the indoor and outdoor air in summer months

When Figure 5 was examined, the lowest and highest average indoor temperature were 18.82 °C and 26.84 °C in Barn-I, 20.02 °C and 31.66 °C in Barn-II, respectively. the average indoor temperature values could be kept at suitable levels by the effect of the misting system in the Barn-I. It has been also seen that there was a slight deviation from 25 °C which is accepted as the optimum design criteria in summer conditions. In Barn-II, the average indoor temperatures varied among wider limits. This situation caused to an increase in temperature stress of water buffaloes, resulting in reduced feed consumption and reduced milk yield. When the average relative humidity values were examined in Figure 6, it varied between 50.81% and 83.55% in the Barn-I, while these values varied between 44.53% and 76.92% in the Barn-II. When the optimum relative humidity values accepted for the summer season were compared with 80%, it has been seen that the average relative humidity values of Barn-I were slightly higher by the effect of the misting system. However, it could be said that water buffalo welfare was not at a level that would cause too many problems. In Barn-II, the average indoor relative humidity values were positive for animal welfare.

Daily changes of average temperature and relative humidity values of Barn-I, Barn-II and outdoor air in the autumn season were given graphically in Figure 7 and Figure 8.

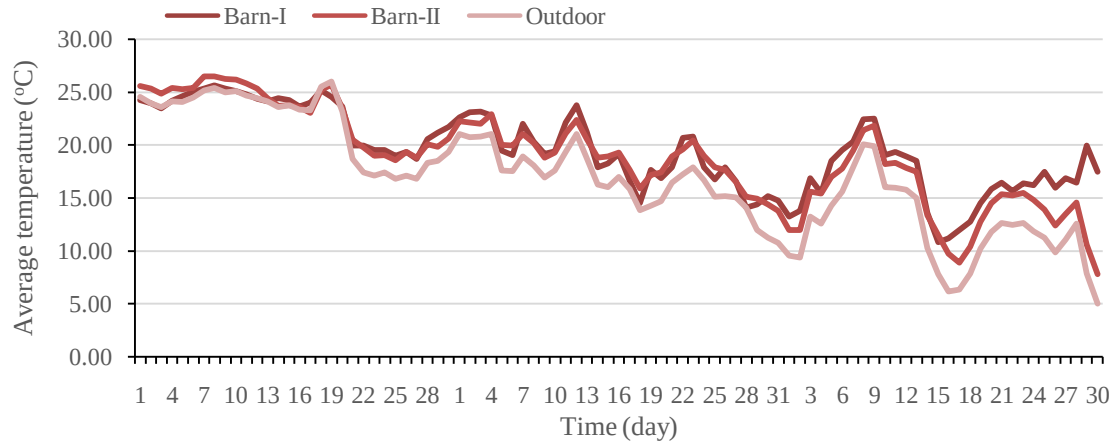

Fig. 7. Average temperature values of the indoor and outdoor air in autumn months

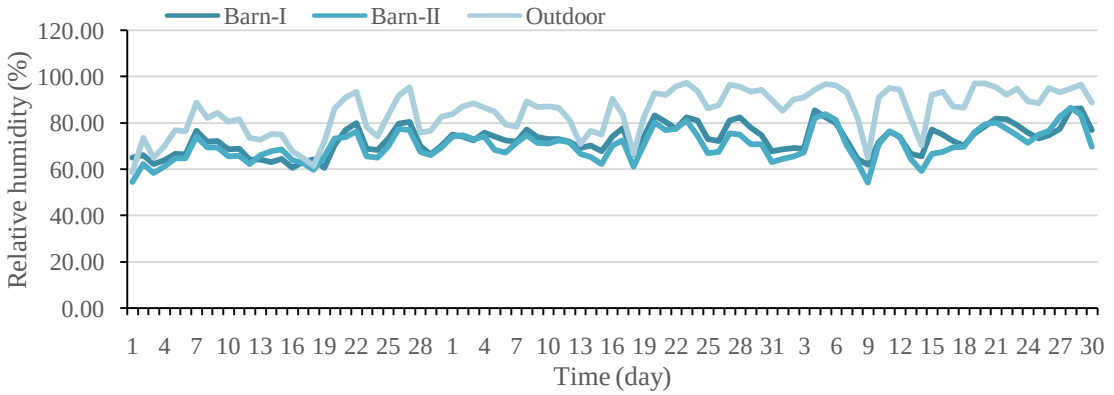

Fig. 8. Average relative humidity values of the indoor and outdoor air in autumn months

When Figure 7 was examined, the lowest and highest average temperatures were 10.87 °C and 25.69 °C in Barn-I, 7.81 °C and 26.54 °C in Barn-II, respectively. Based on the optimum temperature of 18 ° C for the transition season, the recorded average temperature values were not at a stress level for animal welfare in Barn-I and Barn-II. When the average relative humidity values were examined in Figure 8, it varied between 60.51% and 86.12% in the Barn-I, while it varied between 54.24% and 86.56% in the Barn-II. When the relative relative humidity values were compared with 75%, it could be

said that the relative humidity value changes of the Barn-I and Barn-II induced partial problems for water buffalo welfare.

IV. CONCLUSİONS

In this research, the effects of the on temperature and indoor relative humidity value changes on animal welfare were investigated for different seasons. According to the obtained data, the temperature and relative humidity values were not a problem in terms of buffalo welfare under controlled barn conditions for all seasons. For current farming conditions, the increase in the indoor relative humidity for the winter season and the indoor temperature above 25 ^{o}C in the summer season had a negative effect on the animal welfare. In order to control the climatic environment at an optimum level, a good ventilation system should be planned in closed buffalo barns. In addition, in order to eliminate the heat stress that may occur during the summer months, it will be beneficial to install a misting system in the barn or in the paddock area.

ACKNOWLEDGMENT

This work contains a part of TOVAG 115O602 project supported by TUBITAK. We are grateful to Presidency of TUBITAK for supporting the project.

REFERENCES

[1] I. Kocaman, A Research on the Investigation of the Physical Status of the Tie Stall Dairy Cattle Barns and Environmental Condition in Inanlı and Turkgeldi Livestock Farming Administrations, PhD Thesis, Thrace University, Institute of Natural and Applied Sciences, Edirne, 1998.

[2] A.V.Yaganoglu, 'Regulation of environmental conditions in animal barns', Journal of Atatürk University Faculty of Agriculture, 1986(17), 1-4.

[3] T. Ekmekyapar, Regulation of Environmental Conditions in the Animal Barns, Atatürk UnivesityScience, Erzurum, 1991.

[4] M. Okuroglu, and L. Delibas,'Suitable environmental conditions in the animal barns', Turkey, vol.2, pp. 142-149, May 1986 [Symposium of Animal Husbandry, Turkey, p. 405, 1986].

[5] M. M. Shafie, Physiological Responses and Adaptation of Water Buffalo, Florida, USA, CRC, 1985.

[6] N.H. Noton, Farm Buildings. London: College of Estate Management, 1982.

[7] C.H.Wathes and D.R. Charles, Livestock Housing. UK: Animal Science and Engineering Division Silsoe Research Institute.1994.

[8] Anonymous,Meteorological Data in Catalca District of Istanbul Province. Metorology General Directorate, Ankara, 2019.

[9] S.Mutaf, S.Alkan and N. Seber, 'Design principles of animal shelters in ecological agriculture', Turkey, vol 2, pp. 212-230, July 2004 [1'st International Congress on Organic Animal Production and Food Safety,Turkey, p. 325, 2004].

[10] S. Mutaf, The Climatic Environment and Detection Principles of Animal Barns with Engineering Approach, First edition, vol.1. Ankara, 2012, pp. 236-243.

International Journal of Innovation Engineering and Science Research
(ISSN: 2581-4591)
www.ijiesr.com

MANAGEMENT OF REHABILITATION OF PRODUCTIVE INFRASTRUCTURE OF SECTIONS WITH HIGH RISK OF DEGRADATION

OLAR HORATIU RAUL
PhD student DRILLING PRODUCTION DEPARTMENT
The **Petroleum-Gas University of Ploieşti**, UPG PLOIESTI
Ploiesti, ROMANIA

AVRAM LAZAR
PhD Habil. DRILLING PRODUCTION DEPARTMENT
The **Petroleum-Gas University of Ploieşti**, UPG PLOIESTI
Ploiesti, ROMANIA

STAN MARIUS
PhD MECHANICAL DEPARTMENT
The **Petroleum-Gas University of Ploieşti**, UPG PLOIESTI
Ploiesti, ROMANIA

ABSTRACT

In the extraction process, over time, it was found that there are a number of inconsistencies between the cumulative of the extracted gas and the forecast one. Due to the fact that the recovery factor is not at the level of the forecasted one, it was considered that complex inventories and investigations of all aspects involved in the process of natural gas production were considered, namely: improving the performance of the gas wells, of the separation, collection and gas transport, gas drying stations, gas compression stations, and last but not least the improvement of the human factor's performance, all these aspects being materialized in a technical-economic project for the rehabilitation of a gas structure. The rehabilitation of mature natural gas fields begins with the acquisition, processing, correlation and interpretation of all production data and geological data to determine the dimensions of the porous-permeable collectors, interpretations that rebuild areas of interest for future exploitation in accordance with the new gas reserves. Established with the new possibilities of exploitation of gas wells and surface infrastructure.

Keywords—*management;risk; style; recovery factor; rehabilitation*

I. INTRODUCTION

For the most accurate estimation of the natural gas reserve in a deposit, the most accurate values of the porosity, permeability and saturation in fluids are needed, values that are obtained after analyzing the core samples, but also from the core diagrams of each well. .

The most important geophysical method for mapping areas that may contain hydrocarbons is seismic prospecting, which consists of producing at certain points in the area under analysis, some elastic waves that propagate deep, returning to the surface after contact with separate boundaries. of the investigated layers, thus recording their arrival time on the surface.

When conducting seismic surveys, information about neighboring collectors, of small dimensions that have not been known until now, will be seen, besides information related to the shape and dimensions of the collector being investigated.The formatter will need to create these components, incorporating the applicable criteria that follow.

II. Assessing The Potential Of A Productive Horizon

Assessing the potential of a productive horizon, and predicting different extraction rates can be done through two-dimensional numerical models. The use of two-dimensional models elucidates which areas are drained in different percentages of the horizon, and if an opportunity to increase the operating size is possible by digging new probes.The two-dimensional numerical model applicable to the gas horizon has as theoretical support the differential equation of diffusion [1],[2]:

$$k_x \frac{\partial^2 U}{\partial x^2} + k_x \frac{\partial^2 U}{\partial y^2} + q = c\frac{\partial U}{\partial t} \quad (1)$$

The main characteristic of the natural gases exploited from the Transylvanian depression is given by the higher calorific value of over 10.4 Kwh / mc, and the percentage of methane in the gases is over 99%, which is why it can be considered a single component gas.

The implementation of the whole scenario of reactivation of natural gas wells, in conjunction with the drilling of new wells, or the deepening, the resetting of some of them, must lead to maximum values of the gas recovery factor. The discretization network is chosen based on the geometry of the spectrum of the current lines, the purpose of the study and the type of differential equations correlated with the initial conditions. In general, the rectangular lattice of constant or variable pitch is preferred. A rectangular network of constant pitch can be sized so that any block in the network does not contain more than one probe, or certain blocks include more probes, as desired, either to study the performance of the probes and the distribution of pressure, or to analyze the overall behavior of a deposit. The purpose of the rectangular variable step network is to reduce the step in the immediate vicinity of the well, which is achievable by changing variables, and aims to study the effects of pressure gradients in a certain area in the immediate vicinity of a well.Solving the equation with finite differences including for the two-dimensional space implies its notation in each inner node of the network, we arrive at a system of algebraic equations. of the form

III. Management Of Horizon Exploitation Through The Model Used

The calculation of the pressure values from all the blocks of a productive surface wanted to be analyzed by using two-dimensional numerical models is the engineering way in tracking the behavior of the productive formation. The result obtained by numerical modeling is improved with the help of observations related to the production behavior of the wells in association with the interpretation of the production data. These models give an overall picture with the distribution at a given moment of pressure throughout the production horizon.

If there are differences in the dynamic pressures of the wells on the same objective it means that there is a certain pore blockage. Thus it is advisable to carry out dynamic investigations in all the wells on the horizon to see the updated values regarding the defining parameters in the gas extraction process.

The reconfiguration of the geological models in the three-dimensional space, and then the simulation of the gas movement in the permeable porous environment is summarized in the following stages:

- Construction of the database that includes the parameters of each well on the deposit;
- Seismic interpretation;
- Geological modeling and facies modeling with the purpose of the 3D geological model, the stage in which the structural maps are also prepared.

Petr Petrophysical modeling, where the petrophysical parameters of the core are zonal values, which make up the starting points in the attribution of the average values throughout the hydrodynamic unit. In the petrophysical modeling, the results of the PNN investigations carried out in the wells are taken into account.

- Evaluation of current resources and reserves;
- Modeling and numerical simulation, where the specific is given by the simulation of the production history and the comparison of data with those existing on the site.:

REHABILITATION OF THE PRODUCTIVE INFRASTRUCTURE OF THE SECTIONS

Here we can talk about the rehabilitation of the natural gas production infrastructure, as well as the modernizations necessary to increase the recovery factor, to fulfill the production plan, but also for the need to deliver gas under quality conditions imposed by ANRE, mentioning the following aspects that must be met. :

- Separation of probes

Most of the probes were produced on the same pipeline, and the correct tracking of the parameters was not possible, which is why they went to their separation, and currently we have 17 separations to complete. The probes being separated can be measured with a flow calculator, and the calibration of the impurities is done correctly.

- Unscrewing, and cleaning the impurities separators

Most of the separators were clogged and we went through their digging, cutting and cleaning, and mounting them again.

- Establishing the direction of gas consumption

We have gas structures that can be directed to several directions of consumption, according to requirements.

- Real-time data automation and transmission

This year we have finished installing multivariable sensors on each probe and flow calculators on each group of probes, plus data transmission panel, so that the behavior of the probes can be monitored in real time from the computer of the technological engineer.

Annual maintenance of surface infrastructure, which includes gas pipelines, natural gas drying stations, natural gas compression stations, transmission, centralization and tracking parameters of dynamic wells, objectives to be pursued, inspected , corrects by the employees of the Company, or by third parties in collaboration with the services provided within the Gases Production Units, in order to maintain the production capacities in a continuous flow.

There is a lot to talk about here, but we will deal in particular with the probe-inflow area system, which is the connection area between the infrastructure mentioned above and the gas deposit itself. The inflow area of the probe layer corresponds to the perforated range.

Besides the fact that the well is a mining construction, it represents the production / injection system of the hydrocarbons, but also the source of confirmations / infirmations of the geological and physical models built, so that the rehabilitation of the productive installations is dependent on the positive results obtained in the process of stimulating the inflow. of gas.

Following the technical inspections of all the wells, and of the productive infrastructure of a gas structure, we will select the wells that require reactivation or simple intervention operations on them, the operations being executed both in the well and in the area of well-stratum influx. The rehabilitation of the natural gas wells requires the imposition of complex operations in the productive area as well as in the well, where the rehabilitation of the system of influence of the stratum-probe depends on the safety in operation of the well, for which specific investigations are carried out.

The construction of the natural gas wells represents practically a well dug up to several thousand meters tubed with steel bins, where on the outside there is cement paste for consolidation and selective exploitation of the objectives. The tubular material is chosen so that it can withstand the entire life of a probe, all the forces acting on it. The probe is then equipped and put into operation.

Of the range of tubular material with which a well is equipped, the tubing and the operating column, due to agents such as: oxygen, sands, hydrogen sulfide, carbon dioxide, are the most exposed to

corrosion. Agents are found in fluids circulating or stationary in the tubular material during operations and RK operations, or come from the layers communicated with the operating column.

The tubular material is subjected to the action of pressure and temperature, and on the tubing lining it acts the dynamic efforts of bending, torque and traction, being able to generate changes in the diameters of the column and of the tubing, cracks, or even breaks.

The degradation of the columns and the tubing of the probes is based on mechanisms of destruction that can be eliminated by applying the methods:

- Elimination of the causes of aeration of circulating fluids;
- Use of corrosion inhibitor;
- Increased ph value;
- Use of oxygen and hydrogen sulphide consumers;

Most natural gas wells are equipped with D = 27/8 inch tubing and D = 51/2 inch operating columns. Checking the integrity of the extraction pipe lining is done by deep or surface blasting, and by surface diagnostics, pressure tests and metallographic expertise. Column patterning is a coarse method for determining the inside diameter, so an effective method is to insert multifinger devices into the well using a geophysical cable [3]. [5].

Fig. 1 Types of multifinger devices

The accuracy of the column investigation is high the higher the number of sensors. The sensors of the device are arranged truncated, and the vertical movement of the sensors generates an electrical signal [4].[5].

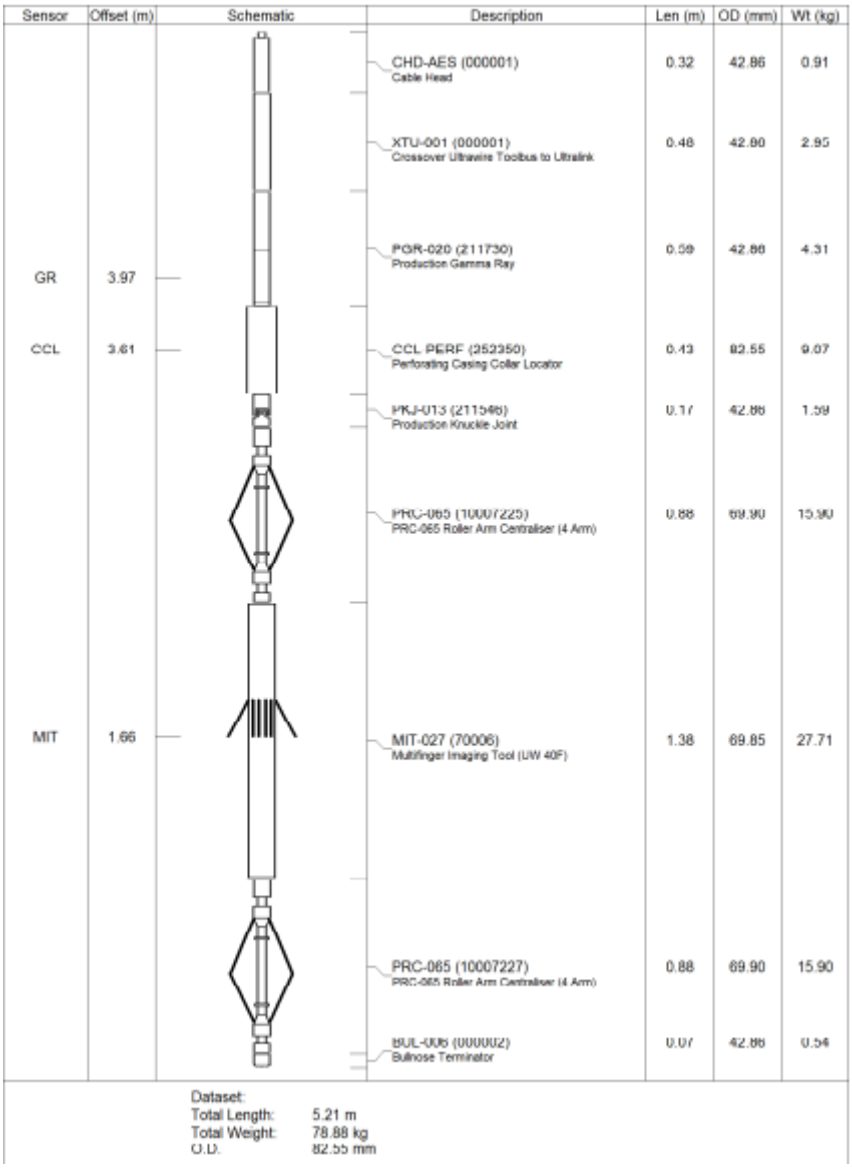

Fig. 2Sketch multifinger device

Inspection of the tubular material of the columns of the probes using the multifinger equipment identifies problems as:

- Increasing the inner diameter of the columns, thus decreasing the wall thickness, due to the action of erosion and corrosion;
- Exact determination of the areas with deposits inside the pipe;
- Location of equipments with nipples, packers, circulation valves;
- Detection of cracks;
- Pipe deflections

After analyzing the data from the probe "Z" with the characteristics mentioned below, the results were obtained:

Data of the analyzed probe:
WHAT THE. 2.9 / 16 " x 210 atm. snubbing.
Col. 5.½ " x 1595m.

- Mass flange distance = 3.20m.
- OGL; 881m. (879m deposit)

- Perf; 856-836 = 16m. selective.
- The barges with the highest penetration:
- Penetration of 100.00% (6.00mm) in drill 86 at depth 839.0m
- Penetration of 100.00% (6.00mm) in bead 87 at depth 853.9m
- Penetration of 100.00% (6.00mm) in drill 88 at depth 856.3m
- Penetration of 90.42% (5.43mm) in drill 85 at 836.4m depth

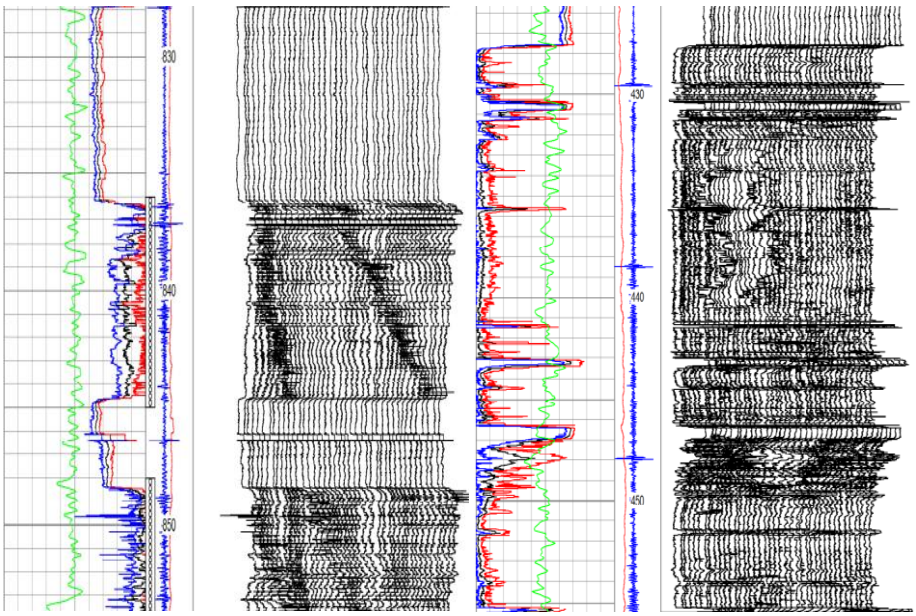

Fig. 3Diagrams resulting from the investigation with the multifinger device

- The casing with the highest penetration:
- Penetration of 100.00% (6.00mm) in drill 86 at depth 839.0m
- Penetration of 100.00% (6.00mm) in bead 87 at depth 853.9m
- Penetration of 100.00% (6.00mm) in drill 88 at depth 856.3m
- Penetration of 90.42% (5.43mm) in drill 85 at 836.4m depth. The range 427.6m-480.7m presents deposits / cement ring (in the work program it is mentioned that in 2008, cementation under pressure was executed to repair a detected break at 435m). For this reason, a valid analysis could not be performed on this range because the inside diameter on this area is 114-115mm. It is recommended that this area be cleaned to repeat the multifinger operation and determine the condition of the 5 ½ column of the probe.
- In case of detection of certain special situations such as loss of material in certain areas, cracks or cracks, the isolation of the sensitive area is applied with the help of a packer, by piping the respective column, allowing the work to continue. For technical-economic reasons, a certain portion of the initial trajectory of the well must be given up and a new, directed trajectory must be drawn from a set depth.

With the help of cementing acoustics, by introducing equipment into the well, Radial Bond Log, we can analyze the situation of the cementation of the column [2].

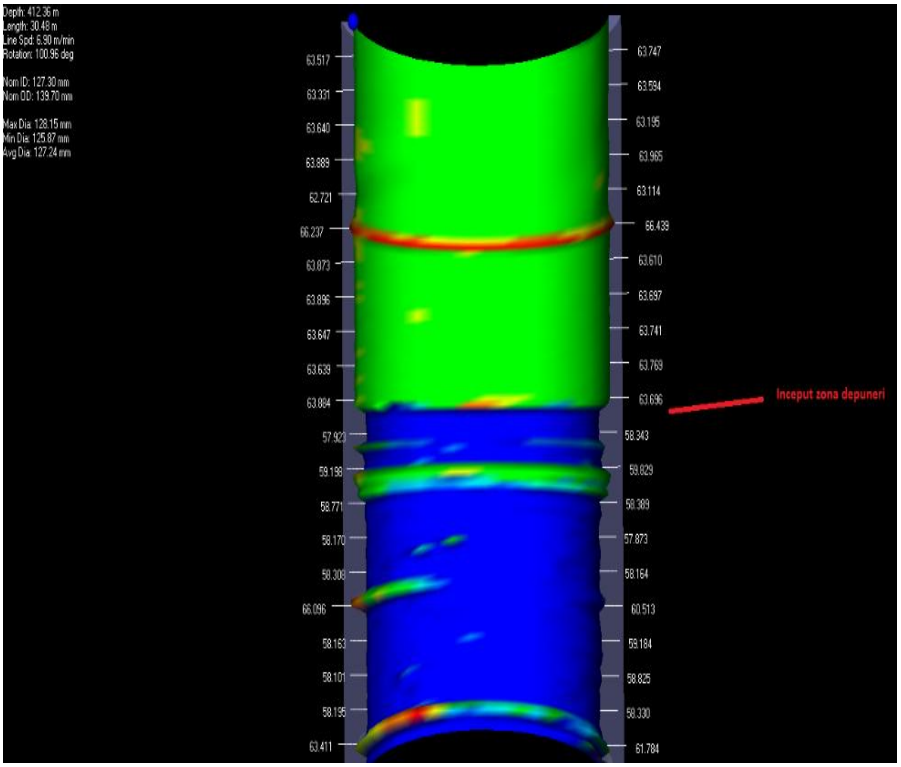

Fig. 4 Highlighting a deposit

IV. MANAGEMENT NVESTIGATION OF PRODUCTIVE GAS WELLS

a) By the production core method.

Natural gas wells have porous-permeable layer perforations on portions from several meters to hundreds of meters. Initial gas production was obtained by opening the layers with similar hydrodynamic parameters, and when the energy of the open layers decreased, they were added to other layers, so that a probe had opened and communicated several layers, which produced different natural gases as well. water, thus transferring gaseous mass from one layer to another. Due to the errors of measurement of the length of the geophysical cable with the help of the signal required for detonation, the massive perforations communicate non-productive areas of natural gas and aquifers, so errors of measurement of several meters at great depths lead to the complete failure of the area where there is natural gas corners.

Reaching the very high recovery factors, in some cases over 90%, the exploitation of all the porous-permeable layers of the deposit, the passing of the receptivity tests, can be the premises of the massive stocks of reservoir water, which is unusable, and must be reinjected into the wells with this deposit. destination.

- The new methods of investigation can detect all the layers potentially producing fluids, as well as the contribution of each one in the total flow of the well, both gas and water.
- Understanding the behavior of the deposits can be done by the production logging method, known as Production Logging Tool (PLT). The principle of this method consists in determining the apparent speed of movement of the fluid near the perforations, and then of the flowmeter, the flowmeter that detects the different local velocities of the fluids coming out of the layer, having in its composition a number of blades centered on an axis so that rotate due to the fluid ascension flow as well as the oscillation of the device's movements in the fluid mass. The

purpose of this investigation is to make available to the engineers involved in the reactivation documents necessary to understand the behavior of the respective deposit.

- The first purpose of the production core is given by determining the location of the sources of water and those of natural gas, where the solution of the inflow of the reservoir water can be solved by cementing under pressure the perforated area, and then the reinforcement of the porous-permeable layer.
- Methods of hydrodynamic investigation of natural gas wells:

From the necessary steps to be carried out for the rehabilitation of a deposit, we deduce the dependence on the need to reevaluate the hydrodynamic parameters of the wells. The importance is given by determining the maximum flows that a well can have and the factors that limit these flows, by the coefficients of resistance to the gas filtration to the productive area and the determination of the potential flows of the wells. These hydrodynamic research methods are divided into two categories according to the hydrocarbon motion regime in the porous-permeable environment, thus distinguishing investigations of the formations in the stationary and non-stationary motion regime.

Closing probes investigation:

With the help of the method it is desired to reassess the physical and hydrodynamic parameters of the production layer, namely: effective permeability, flow capacity, productivity indices, phase mobility, static pressure. The permeability of the area adjacent to the zone, the flow capacity of the fluids in that area, are dependent on the size of the skin factor, which is very important in evaluating the wells performance. Specific to this type of research is the fact that the probe is in production for a high period of time so that in the area of inflow layer-well the pressure is evenly distributed, and then the probe is closed to recover the static pressure.
After interpreting the parameters from the surface of the wells (static pressure at tubing and column, dynamic pressure at tubing and column, before and after the depressogenic organ (nozzle, nozzle), flow, impurities), a procedure is established for further investigations of the well, of the area influx and surface infrastructure.In order to determine the value of the average static pressure of the horizons of the gas structure, the static pressure measurements are carried out at the eruption head of the wells, using the formula [3]:

$$P_{zmed}{}^{(t)} = \frac{\sum_{i=1}^{n} P\text{adz}\, hz}{\sum_{i=1}^{n} hz} \qquad (2)$$

Where,
Padi - is the value of the static depth pressure of the probe z
hz - the effective stratigraphy of the layer

The above relationship is applicable also for the gas horizons put in communication, but the accuracy of the result is given by the interpretation of the bottom measurement in the wells in which there is communication between the horizons.
The gas storage coefficient is given by the ratio between the variation of the volume of gas in the well and the variation of pressure in the well of the well [3]:

$$c = \frac{\Delta Vs}{\Delta p} = \frac{Q \cdot bg \cdot \Delta t}{\Delta p} \qquad (3)$$

bg - the volume factor of the gases

The time of storage of fluids in the well can be determined from the relation:

$$t_{ad} = \frac{k \cdot t_c}{m \cdot \mu \cdot \beta_T \cdot r_s^2} \qquad (4)$$

β_T - is the total compressibility coefficient of the fluid

The decrease of the skin factor will generate significant increases of the recovery factor, a skin factor that can be calculated under the conditions of non-stationary gas filtration, taking as a basis the pressure value at one hour after the closure of the well, as follows [2]:

$$S = 1.151\left(\frac{P^2_{\Delta t=1h} - P^2_{\Delta t=0}}{i} - log\frac{k}{m\cdot\mu\cdot\beta_T\cdot r_s^2} - 0.351\right) \quad (5)$$

The skin factor is composed of a multitude of factors, taking into account all the aspects related to the porous-permeable layer in the area of layer-probe influx [2].

$$S = S_b + S_p + S_{\overline{h}} + S_S + S_\partial \quad (6)$$

Probe factors are:

S_b - due to the blockage;

S_p - due to imperfection after opening mode;

S_h - due to imperfection after the degree of openness;

S_S - due to the exploitation at high differential pressures defending the non-linear motion around the well;

S_∂ - due to the oblique trajectory of the gas well;

The investigation of the probes at the opening consists of producing a probe for a certain period of time at a constant flow rate and with the recording of the variation of the depth pressure, thus obtaining the stabilization curve of the bottom dynamic pressure.

The isochronous investigation of the probes is a complex method that consists in alternating the closing and opening of the probe at equal times, with the recording of static and dynamic parameters.This method being very flexible does not destabilize the gas production over a certain investigated horizon, the closing and opening times being of the order of several hours.

CONCLUSIONS

Natural gas production is a complex activity, which has been proven over the course of more than 100 years of exploitation of the deposits that contain these hydrocarbons, as well as the dependence on certain factors and conditions.
Romania has the largest market for natural gas in Central Europe and was the first country to use natural gas for industrial purposes. The natural gas market reached record size in the early 1980s, following the implementation of government policies aimed at eliminating the dependency on imports. The application of these policies has led to an intensive exploitation of internal resources, resulting in the decline of domestic production.

Acknowledgment

I wish to bring my thanks to my teachers from the University Of Lucian Blaga Din Sibiu, the university professor dr. ing. Avram Lazar we work from the University Of Petrol Gas From Ploiesti, and from the company ROMGAZ S.A.

REFERENCES

[1] Giura, Lucian, Contributii la istoria gazului metan din România, Ed. Univ. Lucian Blaga, Sibiu 1998

[2] Avram, Lazar, Maloș, Mihail, Combaterea dificultăților și accidentelor tehnice de foraj, Ed. Univ. Petrol Gaze din Ploiești 2013

[3] Ştefănescu, Dan Paul,Practica extracţiei gazelor naturale. Vol I, Vol II. Ed. Univ. Lucian Blaga, Sibiu

[4] Ştefănescu, D. P. – Introducere în Reabilitarea Zăcămintelor Mature de Gaze Naturale – Teorie şi Studii de Caz, Editura Universităţii "L. Blaga", Sibiu, 2011

[5] Ştefănescu, D. P. – Introducere în Reabilitarea Zăcămintelor Mature de Gaze Naturale – Teorie şi Studii de Caz, Editura Universităţii "L. Blaga", Sibiu, 2012

International Journal of Innovation Engineering and Science Research
(ISSN: 2581-4591)

www.ijiesr.com

Power of Canola Biodiesel Blends in A Tractor Diesel Engine

Oguzhan EROL

University of Tekirdag Namik Kemal, Çorlu Vocational School Automotive Technology Program, 59030-Çorlu-Tekirdag, Turkey.

Yilmaz BAYHAN

University of Tekirdag Namik Kemal, Department of Biosystems Engineering, Faculty of Agricultural, 59030-Tekirdag, Turkey

ABSTRACT

The objective of this aimed to determine the effects of diesel fuel and canola biodiesel on engine power. For this purpose, power of engine was determined for the fuels prepared by mixing certain ratios of canola biodiesel with the petroleum based diesel fuel. In this research, the fuels obtained by mixing %5 (B5), %10 (B10), %20 (B20), %50 (B50), %80 (B80) of canola biodiesel with diesel fuel (B0), canola biodiesel (B100) and diesel fuel had been used. These fuels were tested in a direct injection, air–cooled diesel engine with four cylinders. The tests conducted on the engine were carried out according to TSE 1231 standard. The change values of power obtained in this study were found significantly different according to the statistical analysis performed. Whereas the maximum power value was obtained for B0 fuel as 66 kW at 3500 cycle/min while the minimum power value was 61,4 kW for B100 fuel. The engine power values of B0 fuel mixed with canola biodiesel at ratios of 5%, 10%, 20%, 50%, 80% and 100% canola biodiesel at different engine speeds are determined. As the ratio of biodiesel mixed with B0 fuel increases, there happens decrease at engine power. When usage of biodiesel – diesel mixture at different ratios being from B5 to B100, there showed decreasing in effective power changes as comparing with B0 fuel usage at all engine speeds. At high engine speeds, there observed that the effective power values of B5 fuel decrease a little bit as comparing with B0 fuel. In this study not questioning how the effects will be as lifetime of fuel pump goes up, there happens a decrease at power values of B10, B20, B50, B80 and B100 fuels as depending on the decrease of burning affectivity by the viscosity.

Keywords— *Biodizel, Canola oil, Power, Torque*

I. INTRODUCTION

Gradual depletion of energy reserves, the rise of petroleum prices and environmental concerns have accelerated the need to find suitable and sustainable renewable fuels. Biodiesel, being eco-friendly, renewable and non-toxic in nature, has much potential to be used as an alternative to petroleum diesel [1].

Due to environmental concerns and the rising cost of fossil fuels such as diesel, the search for alternative fuels like biodiesel has attracted more attention. Renewable fuels such as biodiesel continue to be of interest to achieve a sustainable energy economy, thus reducing dependence on fossil fuel utilization [2]. It was further stated that the use of renewable transportation fuels is increasing, and a national standard of 5% in the United States has been proposed in the energy-related legislation [3,2]. The fuel and energy crises of late 1970s and early 1980s as well as accompanying concerns about the depletion of the world's non-renewable resources provided incentives to seek alternatives to conventional, petroleum-based fuels. Biodiesel fuel is an environmentally clean and renewable energy source. It is usually produced from animal fats or vegetable oils by the transesterification reaction. The oxygen content, which is about 11–15 wt.%, helps biodiesel enhance the combustion process and reduce pollutant emissions from the diesel

engine [4]. Biodiesel as an alternative fuel in diesel engines has a great potential of reducing noxious emissions such as CO, CO2, HC, PM, Sox and PAH [5,2]. The major threat facing the use of biodiesel fuel is characterization of spray and combustion processes of this fuel injected by diesel engines in common rail systems [3,2].

In this study, it was aimed to determine the effects of diesel fuel and canola biodiesel on engine performance and torque rise. For this purpose, engine performance and torque rise tests were conducted for the fuels prepared by mixing certain ratios of canola biodiesel with petroleum-based diesel fuel.

II. EXPERIMENTAL SETUP

The experiments were conducted at Namık Kemal University Çorlu Vocational School Automotive Technology Program Engine Test Laboratory. In the experiments, a four-cylinder, four-stroke, air-cooled Fiat 8040.02 diesel engine was used as the test engine. This engine is used in the Fiat 640 Model tractor. The general specifications of the diesel engine are given in Table-1. There is a CAV-made injection pump and an injector coupled with the engine. Filters were made by the Lucas company. The CAV injector pump: the CAV transfer pump is the positive type. It has two vanes sliding inside an eccentric liner in the hydraulic head. The transfer pump rotor is carried at the end of the distributor rotor. The capacity of the transfer pump is considerably in excess of injection pump requirements. Injection pump was previously tested with diesel before starting the experimental process.

TABLE I. THE GENERAL SPECIFICATIONS OF THE DIESEL ENGINE

Engine	FIAT
Model	50 NC
Type	Water-cooled, four stroke
Compression	Direct injection (DI) and naturally aspirated
Number of cylinders	4
Bore and stroke	104×115 mm
Displacement	3908
Compression ratio	17:01
Nominal rated power	90 HB
Maximum torque speed	1700 rpm
Combustion chamber	Swirl chamber

The production of biodiesel from canola oil was carried out using the transesterification method. The properties of the refined canola biodiesel were defined according to the DIN EN 14214 standards. The relevant properties of the test fuel used in the study are given in Table-2.

TABLE II. SPECIFICATIONS OF THE REFINED CANOLA OIL

		Specification	DIN EN 14214
Fuels	Result	Min	Max
Density at 15 ºC(kg/m3)	888	860	900
Specific combustion enthalpy (MJ/kg)	39,8		
Cetane number	51,3	51	---

Iodine number	129,7	---	130
Kinetic viscosity (40 ºC mm2/s)	4,4	3,5	5,0
Sulfur content (mg/kg)	≤ 1 ppm	---	10
Percentage of humidity (%)	0,13		
Acid value (mg KOH/g)	0,336	---	0,5
Diglyceride content % (m/m)	≤ 0,2	---	0,2
Triglyceride content % (m/m)	≤ 0,2		0,5
Monoglyceride content % (m/m)	≤ 0,8pm	---	0,8
Total Glycerol % (m/m)	≤ 0,25	---	0,25

An external tank was prepared by cancelling the fuel tank of the four-cylinder diesel engine. A line was installed through the external tank to the diesel (B0) fuel supply tank. A line steered from the fuel supply pump extended to the fuel meter mechanism. The diesel (B0) fuel running through the metering mechanism was conveyed to the fuel injection pump by means of a line. Another line steered from the fuel return system was again steered to the fuel meter. The data about the metered fuel were gathered in the electronic power meter unit, whereupon the gathered data were transferred to a computer (Figure-1). The engine connected to the dynamometer by the shaft gear was fired up at the maximum speed. The power, torque and fuel consumption values at different speeds could be recorded by means of a hand-controlled unit. Before starting the experiment for each fuel mixture, the engine was started with the fuel to be experimented on in order not to leave any residue from the other fuel type.

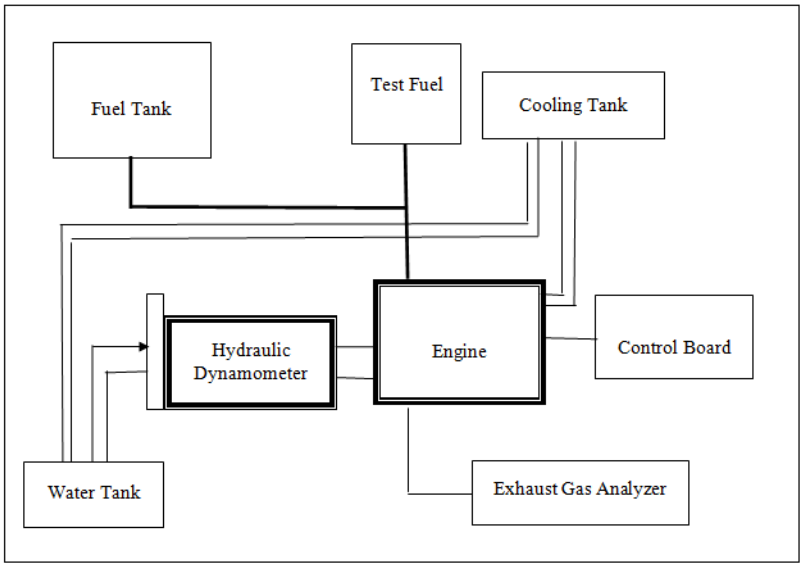

Fig. 1. View of the experimental setup

Effective power is the power obtained from the flywheel which is the exit point of the power taken from the engine. This power is the real engine power that takes into account factors that are ignored in terms of internal power such as friction losses, and power spent on supporting pieces in lubrication, ignition and valves [6] . Equation (1) was utilized in determining the effective power of the engine.

$$Pe = \frac{Mdxn}{9550} \qquad (1)$$

Here;

Pe : Effective power (kW),

Md : Torque of the engine (Nm),

n : Engine speed (rpm).

In the experiments, the engine was initially run at the idling speed to return to normal operating temperatures. The engine oil and intake air temperatures were maintained at about 85 ± 2 °C and 25 ± 1°C throughout all testing conditions, respectively. The engine tests were operated at speeds of 1100, 1400, 1700, 2300, 2600, 2900, 3200, 3500 and 3800 rpm. At these speeds, the engine was operated at full throttle, and the following loads were applied to obtain the power values of the engine (Table-3).

TABLE III. THE LOAD VALUES OBTAINED FROM DIESEL (B0) OIL AND BIODIESEL – DIESEL MIX FUELS AS TO ENGINE SPEED

Engine Speed (rpm)		1100	1400	1700	2000	2300	2600	2900	3200	3500	3800
Load Values (N)	B0	332,07	339,37	346,09	333,42	315,64	303,28	289,90	272,00	252,81	192,40
	B5	325,03	335,34	337,81	326,09	310,96	298,98	286,59	269,66	248,83	189,83
	B10	318,25	331,90	328,45	319,23	307,72	298,85	281,42	266,42	246,09	187,43
	B20	307,05	321,37	320,42	311,75	300,94	290,88	278,00	260,17	242,65	185,59
	B50	301,40	310,54	313,02	304,82	292,65	286,26	274,41	257,04	240,80	182,22
	B80	293,59	301,86	305,00	298,16	288,09	280,57	268,77	252,65	236,51	176,05
	B100	289,43	295,13	297,89	296,22	282,96	275,75	264,16	248,63	233,97	174,94

III. RESULT AND DISCUSSION

A-Change of Power

The results of the multiple comparisons test (Duncan) of effective power changes which were obtained from the B0 fuel, B100 fuel and biodiesel fuel mixed with B0 at different ratios by using different speeds during the engine test experiments are given in Table-4.

TABLE IV. EFFECTIVE POWER VALUES OF DIESEL (B0) FUEL AND BIODIESEL – DIESEL OIL MIXTURES A DEPENDING ON ENGINE SPEEDS

Engine Speed (rpm)			1100	1400	1700	2000	2300	2600	2900	3200	3500	3800
Ort + sh		Fvalue	25,5**	33,5**	40,9**	46,8**	51,7**	56,64**	60,3**	62,8**	63,7**	54,4**
Effective power (kW)	B0	Rep:3	$27,4^{a}$	$35,6^{a}$	$43,9^{a}$	$49,8^{a}$	$54,2^{a}$	$58,9^{a}$	$62,7^{a}$	$64,9^{a}$	$66,0^{a}$	$54,4^{a}$
	B5	Rep:3	$26,8^{b}$	$35,2^{b}$	$43,1^{b}$	$48,9^{b}$	$53,6^{b}$	$58,3^{b}$	$62,3^{b}$	$64,7^{a}$	$65,3^{b}$	$54,1^{b}$
	B10	Rep:3	$26,2^{c}$	$34,8^{c}$	$41,9^{c}$	$47,9^{c}$	$53,1^{c}$	$58,3^{b}$	$61,2^{c}$	$63,9^{b}$	$64,6^{c}$	$53,4^{bc}$
	B20	Rep:3	$25,3^{d}$	$33,7^{d}$	$40,8^{d}$	$46,8^{d}$	$51,9^{d}$	$56,7^{c}$	$60,4^{d}$	$62,4^{c}$	$63,7^{d}$	$52,9^{c}$
	B50	Rep:3	$24,9^{e}$	$32,6^{e}$	$39,9^{e}$	$45,7^{e}$	$50,5^{e}$	$55,8^{d}$	$59,7^{e}$	$61,7^{d}$	$63,2^{d}$	$51,9^{d}$
	B80	Rep:3	$24,2^{f}$	$31,7^{f}$	$38,9^{f}$	$44,7^{f}$	$49,7^{f}$	$54,7^{e}$	$58,4^{f}$	$60,6^{e}$	$62,1^{e}$	$50,2^{e}$
	B100	Rep:3	$23,9^{g}$	$31,0^{g}$	$38,0^{g}$	$44,4^{f}$	$48,8^{g}$	$53,8^{f}$	$57,4^{g}$	$59,7^{f}$	$61,0^{f}$	$49,8^{e}$

**The means were taken at P<0.01. Means having the same letters are not significantly different at the probability of 1%.

It was observed that the effective power value obtained from B0 fuel usage was higher than all the other effective power values obtained from the other biodiesel mixtures during the experiments conducted at all engine speeds. By analysis of variance, it was observed that there was a statistically significant difference based on speed in terms of power changes among the fuels (p<0.01). According

to Duncan's multiple comparison test conducted to determine the statistical differences among the groups, it was found that all groups were significantly different ($p<0.01$). The highest power values were obtained at 3500 rpm for all fuels that were used for the experiments. When the engine speed was at 3500 rpm, the effective power value of the B0 fuel was 66 kW. At the same speed, the effective power value of the B100 fuel was 61.4 kW. The maximum power of the B100 fuel was decreased by 6.97% as compared to the B0 fuel. At the same engine speed, the effective power value of the B5 fuel showed a 1% decrease in comparison to the B0 fuel. At 1700 rpm, the effective power value of the B0 fuel was 43.9kW. At the same engine speed, the effective power value obtained from the B100 fuel was 38 kW. The B100 fuel showed a 12.45% decrease in comparison to the B0 fuel. At the same engine speed, the effective power value of the B5 fuel realized a 1.9% decrease in comparison to the B0 fuel. As seen in Table-4, the effective power change showed an increase until 3500 rpm, but at higher speeds, it decreased. The effective power change during the engine performance experiments conducted at full throttle and loading is seen in Figure-2.

In all experiments, the effective power values obtained by usage of the B0 fuel were found to be higher than the power values of the biodiesel mixture fuels. The maximum engine power value of the B0 fuel was achieved at 3500 rpm. At the same engine speed, the maximum effective power values of the B5, B10, B20, B50, B80 and B100 fuels showed decreases at ratios of respectively 1.06%, 2.12%, 3.48%, 4.24%, 5.90% and 7.12%. As the ratio of biodiesel which was obtained from Canola oil and mixed up with the B0 fuel increased, there was a decrease in the ratio of power. The reason for this decrease was that the thermal value of biodiesel fuel is less than the thermal value of the B0 fuel. The other reason for this engine power decrease was that the density and viscosity of canola biodiesel are higher than the B0 fuel. High viscosity and density cause the fuel not to be atomized in the injector on the desired level. This situation extends time of ignition, which effects combustion and contributes to poorer combustion outcomes. As in these results, a previous study [7] found that the engine power showed a 6.27% decrease by using biodiesel as compared to the B0 fuel at 3000 rpm, and the reason for decreasing of engine power depended on some specifications as viscosity, density and thermal values. In their study, some authors [8] declared that there happened a 4.2% and 5.7% decrease as using fish oil and methyl ester mixed fuels, in comparison to B0. Another study [9] reported that the differences between the power values of petroleum-derived B0 fuel and power values obtained from canola biodiesel mixed fuels were on acceptable levels, and these differences were caused by the thermal value, density and high viscosity of canola biodiesel fuel. Additionally, Eliçin, [9] also stated that the power values obtained from canola biodiesel and biodiesel – diesel mixed fuels were found to be lower because the thermal value of canola biodiesel fuel is lower than the thermal value of the B0 fuel.

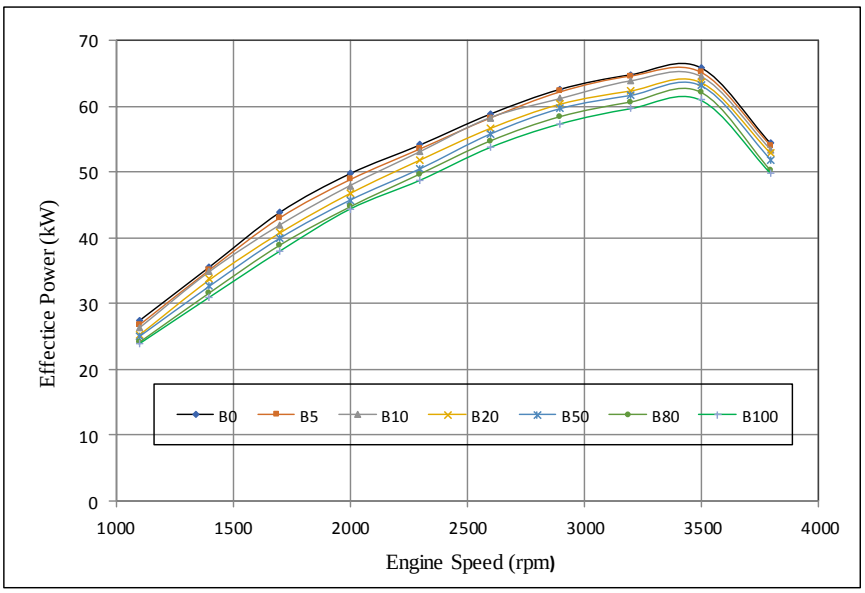

Fig. 2. The effective power changes of diesel (B0) fuel and biodiesel – diesel fuel mixture fuels according to engine speed

IV. CONCLUSION AND COMMENTS

In this study, possibilities of canola biodiesel being used as an alternative fuel in diesel engines without any modification were investigated. The engine power values of the B0 fuel mixed with canola biodiesel at ratios of 5%, 10%, 20%, 50%, 80% and 100% canola biodiesel at different engine speeds were determined. Here under:

- As the ratio of biodiesel mixed with B0 fuel increases, there happens decrease at engine power. While using biodiesel – diesel mixtures at different ratios from B5 to B100, there is a decrease in effective power changes as comparing to the B0 fuel at all engine speeds. At high engine speeds, the effective power values of the B5 fuel decrease a little bit in comparison to the B0 fuel. In this study not questioning how the effects will be as the lifetime of fuel pump goes up, there is a decrease in the power values of the B10, B20, B50, B80 and B100 fuels depending on the decrease in combustion efficiency caused by the viscosity.

As to the data obtained from that study, the following recommendations may be made:

- B5 fuel may be used without any need for modification or with a little bit of change in engines.
- In terms of engine performance and emission values, it may be used as an alternative fuel because the obtained values are close to the values of the B0 fuel.
- Biodiesel usage will contribute to sustainable future and community health because of its more unpolluted combustion products.
- B5 fuel may be used as an alternative fuel because of the reasons as having no risk for the environment and living being and providing opportunity of usage of waste products.
- B5 fuel may be used as an alternative fuel to B0 fuel which is indispensable especially in the transportation sector.

REFERENCES

[1] M.A. Fazal, S. Rubaieeb and A. Al-Zahrani, "Overview of the interactions between automotive materials and biodiesel obtained from different feedstocks" Fuel Processing Technology, vol. 196, pp.1069178, December 2019.

[2] O.A., Kuti, J. Zhu, K. Nishida, X. Wang and Z. Huang "Characterization of spray and combustion processes of biodiesel fuel injectedby diesel engine common rail system" Fuel, vol.104. pp.838-846, February 2013.

[3] J.P Szybist, A.L. Boehman, J.D. Taylor and R.L. McCormick "Evaluation of formulationstrategies to eliminate biodiesel NOxeffect" Fuel Process Technology, vol. 86, pp.109–1126, June 2005.

[4] H.K. Suh, H.G. Roh and C.S. Lee" Spray and combustion characteristics of biodiesel/diesel blended fuel in a direct injection common-rail diesel engine". The American Society of Mechanical Engineers, Journal of Engineering for Gas Turbines and Power, vol.130, pp. 2807–2815, May 2008

[5] T. Fang, Y.C. Lin, T.M Foong and C.F. Lee, " Biodiesel combustion in an optical HSDIdiesel engine under low load premixed combustion conditions" Fuel, vol.88, pp. 2154–2162, November 2009.

[6] B. Alpgiray, "Determination of the Effect of Rapeseed Oil Diesel Engine Performance and Emissions Characteristics" Master's thesis, Ankara University, Graduate School of Natural and Applied Sciences, May 2006.

[7] E. Çengelci, H. Bayrakçeken and F. Aksoy, "Bir Dizel Motorunda Hayvansal Yağ Metil Esterinin Kullanımının Motor Performansı ve Emisyonlarına Etkisi" 6th International Advanced Technologies Symposium (IATS'11), pp. 113-116, Elazıg-Turkey, 16-18 May 2011.

[8] R. Behçet and A.V. Çakmak, "Bir Dizel Motorda Yakıt Olarak Kullanılan Balık Yağı Metil Esteri Karışımlarının Motor Performans ve Emisyonlarına Etkisi" 6th International Advanced Technologies Symposium (IATS'11), pp. 161-165, Elazıg-Turkey, 16-18 May 2011.

[9] A.K. Eliçin, "Experimental investigation of the effect of air intake pressure on the performance and emission characteristics in a small diesel engine using biodiesel" PhD. Thesiss, Ankara University, Graduate School of Natural and Applied Sciences, Department of Agricultural Machinary, June, 2011.

International Journal of Innovation Engineering and Science Research
(ISSN: 2581-4591)
www.ijiesr.com

Forensic Analysis of Amazon Alexa and Google Assistant Built-In Smart Speakers

Ilkan Yildirim, ErkanBostanci, Mehmet SerdarGuzel
Department of Forensic Informatics, Institute of Forensic Sciences
Ankara University, Ankara, Turkey

ABSTRACT

People's communication with machines is evolving. The process that started with the buttons has evolved to the touchscreen and now people can command to machines just talking with them. The use of smart home assistants, which allows people to control their smart homes, access mail accounts and even order, is becoming increasingly popular. For this reason, it is possible that they will be found at crime scenes soon and carry the value of digital evidence. In this study, the best-selling products Alexa Echo and Google Home were examined in terms of forensic evidence and the data containing digital evidence were found. Then fake activities were created by changing device name, creating fake routine creation and custom skill development. As a result of the investigations, for the cyber security experts or academics working in this field the information was provided about which kind of digital evidence could be found in smart home assistant's activities. Also, difference between real activity and fake activity were elicited against anti-forensic.

Keywords—*IoT Forensic, Alexa, Google Assistant, Anti-Forensic, Fake Activity*

I. INTRODUCTION

People have discovered new ways to communicate with machines throughout history. People had started to use punch cards, and QWERT keyboards, and today continue with touch screens and speech commands with smart assistants like Google Assistant, Amazon Alexa, Siri and Cortana.

Speakers with integrated smart assistants are capable of control IoT devices like lights, TV, door and multimedia systems at home. Number of smart speaker sales increasing exponentially. Almost all home will have this kind of device and, they will be found in crime scenes soon.

Many of latest technology electronic devices have system logs such as cameras, drones and cars. These are valuable assets for the forensic investigations. Not only technology makes people life easier, but also criminals use it for anti-forensic activities[1]. For this reason, cyber security experts should take an action first to protect innocent people.

This study has two parts. In the first part Amazon Alexa with its smart speaker Echo Plus 2nd Generation and Google Assistant with its smart speaker Google Home Mini have been examined to find out whether there are digital evidences. In the second part, anti-forensic cases were created and compared with first part's digital evidences.

The rest of paper organized as follows: Section 2 includes review of background, Section 3 has related works, Section 4 has method, Section 5 includes evaluation, and last part Section 6 consist of conclusion and future work.

Smart speakers have integrated smart assistants that take input from users' speech, then convert it to text, apply NLP on this text, take an action and reply to user as an informative voice message. They can control IoT devices i.e. smart home, order something from anywhere and send money. People can do whatever they want with smart speakers like using their computers or mobile phones. The

difference between smart speakers and other computers, there is no GUI on smart speakers. They are using VUI as a user interface. Because of that, they are listening the environment all time until user uses the wake-up words to activate smart speakers.

To make user commands Alexa have skills and Google Assistant have actions. In this kind of devices more skills or actions means more capability. Skills and actions are almost same, both have development kits for the developers. At the end of 2018, Amazon announced that they have 70.000 skills, and they are increasing 192 per day worldwide [2]. Google Assistant actions reached 4.253 in January 2019; this number rose about 2.5 times last year compared [3].

At fig 1 number of unit sales of smart speakers are increasing exponentially. The study about global smart speaker unit sales shows that only the Q4 sales 8.5 times increased from 4.2 million to 38.5 million between 2016 and 2018 [4].According to research firm Arizton's report about smart speaker market, the size was $991 million in 2016 and will grow $4.8 billion in 2022 [5].

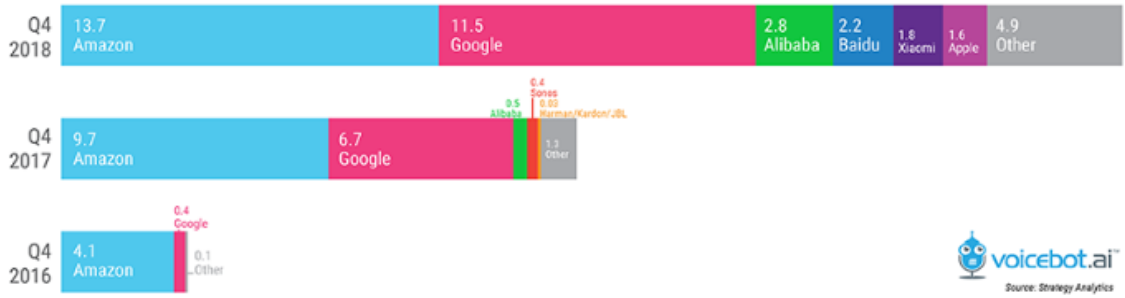

Fig.1. Number of Smart Speaker Unit Sales (Million)

There are studies about IoT forensics and smart speakers. Smart speakers are listening environment until hearing wake-up words. There is a study about smart speaker Alexa whether listening environment until wake-up words or recording everything to process data. They have used network forensic tools 21 days. The traffic was encrypted. They couldn't find any evidence about Alexa is listening all time [6]. Scope of another study consists of cloud-based asset analysis, voice command tests, application analysis and firmware analysis. The goal was emphasizing vulnerabilities of Alexa. As a result of that, they found that Alexa is recording environment sounds after hearing wake up words even if there are no meaning in this sentence[7].

Some of the studies are held on about forensic investigation processes for the smart home ecosystems. Researches were analyzed Echo Dot with Alexa, and they found evidences. First, they analyzed network traffic data to find API of Alexa. Then they send request to gather evidence. They found activity records, personal information etc. As a result, they created a tool theoretically for this purpose [8].

The study about Alexa vulnerability called "Skill squatting attacks" that focuses on accent of command. They used 11.460 American English words experimentally to see percentage of Alexa's misunderstanding. After realizing there is a systematic misunderstanding on Alexa, they attacked by using these words. They called this attack type called as "skill squatting attacks"[9]. Another vulnerability case study attack applied theoretically on Amazon Alexa and Google Home by ordering something fake and unlocking the door remotely.

The researchers mention about many of the forensic studies about smart speakers were holding on theoretically. They showed that there are some studies about smart speaker Amazon Echo and IoT

forensics Z-wave protocol practically and emphasized that researchers should give importance to this issue[10].

II. METHOD

In this study, experimental environment was arranged in order to produce data. LM-G710EM model number LG ThinQ Q7 mobile phone with Android 8.0.0 is used. For the smart home environment Google Home Mini H0A and Amazon Alexa Echo Plus 2nd Generation L9D29R used as smart speakers with their android mobile applications. 2.11.1.8 version of Google Home application and Amazon Alexa version 2.2.271281.0 version was installed. Amazon Alexa application does not work in Turkey. Therefore, the Google Play account settings have been changed to the United States. The SENGLED bulb R11-G13 was connected to Echo and GE C-Life Smart Bulb A19 was connected to Google Home Mini by using wireless.

Fig.2. Google Home Mini ve Amazon Echo Plus 2nd Generation

Alexa Skill was created by using Alexa Skills Kit in Amazon Web Services Lambda functions. In order to create fake activity, an intent code was written by using node.js. In this skill user commands for sum of two numbers, Alexa response as multiply of these two numbers. Same skill was built as a Google Action by using Google Dialog flow Fulfillment inline editor. In figure 3 shows that interaction between Alexa Skills Kit and Alexa Voice Services. Alexa allows developers to use both.

Fig.3. Alexa Web Services[11]

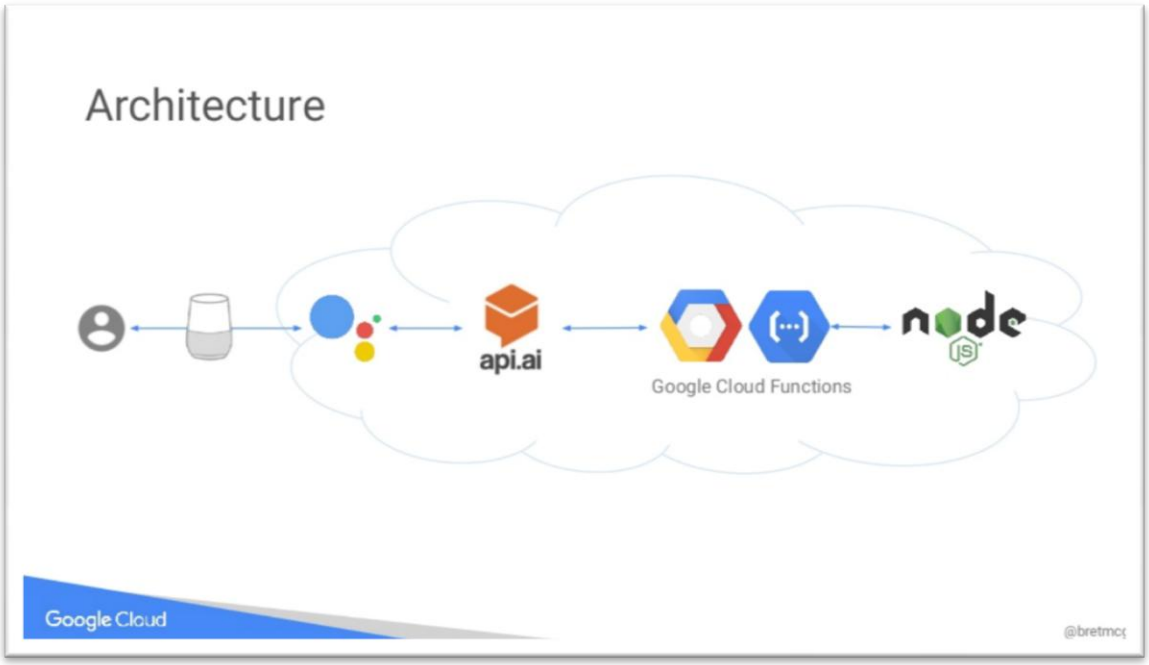

Fig.4. Google Assistant Architecture [12]

In figure 4 there is google cloud architecture, google device listens user that sends the audio to google assistant. Google Assistant uses the api.ai and Google Cloud Functions with nodejs.

TableI. CASE DETAILS

Cases	***Command***	***Command Type***	***First State***	***Expected Action***	***Expected Action***
1	Turn on light	Daily	Lights Off	Lights On	Lights On
2	Turn on horse	Edited Device Name	Lights Off	Lights On	Lights On
3	Turn on TV	Custom Routine	Lights Off	Lights On	Lights On
4	"Fake activity", "Add 5 and 6"	Skill/Action	-	Add	Multiply

In first case, as a regular user, "turn on light" command sent to both smart speakers. This is daily common usage of smart home devices. For this reason, this case was used as a reference point to compare other cases. The other cases are for the Anti-Forensic to mislead forensic investigator.

For the second case, name of device changed from "light" to "horse", then "turn on horse" command send to both smart speakers.

In third case, the routine was created. The invocation of the routine sentence was chosen as "Turn on TV", then routine action was set as turning on the light, and routine response set as "Ok." same as daily activity. After that "Turn on TV" command sent to both devices.

The last case was about creating custom skills by using developer kits of both devices. For the summation intent of two numbers, multiplication response was created. Firstly, invocation word, then "Add 5 and 4" commands sent to both devices.

Google Home application and Amazon Alexa application have activity histories. For the four cases, these activity histories were found in user privacy settings menu, after clicking this, applications redirect to the web pages.

III. EVALUATION

As a result of the first "turn on lights" daily case, the digital evidences were found in Alexa and Google Assistant's activity histories. Every user can see these histories on the mobile applications or the web interface of Amazon Alexa or Google Assistant's activity history. For the more advanced users, they can get these information by using the APIs. Table II shows the Google Assistant's activity details.

TABLE II. GOOGLE ASSISTANT ACTIVITY DETAILS

Google Assistant History	**"Turn on Lights" Command**
User Command's Text	Said turn on lights
User Command's Voice Recording	Play Button to Listen Recording
Time stamp	Today at 1:18 PM
Assistant's Response	Ok, turning the Light on.
Device Type	Smart Speaker
Device's Approximate Location	Google Map Image
Started By	Hotword
Action Type	com.google.homeautomation

Table III shows the Alexa's activity details.

TABLE III. AMAZON ALEXA ACTIVITY DETAILS

Alexa History	**"Turn on Lights" Command**
User Command's Text	"turn on light"
User Command's Voice Recording	Play Button to Listen Recording
Time stamp	Today at 02:07 PM
Assistant's Response	"ok"
Device Name	<user>'s Echo Plus

Both activity history has user command text, its voice recording, time stamps, and assistant's response. While Google is storing device type like Google Home or Android Application, Alexa is just storing the device name. In addition to Alexa, Google is storing approximate location of device, started by and action type. At the fig 5 shows that amazon Alexa history on its mobile application.

For the second case, the device names were changed from "light" to "horse" in both mobile applications to mislead forensic investigator. As a result, for the second case activity, there were no difference between daily case and this case in activity history records both Amazon Alexa and also Google Assistant. Thus, to find what horse is, forensic investigator should record device names by using mobile application if the user didn't change the name of devices.

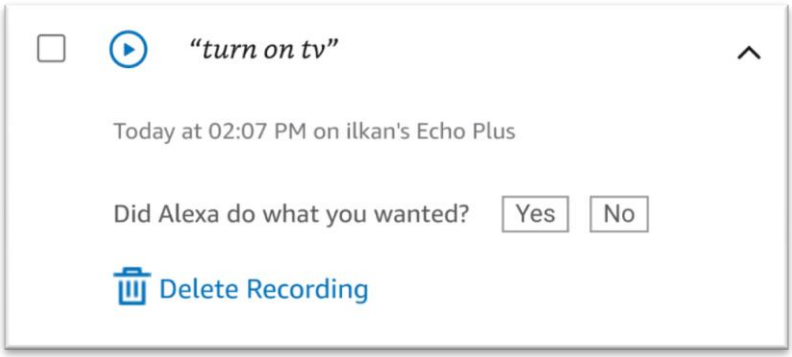

Fig.5. Amazon Alexa 3nd Case Activity History

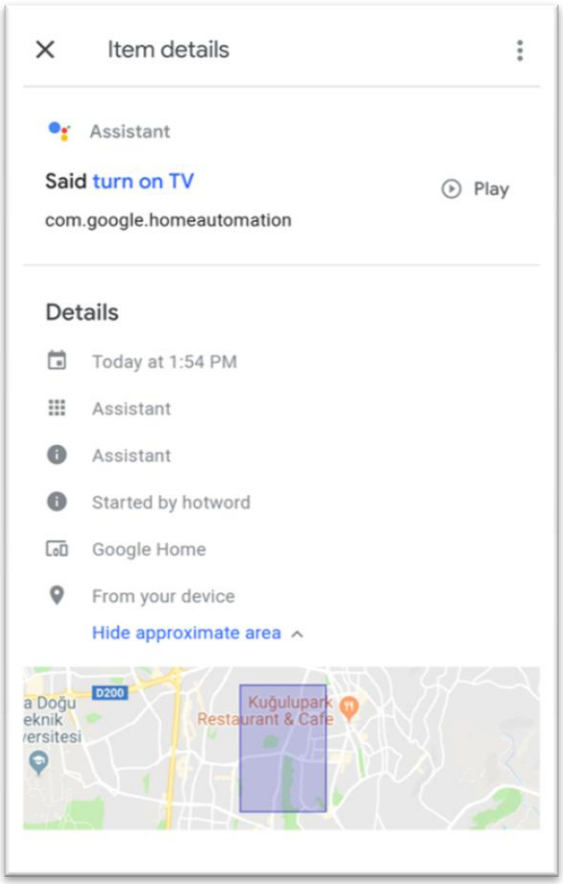

Fig.6. Google Assistant3nd Case Activity History

In third case, created routine command's activity history recordings were different according to daily activity history. In both activity history, the missing part was assistant's response although it was defined. This is the clue for the forensic investigators. At this point they should record all the routines carefully.

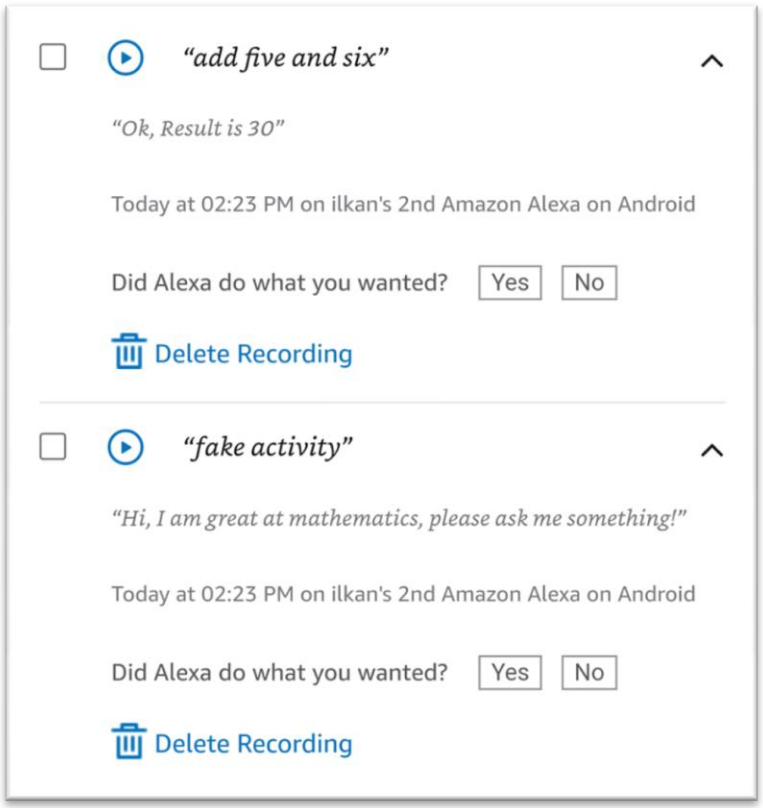

Fig.7. Amazon Alexa Custom Skill Activity History

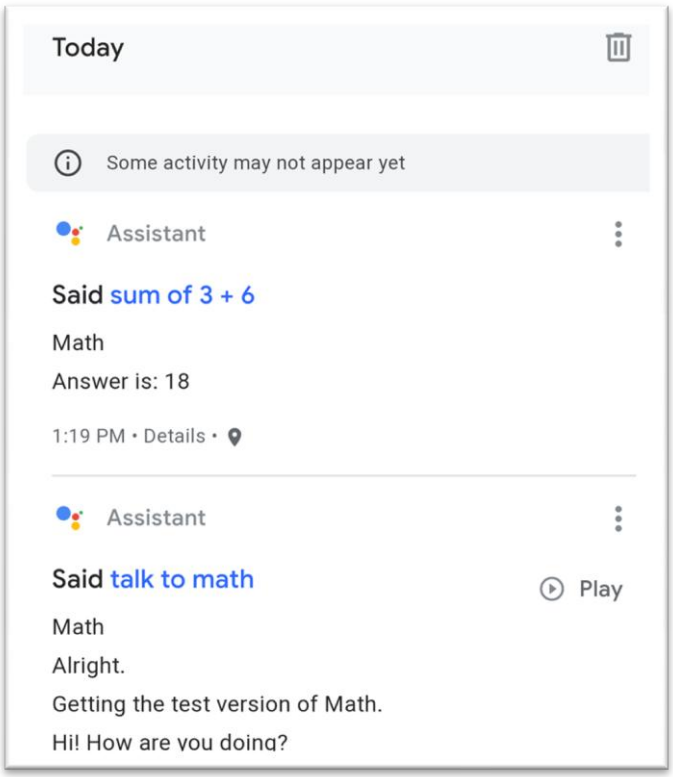

Fig.8. Google Assistant Custom Action Activity History

The last case creating custom actions' and skills' activity initiation history were same as daily case. At the fig 8 Google Assistant's intent activity histories were different than daily case which activity recording's missing parts were user command's voice recording and assistant's response. There was no missing part Alexa's in activity history which was same as daily case. At this point the only clue for the forensic investigators in Google Assistant's histories. At the fig 7 For the Alexa part, criminals can create anti-forensic fake activities easier by comparison to Google Assistant.

It was seen that both products store user data using cloud computing to improve their products and according to GDPR [13] they should present these data to users in readable format. That makes life easier for the forensic investigators.

IV. Conclusion

In this study, Amazon Alexa Echo and Google Home Mini smart assistants were selected by looking at the number of unit sales in the market and analyzed with forensic perspective. First, daily user command sent to both devices and its activity recording, then which compared with anti-forensic fake activities such as changing device name, creating routine and building custom skills in order to mislead forensic investigator. Clues and vulnerabilities were unearthed for these cases from activity histories.

Illogical requests with customized skills or actions allow users to perform different operations and create fake activity history recordings. Preventive studies can be done by Alexa and Google Assistant team.

Forensic analysis of smart assistants is a new field of study. The research has been done on Android devices, but it is obvious that there isn't any difference for IOS devices as both applications are directed to the web browser for activity histories. Criminal experts have no chance to take an image of device for analyzing, because all the data are uploading to cloud servers, but can request these data from Amazon and Google companies.

References

[1] D. Lillis, B. A. Becker, T. O'Sullivan and M. Scanlon, "Current Challenges and Future Research Areas for Digital Forensic Investigation," in *The 11th ADFSL Conference on Digital Forensics, Security and Law (CDFSL 2016)*, Daytona Beach, FL, USA, 2016.

[2] B. Kinsella, "There are Now More Than 70,000 Alexa Skills Worldwide, Amazon Announces 25 Top Skills of 2018," 14 12 2018. [Online]. Available: https://voicebot.ai/2018/12/14/there-are-now-more-than-70000-alexa-skills-worldwide-amazon-announces-25-top-skills-of-2018/. [Accessed 06 06 2019].

[3] "Google Assistant Actions Total 4,253 in January 2019, Up 2.5x in Past Year but 7.5% the Total Number Alexa Skills in U.S.," 15 02 2019. [Online]. Available: https://voicebot.ai/2019/02/15/google-assistant-actions-total-4253-in-january-2019-up-2-5x-in-past-year-but-7-5-the-total-number-alexa-skills-in-u-s/. [Accessed 06 06 2019].

[4] B. Kinsella, "Amazon Increases Global Smart Speaker Sales Share in Q4 2018, While Google Rise Narrows the Gap and Apple Declines," 20 02 2019. [Online]. Available: https://voicebot.ai/2019/02/20/amazon-increases-global-smart-speaker-sales-share-in-q4-2018-while-googles-rise-narrows-the-gap-and-apple-declines/. [Accessed 02 06 2019].

[5] Arizton, "Arizton Says Smart Speaker Market $4.8 Billion in 2022 - Voicebot," 4 1 2018. [Online]. Available: https://voicebot.ai/2018/01/04/arizton-says-smart-speaker-market-4-8-billion-2022. [Accessed 5 5 2019].

[6] M. Ford and W. Palmer, "Alexa, are you listening to me? An analysis of Alexa voice service network traffic," *Personal and Ubiquitous Computing 23(1),* pp. 1-13, July 2018.

[7] H. Chung, M. Iorga, J. Voas and S. Lee, "'Alexa, Can I Trust You?'," *Computer 50,* pp. 100-104, 2017.

[8] J. P. S. L. Hyunji Chung, "Digital forensic approaches for Amazon Alexa ecosystem," *Digital Investigation Volume 22, Supplement,* pp. Pages S15-S25, August 2017.

[9] D. Kumar, R. Paccagnella, P. Murley, E. Hennenfent, J. Mason, A. Bates and M. Bailey, "Skill squatting attacks on amazon alexa," *SEC'18 Proceedings of the 27th USENIX Conference on Security Symposium*, pp. 33-47, 2018.

[10] C. Shin, P. Chandok, R. Liu, S. J. Nielson and T. R. Leschke, "Potential Forensic Analysis of IoT Data: An Overview of the State-of-the-Art and Future Possibilities," in *2017 IEEE International Conference on Internet of Things (iThings) and IEEE Green Computing and Communications (GreenCom) and IEEE Cyber, Physical and Social Computing (CPSCom) and IEEE Smart Data (SmartData)*, Exeter, 2017.

[11] Amazon Web Services, «Creating IoT Solutions with Serverless Architecture & Alexa,» 01 Şubat 2014. [Online]. Available: https://www.slideshare.net/AmazonWebServices/creating-iot-solutions-with-serverless-architecture-alexa. [Accessed: 01 Haziran 2019].

[12] B. McGowen, «Google Home and Google Assistant Workshop: Build your own serverless …,» 28 July 2017. [Online]. Available: https://www.slideshare.net/bretmc/google-home-and-google-assistant-workshop-build-your-own-serverless-action-on-google-app. [Accessed: 02 Haziran 2019].

[13] GDPR, "General Data Protection Regulation GDPR," 2018. [Online]. Available: https://gdpr-info.eu/art-12-gdpr/. [Accessed 01 06 2019].

Morphological and biometric characterization on indigenous Lampuchhre sheep in Terai region of Nepal

Bhojan Dhakal, Scientist
Nepal Agricultural Research Council (NARC),NASRI, Kathmandu, Nepal

Sabita Subedi, Goat Development Specialist
ISFP/KUBK, PIU, Pyuthan, Nepal

Ram Bahadur Rana, Senior Technical officer
Nepal Agricultural Research Council (NARC), Kathmandu, Nepal

Naba Raj Poudel, Scientist
Nepal Agricultural Research Council (NARC), Kathmandu, Nepal

Megh Raj Tiwari, Director
National Animal Science Research Institute, NARC, Nepal

Tek Bahadur Gurung, Executive Director
Nepal Agricultural Research Council (NARC), Kathmandu, Nepal

ABSTRACT

A comprehensive study was conducted to find out the prevailing production system of Lampuchhre Sheep (*Ovies aries*) in Western and Eastern Terai region of Nepal.Different morphological and biometric information were measured in farmer field including household survey mostly focused on sheep production in current farmers' management scenario by purposive sampling technique. Morphological and biometric parameter such as: parity, number of lambs, feeding regimes were taken according to cross- sectional household survey and focus group discussion. Moreover, the major morphological parameter namely head length, ear length, tail length, body length, neck length, fore feet, rear feet of the Lampuchhre sheep were recorded to establish a reliable regression function (equation). The multiple regression analysis provided a model equation for estimating body weight relationship among all the morphological traits. Moreover, body weight and body length had positive association with a linear functional relationship. The model equation observed was: Body weight= (-61.82)+ 0.449 (Body length)+ 0.857 (Heart Girth)+ (-0.1) Barrel height).Body length and heart girth had highly significant ($p<0.01$) relationship while the barrel height had non-significant effect ($p>0.05$) in the overall modelling. The majority of the morphological traits were found to be highly correlated in two-tailed. Body weight was correlated ($p<0.05$) with majority of the parameters except horn length, barrel height and neck length. These phenotypic information served as a basis for designing appropriate conservation and breeding strategies for sheep in the study area. However, it should be

substantiated with genetic characterization to guide the overall sheep breeding and conservation programs.

Key words: Lampuchhre sheep, modelling, characterization, potentiality

I. INTRODUCTION

Sheep generally seems to have least attention to the researcher in Nepal, despite its wide adoption in divergedagro climatic condition and widespread availability from hills to mountains. Additionally, Lampuchhre Sheep which generally found in southern part of Nepal, in warm Terai region, lags behind the research and extension program. Despite the facts, it plays a pivotal role on rural heritage and value chain due to its social values mostly among ethnic communities, which they need during the social occasions and rituals.

Sheep husbandry was carrying by the modern generation as family tradition and other ethnic communities are likely to be hesitant especially to Lampuchhre sheep, therefore it was likely that to encourage the sheep farming in Terai community would be essential.

The study of different morphological parameters of various known groups of sheep especially indigenous one which has diversified allocation in multiple environmental conditions with distinguishing characteristics is always a major concern for the animal science researcher for years. There is limited research on determining the appropriate equation/function to determine the weight of animals. The different morphological parameters of the sheep have certain level of the functional relationship with the body weight gain. The average meat production is always correlated with the body weight of the animals. The selection process of the any breeds possibly can be determined by using weight function of the animals. Identifying the major factor/parameter that have major functional relationship on the body weight might play role during selection process of animals for breed improvement program in the farm without addition of blood level of other foreign/imported breed.

Fisher (1936), Lachenbruch (1975), Krzanowski and Hand (1997), Desu and Geisser (1973) defined that discriminant analysis was extensively used in various fields where mostly linear discriminate function (LDF) was the main classification function obtained for classifying the known observations.Animal genetic resource (AnGR) characterization encompasses major activities associated with the identification, quantitative and qualitative description of breed populations and the natural habitat and production where their successful adoption may present or not (Asamoah-Boaheng and Sam, 2016). This research tries to cover upon these characterizations.

The aim of this study is to determine the major morphological parameter/physical traits including its reproductive parameters to identify variable selection criterion for developing weight gain function aiming to improve selection process. This would help on juxtaposing for breed enhancement program as well as estimation of body weight with functional equation. This will reduce the time burden for weighing sheep and arrangement of facilities for direct weight measurement process among these nomadic herder. Yanusa et al. (2013) published his paper in the International Journal of Biodiversity and Conservation, Volume 5 investigated that tail of the sheep can be most distinguishing character in his stepwise multifactorial discriminant analysis. The purpose of the discriminant analysis is to classify the observation or several observation into already known groups. (Hardel and Simar 2007).

II. METHODOLOGY

Different district of Eastern and Western Terai were selected for the study such as Sunsari, and Banke respectively. Cross sectional purposive random sampling method was used for household survey within 60 farmer / household. Lampuchree and Kage sheep growing farmers were selected for the study. Focus group discussion, face to face interview and direct farm observation was conducted to collect the data on prevailing situation within herders, farmers, wool merchants, middleman, and meat consumer. The open as well as closed type interview was scheduled to the farmers. The current populations of Kage and Lampuchhre sheep, traditional practices on rearing and other general management practices by the farmer were documented.

Breeding, health and nutritional aspects followed by farmers were categorized based on farmer's perception and secondary information. Along with this, major problems on Lampuchhre Sheep farming was investigated. Morphological/ and reproductive parameters of 60 Terai / Lampuchhre sheep was recorded in Kapilbastu district, Nepal.

Multiple regression analysis was conducted to explain the relationship between multiple independent or predictor variables and one dependent or criterion variable namely sheep body weight. A dependent variable was modeled as a function of several independent variables with corresponding coefficients, along with the constant term. The Multiple regression which requires two or more predictor variables (independent variable) to define the outcome variable (dependent variable) was used to develop the model equation.
The model equation for estimating body weight was observed within four variables namely body length, heart girth and barrel height and for female age of puberty. The regression equation for modelling was as follows.

$$\boldsymbol{Y = a + \beta_1 X_1 + \beta_2 X_2 + \beta_3 X_3 + \beta_4 X_4 + e}$$

Where
Y= body weight of sheep, α= constant, β
The multiple regression equation explained above takes the following form:
y = b1x1 + b2x2 + … + bnxn + c.
Here, bi's (i=1, 2…n) are the regression coefficients, which represent the value at which the criterion variable changes when the predictor variable changes.

Model Summary

Predictors (constant) variable were age at puberty, heart girth(cm), barrel height from the ground (cm), body length(cm). Meanwhile dependent variable was body weight (kg).

Figure1, 2: Lampuchhre Sheep in Kapilbastu, Terai, Nepal

III. RESULTS

Community involved in the household sheep production

Majority (85%) of the Lampuchhre sheep farming communities in Western Nepal were from Gaderiaethnicity as a family tradition since time immemorial. The similar scenarios were found in eastern region of Nepal where majority (89%)of Pal communities were found to be engaged. Some other highly marginalized ethnicity and some minorities group such as Muslim also had family tradition of sheep husbandry (only 4%) mainly in eastern region.

Biometric characteristics of Lampuchhre Sheep

Lampuchhre sheep also known as long tail sheep could be found different region mainly in tropical region of Nepal. It wasindigenous sheep which had its importance on rural heritage and value chain. These sheep breed was generally useful for ritual activities and social beliefs. It was also used for the fighting among each other. The owner of the victorious sheep wasrenounced as a chief who had greater knowledge on management and feeding system of the sheep and can make more robust and healthier sheep. The sheep was generally found in black and white color and sometimes in mixed colors. The average age to attain puberty was 9 month. The number of lambs in their life was 7 lambs and gives one lamb per lactation. The average birth weight of lamb was 1.2 kg with less mortality as compared to other sheep breeds with good disease resistant capacity. The average grazing hours was 12 hours per day.

Morphological information of Lampuchhre Sheep

The major morphological parameter of the male sheep namely head length, ear length, tail length, body length, neck length, fore feet, rear feet are higher as compared to female sheep of similar age. There was a large variation of body weight among female compared to male. It suggested that farmer practices selection procedures for breeding purpose and there was some uniformity in male body weight.The strong variation between the weight of female sheep within and among the herd signified that there was huge possibilities of inbreeding and meanwhile more opportunities for selection to maintain herd quality of greater performances. Uniformity need to be maintainedfor good performances on production parameters among the herd. As Singh et al (1993) described that the average body weight of Lampuchhre sheep is 30 kg which value is far below than result obtained in our study. This was may be due to variation of population from region to region.

Table1. Morphological and biometric parameters of Lampuchhre Sheep breed in Terai

Parameters	Male (n=30)	Female (n=30)	Total (60)
Head Length (cm)	24.80±0.83	23.27±0.75	23.53±0.95
Ear Length (cm)	16.40±0.96	14.37±3.74	14.72±3.50
Tail Length(cm)	38.90±1.52	35.29±2.77	35.91±2.92
Body Length(cm)	74.40±3.05	68.41±4.46	69.44±4.79
Heart Girth(cm)	80.60±2.19	73.85±2.83	75.02±3.74
Barrel height from the ground (cm)	34.50±1.58	31.71±1.52	32.19±1.84
Neck Length(cm)	24.50±1.58	23.56±1.34	23.72±1.39
Fore feet above knee (cm)	23.50±.50	21.78±0.79	22.07±0.99
Fore feet below knee (cm)	24.30±1.56	22.10±1.25	22.48±1.53
Rear feet above hock (cm)	27.50±1.00	25.43±0.88	25.79±1.18
Rear feet below hock (cm)	28.80±0.75	27.37±0.72	27.62±.90
Horn Length (cm)	27.80±16.66	.416±2.04	5.14±12.41
Body Weight (kg)	40.32±3.15	31.17±3.48	32.75±4.87
Age at puberty		6.79±.29	6.79±.29
lambing interval (days)		365.00	365.00
Average age in years	3.00±.71	3.71±1.45	3.59±1.37

Independent sample t test of Phenotypical (morphological) traits

Most of the morphological parameters were significantly correlated with the body weight of the animals. The barrel height had non-significant effect ($p>0.05$) in the overall modelling while body length and heart girth had highly significant ($p<0.01$) relationship. The majority of the morphological traits were found to be highly correlated in two-tailed. Meanwhile, horn length was also significantly correlated ($p<0.01$) with head length, body weight, and heart girth, both feet height above knee and above hock. Furthermore, neck length was significantly correlated with only heart girth and non-significant with all other morphological character measured under this study. Besides these, heart girth was significantly correlated with all parameter except ear length. In case of body weight, it was correlated ($p<0.05$) with majority of the parameters except horn length, barrel height and neck length. Similarly, rear and fore feet height below knee was significantly co-related with all parameters except ear length.

Table 2.F test of physical traits

Parameters		Levene's Test for Equality of Variances		t-test for Equality of Means			Confidence level	
		F	Sig.	t	df	Sig. (2-tailed)	Mean Difference	Std. Error Difference
Head Length in cm	E. V. assumed	.029	0.867	4.068	27	.000	1.52	0.3759
	E. V. not assumed			3.781	5.431	0.011	1.529	0.404
Horn Length in cm	E. V. assumed	36.218	0.000	8.331	27	0.000	27.383	3.287
	E variances not assumed			3.668	4.025	.021	27.383	7.465
Ear Length (cm)	Equal variances assumed	6.066	.020	1.185	27	.246	2.025	1.709
	Equal variances not assumed			2.309	25.293	.029	2.025	0.87719
Tail Length(cm)	Equal variances assumed	.757	.392	2.795	27	.009	3.608	1.290
	Equal variances not assumed			4.084	10.621	.002	3.608	0.883
Body	Equal variances	.015	.902	2.842	27	.008	5.983	2.10496

Length(cm)	assumed							
	Equal variances not assumed			3.649	8.083	.006	5.983	1.639
Body Weight (kg)	Equal variances assumed	.073	.789	5.420	27	.000	9.149	1.688
	Equal variances not assumed			5.805	6.231	.001	9.149	1.576
Heart Girth (cm)	Equal variances assumed	1.100	.304	4.993	27	.000	6.745	1.351
	Equal variances not assumed			5.929	7.124	.001	6.745	1.137
Barrel height from the ground (cm)	Equal variances assumed	.060	.809	3.719	27	.001	2.791	.750
	Equal variances not assumed			3.616	5.646	.012	2.791	.771
Neck Length(cm)	Equal variances assumed	.233	.633	1.385	27	.177	.937	.676
	Equal variances not assumed			1.237	5.262	.268	.937	.758
Fore feet above knee (cm)	Equal variances assumed	1.038	.317	4.644	27	.000	1.729	.372
	Equal variances not assumed			6.262	8.877	.000	1.729	.276
Fore feet below knee (cm)	Equal variances assumed	.601	.445	3.430	27	.002	2.195	.640
	Equal variances not assumed			2.947	5.120	.031	2.195	.745
Rear feet above hock (cm)	Equal variances assumed	.199	.659	4.685	27	.000	2.062	.440
	Equal variances not assumed			4.282	5.358	.007	2.062	.481
Rear feet below hock	Equal variances assumed	.000	.991	3.966	27	.000	1.425	.359

(cm)	Equal variances not assumed			3.850	5.638	.010	1.425	.370
Age in years	Equal variances assumed	2.165	.153	-1.049	27	.304	-.708	.675
	Equal variances not assumed			-1.631	12.528	.128	-.708	.434

Most of the morphological parameters weresignificantlycorrelated with the body weight of the animals.

Partial regression of body weight and body length

Body weight and body length had linear relationship. As body length progress, the body weight also increased.

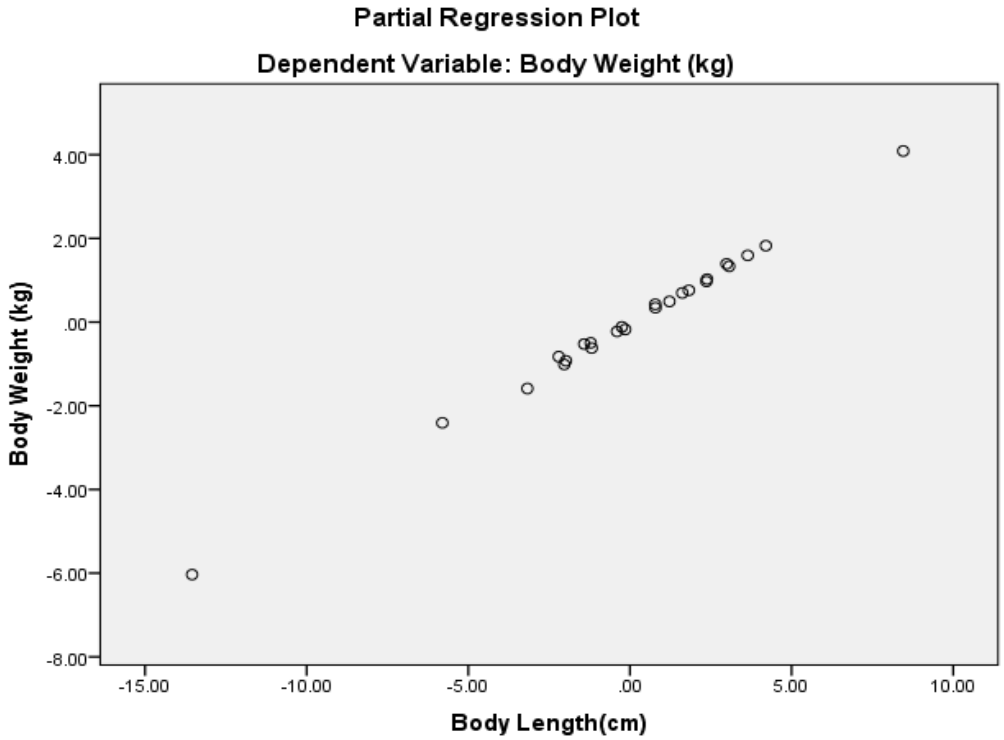

Figure: 3Partial regression of body weight and body length

Fitting of the model

P-P plot of regression standardized residual and dependent variable was measured and the relation was found to be directly correlated which signified that the modelling of the weight measurement wascoincided from each other value. This coincident validated the regression modeling equation of the morphological parameters.

A P-P plot compared the empirical cumulative distribution function of a data set with a specified theoretical cumulative distribution function. The plot showed that our observed value closely lied within the expected line. The majority of the observed value concentrated towards the straight line of the expected value with minimum scatterings of the data. The normal P-P plots of body weight of Lampuchhre sheep showed that the regression equation had a significant result on the hypothesis that, body weight of the sheep could be simulated by regression equation in very efficient way.

The residual probability was coincided with expected probability which signified the fitting of the model coincided with actual value.

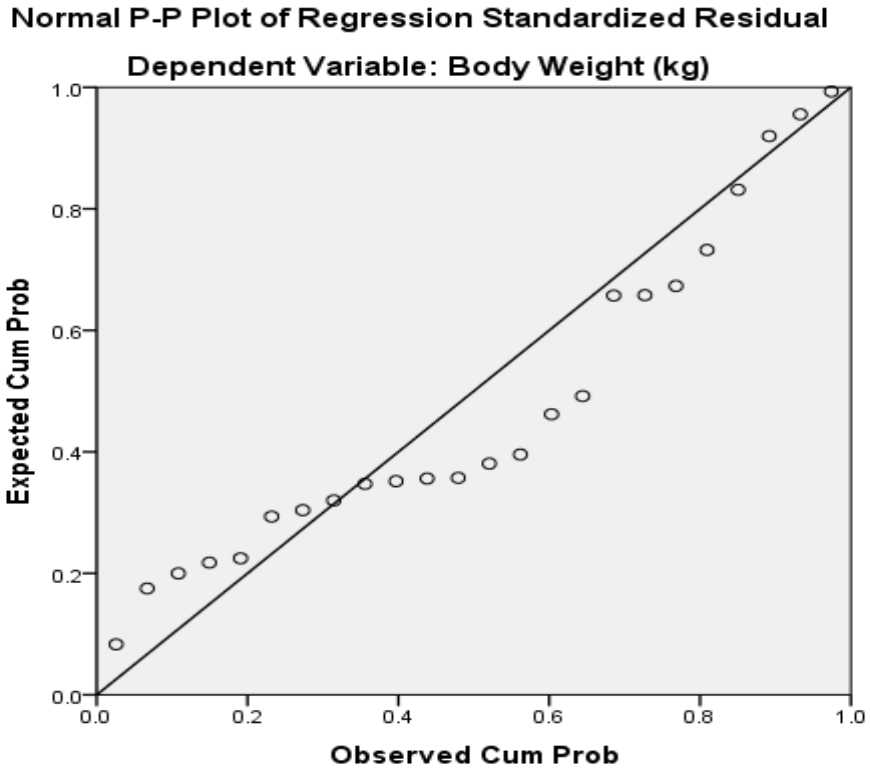

Figure 4.P-P plot of observed and expected probability

Body weight characterizations

To construct a P-P plot, the n non-missing values are first sorted in increasing order: x(1) x(2) x(n) Then the i^{th} ordered value x(i) was represented on the plot by the point whose X coordinate is E (x) and whose y-coordinate was O (y) . Like Q-Q plots and probability plots, P-P plots was used to determine how well a theoretical distribution models of a data distribution. If the theoretical reasonably models in all respects, including location and scale, the point pattern on the P-P plot was linear through the origin and had almost unit slope.

The model equation for estimating body weight was observed within four variables namely body length, heart girth and barrel height and for female age of puberty. The barrel height and age at puberty had non-significant effect (p>0.05) in the overall modelling while body length and heart girth had highly significant (p<0.01) relationship. The regression equation for modelling was as follows.

$$\boldsymbol{Y = a + \beta_1 X_1 + \beta_2 X_2 + \beta_3 X_3 + \beta_4 X_4 + \ e_{ijk}}$$

$$Bodyweight = (-62.73) + 0.449\ (BodyLenght) + 0.857(HeartGirth) + (-0.1)(Barrelheight) + 0.911$$

(Constant)

Table 3. Modelling for the body weight gain of the Lampuchhre Sheep

Parameters	Unstandardized Coefficients		Standardized Coefficients	t values	Significant level
	B	Std. Error	Beta		
(Constant)	-62.731	.911		-68.842	.000
Body Length(cm)	.449	.006	.576	75.384	.000
Heart Girth(cm)	.857	.009	.698	94.482	.000
Barrel height from the ground (cm)	-.010	.017	-.004	-.594	.560

Age at puberty	.023	.088	.002	.259	.799

Fitting of the model on histogram

The histogram followed the normality curve and complemented the finding of the model equation showing body weight (kg) as dependent variable:

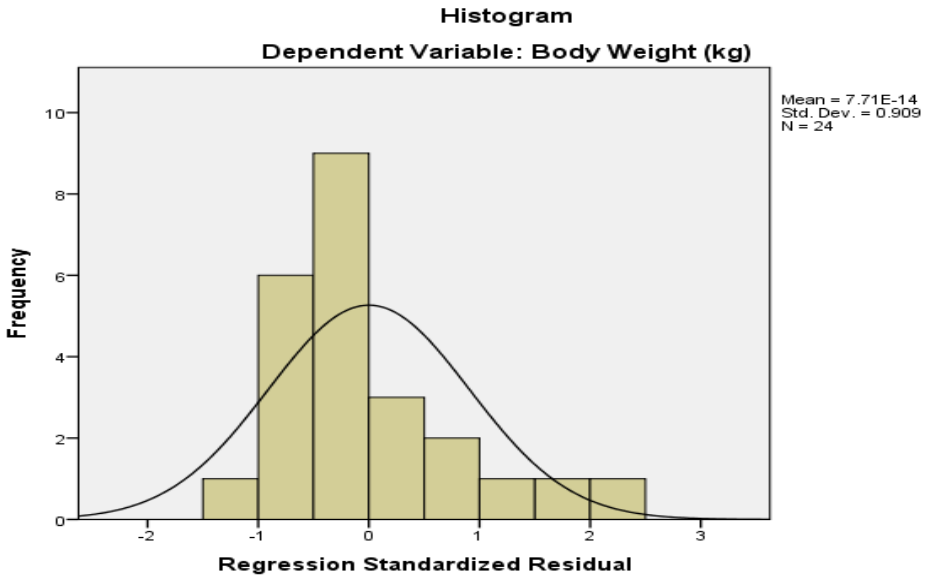

Figure 5.Histogram showing normality of the standardized residuals

Analysis of variance

The ANOVA results showed that the regression equation was highly significant and the model formulated had accuracy at 99% confidence interval. Therefore, we concluded that the predictor of this model can be used at farm and field level for the weight gainfunction of the Lampuchhre sheep.

Table 4. ANOVA of physical traits

Model	Sum of Squares	df	Mean Square	F	Sig.
Regression	278.533	4	69.633	5076.465	0.000
Residual	.261	19	.014		
Total	278.793	23			

Correlation of different physical traits of the Lampuchhre Sheep

Dependent Variable was body weight (kg) and predictors (constant) were age at puberty (for femaleonly), heart girth (cm), barrel height from the ground (cm), and body length (from neck bone to tail bone (cm)

Table 5. Correlation matrix of association between different physical traits

Pearson Correlations (2-tailed)		Head Length in cm	Horn Length in cm	Ear Length (cm)	Tail Length (cm)	Body Length (cm)	Body Weight (kg)	Heart Girth(cm)	Barrel height from the ground (cm)	Neck Lengt h(cm)	Fore feet above knee (cm)	Fore feet below knee (cm)	Rear feet above hock (cm)	Rear feet below hock (cm)
Head Length in cm	Pearson Correlation	1												
	Sig. (2-tailed)													
Horn Length in cm	Pearson Correlation	.519**	1											
	Sig. (2-tailed)	.004												
Ear Length (cm)	Pearson Correlation	.201	.140	1										
	Sig. (2-tailed)	.296	.470											
Tail Length(cm)	Pearson Correlation	.465*	.297	.067	1									
	Sig. (2-tailed)	.011	.117	.729										
Body Length(cm)	Pearson Correlation	.606**	.228	.476**	.530**	1								
	Sig. (2-tailed)	.000	.234	.009	.003									
Body Weight (kg)	Pearson Correlation	.706**	.519**	.380*	.620**	.792**	1							
	Sig. (2-tailed)	.000	.004	.042	.000	.000								
Heart Girth(cm)	Pearson Correlation	.598**	.580**	.239	.548**	.479**	.914**	1						
	Sig. (2-tailed)	.001	.001	.212	.002	.009	.000							
Barrel height from the ground (cm)	Pearson Correlation	.133	.566**	.047	.364	.101	.363	.454*	1					
	Sig. (2-tailed)	.491	.001	.808	.052	.602	.053	.013						
Neck Length(cm)	Pearson Correlation	.007	.091	.011	.360	.038	.348	.463*	.236	1				
	Sig. (2-tailed)	.970	.640	.954	.055	.846	.064	.011	.219					
Fore feet above knee (cm)	Pearson Correlation	.551**	.485**	.031	.436*	.509**	.693**	.650**	.342	.244	1			
	Sig. (2-tailed)	.002	.008	.872	.018	.005	.000	.000	.069	.201				
Fore feet below knee (cm)	Pearson Correlation	.446*	.582**	.189	.481**	.507**	.593**	.520**	.263	-.069	.544**	1		
	Sig. (2-tailed)	.015	.001	.327	.008	.005	.001	.004	.167	.722	.002			
Rear feet above hock (cm)	Pearson Correlation	.457*	.533**	.266	.378*	.429*	.543**	.472**	.297	.191	.511**	.392*	1	
	Sig. (2-tailed)	.013	.003	.164	.043	.020	.002	.010	.118	.322	.005	.036		
Rear feet below hock (cm)	Pearson Correlation	.513**	.570**	.192	.362	.272	.507**	.533**	.340	.218	.417*	.576**	.567**	1
	Sig. (2-tailed)	.004	.001	.319	.054	.154	.005	.003	.071	.256	.025	.001	.001	
	N	60	60	60	60	60	60	60	60	60	60	60	60	60

** Correlation is significant at the 0.01 level (2-tailed)

* Correlation is significant at the 0.05 level (2-tailed)

IV. DICUSSION

The major communities involved in Local Lampuchhre sheep farming wasGaderia and Pal communities. They were used to on keeping sheep since the time immemorial. These sheep might be consider as rural heritage. These sheep were most common among minorities group or within some ethnic groups. The stronger the sheep they have, the greater their social status considered among the villager and farmer. They had weekly customs of allowing the animals for fighting so the winner was mostly used for the breeding purpose for that week. If during the second week, the next animals won the race, whichultimately would get the opportunities for breeding among all the sheep that come heat during that period. This tradition had some advantage for selection of breeding ram in the village and perpetually reduces the chances of inbreeding also. It wasbecause the younger one has greater chance to win, and as the time progress, these were possibilities for other breeding ram in the village to win. The most robust one which had most important vigor and body size with strong body probably would get the chances of their traits to be transferred to their offspring.

Sexual dimorphism was observed among male and female sheep. Due to small number of male sheep taken, the equation was made for the average of male and female sheep. The majority of the morphological traits were found to be highly correlated in two-tailed. The correlation of head length, horn length, tail length, body length heart girth, and knee height of both feet, rear feet above hock were interestingly non-significant ($p>0.05$) to the barrel height from the ground and neck length. Meanwhile, horn length was also significantly correlated ($p<0.05$) with head length, body weight, and heart girth, both feet height above knee and above hock. Furthermore, neck length was significantly correlated ($p<0.05$) with only heart girth and non-significant with all other morphological character measured under this study. Besides these, heart girth was significantly correlated with all parameter except ear length. In case of body weight, it was highly correlated with majority of the parameters except horn length, barrel height and neck length. Similarly, rear and fore feet height below knee was significantly co-related with all parameters except ear length. More interestingly, rear feet above hock was correlated with tail length while rear feet below hock was not correlated.Multivariate analysis was a strong tool for characterizations of physical traits of small ruminants(Traore et al., 2008).Traore et al. (2008) investigation published in Small Ruminant ResearchVolume 80, Issues 1–3 also characterized morphological traits in Burkina Faso's sheep by multivariate analysis.In the similar way, the multivariate analysis of small ruminant was also conducted by Mohammed et al 2016 specifically on morphological characterizationsof goats of Ethiopia.Carneiro et al (2010) described that phenotypic information can be used initially used in mass selection, whereby individuals with better trait values can be chosen to be parents of the next generation (Carneiro et al. 2010).

The weight measure function was easy ways to measure the body weight when carrying weigh balance is not feasible. On the other hand, there wasdifferent weigh equation for different type of sheep. The carcass weight of the sheep would have always dependent on the flesh amount in different body parts of the animals. During the selection and breeding program of the sheep, there was always problems on which part of the animal has the major functional relationship for body weight/carcass weight of the animals. In this scenarios, heart girth had major functional relationship for body mass index of the animals. Therefore there was high possibility of getting more advantage and success in case we select the animals which has most prominent heart girth for better size and growth rate of offspring during the days to come. This would be equally applicable in selecting the ram which had larger heart girth and the longer body length.

The characterizations of sheep in this study will be helpful to livestock farmers and researchers in preserving the genetic resources of some of the indigenous Nepali sheep breeds, as well as to farmers and dealers in livestock products in the production, processing and marketing of livestock and livestock products. However, whether the variations in these morphological traits are caused by adaptive or non-adaptive sources needs to be further verified by comparing between relative levels of population divergence in quantitative traits and neutral DNA markers.

CONCLUSION

Different morphological parameters of the sheep was directly related to the body weight of the sheep. In the nut shell, different morphological parameter of the Lampuchhre sheep was also correlated to each other. Therefore besides body weight, other physical traits could be also considered as a major functional parameters during any kind if genetic improvement program. Moreover the strong variation between the weightsof female sheep within the herd signifies that there was huge possibilities of inbreeding and meanwhile, more opportunities for selection to maintain herd quality of greater performances. This studied tried to open the pathways for studying impact of genotype and manage mental environment on morphological and reproductive parameter of indigenous Lampuchhre sheep within the days to come. Further genetic study may be needed to fully describe this unique sheep population and its genotypic features. The present information when complemented with DNA microsatellites may help in management and in situ conservation of this indigenous Lampuchhre sheep specifically in Terai region of Nepal.

ACKNOWLEDGEMENTS

Numerous individuals and organization supported us while conducting research activities. We are highly grateful to all of them. We would also like to acknowledge the financial and technical support of Nepal Agricultural Research Council (NARC). Support and help obtained from farmers is equally praiseworthy.

REFERENCES

[1.] Traore A,IAlvarez,HH Tamboura,I Fernandez Kabore,B Royo , JP Gutierrez, M Sangare , Ouedraogo-Sanou e , A Toguyeni L Sawadogo, F GoyachGenetic characterisation of Burkina Faso goats using microsatellite polymorphism (2008).

[2.] Asamoah-Boaheng M, & EK Sam. Morphological characterization of breeds of sheep: a discriminant analysis approach. Springer Plus,(2016). 5, 69. Doi: 10.1186/s40064-016-1669-8.

[3.] Desu MM, SGeisser .Methods and applications of equal-mean discrimination. In: Cacoullos T, editor. Discriminant analysis and applications. (1973). New York: Academic Press; 1973. pp. 139–161. [Google Scholar] [Ref list].

[4.] Fisher RA. The use of multiple measurements in taxonomic problems. Annal Eugen. 1936;7:179–188. doi: 10.1111/j.1469-1809.1936.tb02137.x. [CrossRef] [Google Scholar][Ref list].

[5.] Hardel WK, Simar L. Applied multivariate statistical analysis. Heidelberg: Springer; 2007. [Google Scholar] [Ref list].

[6.] Krzanowski WJ and Hand DJ. Assessing error rate estimators: the leave-one-out reconsidered. (2007).Aust J Stat. 1997;39(1):35–46. doi: 10.1111/j.1467-842X.1997.tb00521.x.[CrossRef] [Google Scholar][Ref list].

[7.] Lachenbruch PA.Zero-mean difference discrimination and the absolute linear discriminant function. Biometrika. 1975;62(2):397–401.doi:10.1093/biomet/62.2.397. [CrossRef] [Google Scholar][Ref list].

[8.] Mohammed, Ahmed & Kefelegn, Kebede & Effa, Kefena. Morphological characterization of indigenous goats in Western Ethiopia: implication for community-based breeding programmes.

Animal Genetic Resources/Ressources génétiques animales/Recursos genéticos animales(2016). Retrieved from 1. 1-10. 10.1017/S2078633616000047.

[9.] Lachenbruch PA Some Unsolved Practical Problems in Discriminant Analysis by Department of Biostatistics University of North Carolina at Chapel Hill Institute of Statistics (1975). 1imeo Series No. 1050.

International Journal of Innovation Engineering and Science Research
(ISSN: 2581-4591)
www.ijiesr.com

Lighting on Agriculture and Using Light Emitting Diodes

I.H.CELEN
PhD, Proffessor.,Dept. of Biyosystem Engineering,
Agricultural Faculty, TekirdagNamik Kemal University
Suleymanpasa, Tekirdag, Turkey
icelen@nku.edu.tr

ABSTRACT

In agriculture, light is one of the most important factors affecting productivity. Artificial light sources used to support the energy coming from the sun support the formation of photobiological events. Light sources used in artificial lighting should be suitable for the requirements of plants, safe, environmental and have low energy requirements. LED-type light sources are artificial lighting tools that have become more common in recent years. In this study, the place of light in agriculture, classical lighting and technological features of LED type light sources are investigated. The advantages and operation of LED are emphasized. In addition, effects on plant were tried to be explained.

Keywords—*Light, PAR, Diode, photosynthesis, photon*

I. INTRODUCTION

According to the researches, the world population will be 9.1 billion in 2050. Today, while 49% of the world's population lives in urban areas, this ratio is expected to be more than 70% in 2050 [1]. If traditional farming methods continue to be implemented, new agricultural areas larger than the Brazilian area will be needed to feed this population. 80% of the area suitable for agriculture on a world scale is already cultivated. However, statistics show that 15% are unusable due to poor management. [2].People's learning to mow the land allowed them to move to settled life and to build advanced civilizations. It was a revolutionary change. In the following years, different methods have been developed in order to increase agricultural productivity to meet the nutritional needs of people. By using various chemicals (known as pesticides), insects, weeds and fungi that damage agricultural products can now be neutralized. In addition, many agricultural products can be grown in almost all seasons in the greenhouses where the factors affecting growth such as temperature, humidity and light are controlled. However, these methods will not be enough to meet the food needs in the future due to the increasing world population.

Agricultural practices in which agricultural products are produced in facilities where environmental conditions are controlled are called artificial agriculture, vertical agriculture or landless agriculture. In artificial agriculture, plants are not cultivated in large areas such as in traditional agricultural practices. Instead, it is necessary to establish plants where the conditions necessary for the growth of plants (eg temperature, light, water, carbon dioxide, nutrients) are always kept at optimal value. In this way, it is planned that agricultural products can be grown at the desired place, at the desired season and at the desired time regardless of the external factors such as season and weather conditions.

The basic bond of humans and animals with life is established through plants that perform photosynthesis using light energy. Therefore light; It has always played a very important role in the lives of all creatures. Artificial lighting has come to the fore when the sun is the biggest light source, also when the rays are less, technologies have been developed for this purpose. LED type illumination tools are also a product of technology oriented studies.

II. Conventional Lighting In Agriculture

In agriculture, broad spectrum light sources such as high pressure sodium (HPS) or fluorescent lamps are used as conventional lighting systems, especially for greenhouses. These lamps are excellent light sources for the human eye, but are not the most efficient light sources for plant production due to low blue light levels and other photosynthesis sensitive wavelengths. Light emitting diodes (LEDs), which can produce specific wavelengths by creating a specific light spectrum targeted for maximum plant production, can be said to be a fifty-year technology demonstrating potential in the greenhouse industry. Scientific studies have shown that the most important wavelengths for photosynthesis are in blue and red wavelengths; The peaks in photosynthetic yield are found at 440 (blue), 620 (red) and 670 (red) nm (+/- 10 nm) [3].

Light is an electromagnetic wave energy with particle (photon, quantum) character. Electromagnetic waves that generate light from a source propagate with sinusoidal motion and at constant speed. The rate of propagation to the frequency of sinusoidal motion; wavelength. In the classification made according to wavelength, 380-780 nm range; because it can be perceived by the human eye, it is described as a visible light zone [4].

Plants, chlorophyll formation, photosynthesis, conversion of inorganic substances to organic substances, shoots, leaves, flowers and fruit needs light for the formation [5].The source of light needed for plant development is the sun or artificial light [6,7].The light coming from the sun to the earth is composed of different wavelength rays. The wavelengths of the light in the spectrum between 390 nm and 760 nm are called visible light[5]..In the visible light spectrum, the red-orange light wavelength (600-700nm) is the longest light [8].Plants use visible light in the spectrum when performing photosynthesis [5].The energy of photons with visible wavelengths from the electromagnetic rays emitted by the sun is used by the plants in photosynthesis [9]. Light is not only an energy source for photosynthesis but also a factor that controls and directs different developmental processes for plants [10,11].Many light-related factors, such as light intensity, wavelength, are effective on plant growth parameters (such as node length differences, plant height, branching pattern, leaf sizes and biomass) [12,13,14,15,16,17].The amount of light affects the photosynthesis process. This process is a photochemical reaction within the chloroplasts of the plant cells in which CO_2 is converted into carbohydrate under the influence of the light energy. The spectral composition of red, far red blue, green, yellow or invisible e.g. UV or IR of the different wavelength regions is important for the grows, shape, development and flowering (photomorphogenesis) of the plant. For the photosynthesis, the blue and red regions are most important [3].

The timing / light duration is mainly affecting the flowering of the plants. This is called photoperiod. The flowering time can be influenced by controlling the photoperiod (Fig. 1).

Photosynthetic efficiency is mainly driven by chlorophyll a and b. They are mainly responsible for the photosynthesis and responsible for the definition of the area for the photosynthetically active radiation PAR. It shows further photosynthetic pigments also known as antenna pigments like carotenoids (carotene, zeaxanthin, lycopene and lutein etc.)in Fig.2 [18].

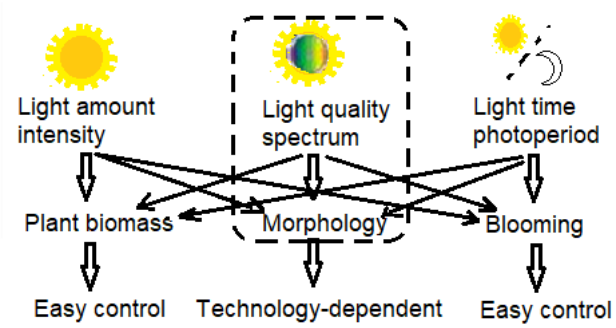

Figure 1. Effect of light on plant [52].

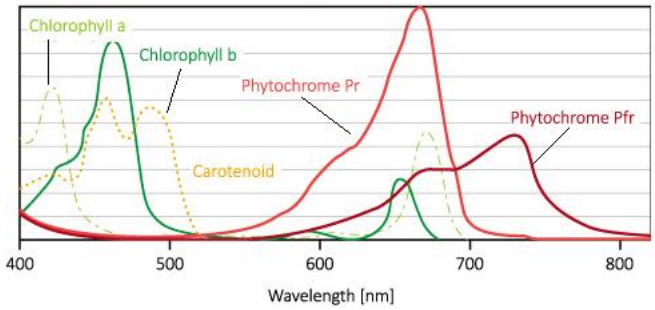

Figure 2.Absorption curves of plants [18].

If we examine traditional plant lighting sources;Incandescent lamps emit light upon the heating up of a metal filament. The fluorescent lamps, high-pressure mercury, high-pressure sodium, and metal-halide lamps are gas discharge lamps since they emit light generated by an electrical discharge through an ionized gas. While gas discharge lamps emit photons by the release of energy from thermionically excited electrons, emission from incandescent lamps consists of thermal radiations. The fluorescent lambs are low-pressure lamps in gas discharge lamps. But high-pressure sodium lamps, the high-pressure mercury lamps, and metal-halide lamps are termed as high-intensity discharge lamps due to the high pressure of gases in the arc tube.

Incandescent lamps, the working principle behind Incandescent lamps, is the phenomenon by which a solid starts emanating electromagnetic radiations in the visible range upon being heated [19]. Their oldest designed lamp consisted of a platinum coil enclosed in an evacuated glass tube, by Rue in 1840.

An incandescent bulb typically consists of a glass enclosure containing a tungsten filament. An electric current passes through the filament, heating it to a temperature that produces light. Incandescent light bulbs usually contain a stem or glass mount attached to the bulb's base which allows the electrical contacts to run through the envelope without gas/air leaks. Small wires embedded in the stem support the filament and/or its lead wires. The enclosing glass enclosure contains either a vacuum or an inert gas to preserve and protect the filament from evaporating. In other words, the bulb is essentially made devoid of oxygen by evacuation or by filling up with an inert gas to prevent the burning up of the filament. The filament is made of a metal It has high melting point and low coefficient of thermal expansion. Tungsten has both of these properties. It has been the only metal used for producing the filament for Incandescent lamps, recently. The two lead-in wires connected to either ends of the filament are connected to the external circuit. The lamp operates when the electrical current flows in from one lead wire, through the filament and out of the second lead wire. Because of the filament has higher resistivity than the lead-in wires, it impedes the flow of electrons. The inelastic collisions between the moving electrons and the electrons within the filament lead to the conversion of the kinetic energy of the moving electrons into atomic vibrational energy. This causes the filament to gradually heat up (2800 K). It then begins to dissipate energy as electromagnetic radiation. It emits radiations in the entire visible range. The intensity of the radiations increases from 400 to 700 nm. A significant portion of the energy is also dissipated as far-red emission which can reach up to 60% of the total PAR (Photosynthetically Active Radiation)[18].

They provide warmth to plants and not produce broad-spectrum emissions. So they are used in indoor cultivation in winter. But because of the low luminous output in exchange of the high electricity input, the operations were not deemed economically feasible. Heat losses and poor electrical efficiency are more important the gain in plant growth and yield. The energy conversion efficiency for the various modern Incandescent lamps ranged between 1 and 5%, with the luminous efficacy never exceeding 20 lumens/watt. Availability of power-efficient and long-lasting gas discharge lamps gradually replaced the Incandescent lamps as a light source for indoor cultivation[18].

The carbon arc lamp is a lamp that produces light by anlectric arc. The carbon arc light, which consists of an arc between carbon electrodes in air, invented by Humphry Davy in the first decade of the 1809s, was the first practical electric light. The application of this lamp was limited owing to the characteristic color of light it gave off. In 1936 Philips launched the first high-pressure mercury vapor

lamps. General Electric became the first to commercially produce fluorescent lamps in 1938. In 1962, metal-halide lamps were developed. Two years later high-pressure sodium lamps emitting bright white light developed were launched commercially[18].

Low-pressure mercury vapor discharge lamps, fluorescent lamps, produce visible light due to the fluorescence of a phosphor coating. They have two type on the basis of their shape and size—tubular and compact. The luminous efficacies of the two designs differ significantly. But their working principle is essentially the same. Both of them consist of an airtight hollow glass tube filled with a mixture of mercury and argon vapors in a low-pressure environment. The inert gas present in the arc tube promotes the ionization of the gaseous metal (mercury) atoms. The two ends of the tube have electrodes composed of tungsten filaments projecting into the vapor mixture. Upon the passage of electricity, the filament gets heated up and starts emitting electrons [20].Since fluorescent lambs work on alternating current, the two electrodes alternately emit electrons every half cycle. The electrons get accelerated toward the opposite electrode through the mercury vapor mixture due to the applied voltage. The electrons collide with the valence electrons of the mercury atoms causing electron impact ionization which leads to the release of more free electrons into the vapor mixture. At this stage, the vapor starts conducting electricity freely. The mobile electrons cause the excitation of the other electrons in the outer orbitals of the mercury atoms. The excited electrons fall back to the ground state and in the process emit radiations in the UVrange. These high-energy UV photons are absorbed by the phosphor coating which fluoresces or starts emitting photons of lower energy. Since the emission spectrum of an fluorescent lamb entirely depends upon the phosphor coating, a wide variety of phosphors have been used for developing white and colored fluorescent lambs.

Energy losses in anfluorescent lamb occur in the ballast which supplies a pulse of high voltage to initiate the discharge. However, a significantly higher amount of energy is lost during the conversion of UV rays into visible light where almost half the energy of each photon is lost as heat. However, the overall energy conversion efficiency of the fluorescent lambs is still below 30% [21]. Because of the white light output that appositely mimics daylight, fluorescent lambs have been a popular source of plant lighting in small- and large-scale operations. Approximately 90% of the photons emitted are in the PAR region. Spectral output of fluorescent lambs cannot be regulated and the surface of the lamp becomes considerably hot during operation.

High-intensity discharge light bulbs and lamps, are a family of gas-discharge arc lamps which create light by sending an electrical discharge between two electrodes and through a plasma, or ionized gas. An additional gas is generally used, and this gas serves as an easy way to classify the major types of High-intensity discharge light lamps: Mercury, sodium, and metal halide. These lamps are known for their high efficiency at turning electricity into light and their long rated life. The Lamps require a ballast in order to generate the initial surge of electricity needed to start them and to regulate their power during normal operation. The basic technology for the gas-discharge lamp has existed for over 300 years, and these same principals also guided innovations in other lighting types such as fluorescent and neon. The invention of the gas-discharge lamp is generally credited to Francis Hauksbee, an English scientist, who first demonstrated the technology in 1705.

At the time, the lamp was filled with air, but it was later discovered that the light output could be increased by filling the lamp with noble gases, such as neon, xenon, argon, or krypton. This technology has further increased light output through experimentation in gas mixtures and improved electrodes, but the functional basics of the high-intensity discharge lamp remain the same. In modern lighting usage, the High-intensity discharge light lamp functions by sending an electric arc between two tungsten electrodes which are housed in an arc tube, usually constructed of quartz. The tube is filled with an amalgam of gas and metal salts. An arc is created with an initial surge of electricity, facilitated by the gas in the lamp. The arc then heats the metal salts, and a plasma is created.This increases considerably the light produced by the arc, resulting in a source of light which is more efficient at creating visible light instead of heat than many traditional technologies such as incandescent or halogen lamps.

The high-pressure mercury lamps contain a mixture of mercury and argon vapors like fluorescent lambs, but the pressure is more higher in an fluorescent lamb. The vapors are maintained in a quartz

arc tube which housed inside an outer envelope made of borosilicate glass filled with nitrogen, to withstand the high pressure and operating temperature. By the emission of electrons from the tungsten electrodes the ionization of mercury atoms is triggered. The frequency of electron impacts on the mercury atoms becomes very high due to the high pressure. The generation of a huge amount of heat occur. In other words, the mercury electrons get ionized to higher excitation states, leading to the emission of radiations at certain wavelengths in the visible range along with the UV radiations. A phosphor coating provided on the outer envelope converts the UV radiations into different visible wavelengths. It results in white light [19].

The high-pressure sodium lamps have greater coverage over the visible spectrum than the mercury vapor lamps. Because there are the presence of sodium vapors along with mercury in the arc tube. Further, the tube is pressurized with xenon. The vapors are maintained within a ceramic or polycrystalline alumina tube which can withstand the corrosive nature of sodium vapors at high temperature and pressure [19].The excitation of mercury and sodium atoms occurs by the bombardment of electrons from the tungsten electrodes. The electron impact ionization coupled with thermal ionization results in electrons jumping to various higher energy states, while falling back to the ground state, the electrons emit electromagnetic radiations covering a wide range in the visible spectrum.

Higher luminous efficacy (80–125 lm/W) and broad emission spectrum of high-pressure sodium lamps have made them a popular source of electrical lighting in public spaces and industrial buildings. A high emission peak in the 560–610 nm range renders a distinct yellow coloration to the light produced which limits its applications. Further, the unbalanced spectral quality in relation to the absorption peaks of chlorophyll a, b and b-carotene makes them unsuitable for promoting photosynthesis and photomorphogenesis. Compared to other conventional sources, high-pressure sodium lamps with high electrical efficiencies of 30–40% are the most energy-efficient light sources used in plant growth [18].

In the metal-halide lamp the inclusion of metal halides along with the mercury vapor and inert gas permits the optimization of the spectral quality of the emitted radiation to a certain extent. Metals such as sodium, scandium, indium, thallium, and dysprosium are used in metal-halide lamps because of their characteristic emission spectra in the visible range. Iodides, and sometimes bromides, of these metals such as sodium, scandium, indium, thallium, and dysprosium are chosen because they are easier to vaporize and ionize than the pure metals as such. Like the other high-intensity discharge lamps, the pressurized gas is maintained within the arc tube and the same mechanism of operation is followed for electron excitation and light emission. However, the outer casing is made of UV-filtering quartz glass to block the UV radiations of mercury. Since the light emitted by the lamp is a mixture of the radiations by the individual metals present in the vapor mixture, changing the combination of the metal halides allows the production of metal-halide lamps with various emission spectra [20].Metal-halide lamps have an evenly distributed spectral output and produce white light with a high luminous efficacy of 100–120 lm/W. metal-halide lamps can be used in plant growth applications due to its high PAR, relative high percentage of blue radiation, and energy efficiency of approximately 25%.

III. LIGHT EMITTING DIODES(LED)

Significant effects of light on plant growth have led to the use of additional light in undergrowth cultivation. Especially during winter months when the light intensity decreases, additional lighting has significant effects on plant growth [22,23]. The use of LED lights has become widespread in recent years for additional lighting before sunrise and / or after sunset [8,24,25,26,27].LED lighting allows the plant to grow in sunless hours[29]. The use of LED lights in different colors according to the development stages of the plants in the greenhouse vegetable cultivation has started to become widespread. For this purpose, red and blue LED light-emitting lamps are widely used and sold [27].

LED lamps, environmentally friendly, long-lasting and convection in electricity consumption compared to all light sources saving occurs because of their being used in many countries and Turkey are also increasingly being used [28,30,31]. LED lamps provide up to 65% energy saving compared to existing lighting technologies [25,28]. In addition, the average lifetime of a normal incandescent bulb is 1000

hours, while the lifetime of LED lamps can range from 20,000 to 50,000 hours. LED lamps provide illumination without damaging the plants as they do not emit ultraviolet or infrared radiation and the system does not contain mercury and lead [28].

LEDs emit light from a semiconductor diode chip. Although the emission of light from Incandescent lamps also occurs from a solid (filament), the cause of electromagnetic radiations is quite different from the LEDs. The Incandescent lamps emit radiations due to the heating up of the filament. LEDs emit light due to the transition of electrons from higher to lower energy orbital's. gas discharge lamps emit radiations due to release of excess energy from electrons too, but the source of energy is thermionic excitation due to the electric arc. In LEDs, the electrons are not impelled into higher excitation states. Simply driven by the electrical potential difference from a higher energy orbital to a lower one.

A LED is a solid-state semiconductor device. It emits light upon the flow of electricity, following the principle of electroluminescence. Electroluminescence is the emission of light when electrons driven by an electrical or magnetic field enter a lower energy orbital and release the excess energy in the form of electromagnetic radiations. The phenomenon was first observed by H.J. Round in 1907 while working with silicon carbide (SiC). Later, in 1955, R. Braunstein reported the emission of infrared radiations from various semiconductor alloys. James Biard and Gary Pittman (in 1961) of Texas Instruments accidentally discovered the emission of infrared radiations from gallium arsenide (GaAs) semiconductor upon the passage of electricity, while working on solar cells. In the same year, Nick Holonyak Jr. designed the world's first LED producing visible light (red) using a gallium arsenide phosphide (GaAsP) diode. Ten years later, Holonyak's student M.G. Craford designed the GaAsP-based yellow LED and high-brightness red and red-orange LEDs. In 1970, improvements in semiconductor fabrication and packaging techniques by Jean Hoerni and Thomas Brandt led to the drastic reduction in the cost of manufacturing LEDs. Initially, the development of light-emitting semiconductor technology was associated with red and infrared radiations. The lack of a viable blue LED hindered the utilization of this technology to plant growth applications. H.P. Maruska designed the first blue LEDs based on gallium nitride (GaN) in 1972. In 1994, Shuji Nakamura presented themdesign for a high-brightness blue LED employing an indium gallium nitride (InGan) diode. The newly developed LED with a peak emission wavelength of 450 nm was found to be suitable for use in studies on plant growth and development. The wavelength matches with the maximum absorption peak of plant photoreceptors of carotenoids[18].

Various semiconductor materials have been used since Holonyak'sGaAsP-based model for fabricating red, green, blue, and white LEDs. Choice of the semiconductor alloy was guided by the need to increase the range of emission wavelength and luminous efficacy of the new LED as compared to its predecessors. Further enhancement in luminous output and power efficiency could be attained by increasing the efficiency of radiative recombination (electron–hole pairing leading to photon emission) within the LEDs. This was achieved via bandgap engineering by the use of heterostructures and quantum wells. Advancements in epitaxial crystal growth techniques enabled the formation of customized heterostructures and quantum wells in LED chips [32].The technology led to the development of power-efficient high-brightness LEDs that have sufficient luminous output with desired wavelength to sustain optimal plant growth. Such LEDs are made from binary direct bandgap alloys from groups III–V elements of the periodic table, namely aluminum gallium arsenide (AlGaAs), aluminum gallium indium phosphide (AlInGaP), and aluminum indium gallium nitride (AlInGaN). Availability of high-brightness LEDs with spectral output matching with the action spectra of photosynthesis and photomorphogenesis created the platform for the LED-based plant illumination system [33].

We know that LED luminaries can become the smart solutions for sustaining plant growth in controlled environment agriculture and regulating morphogenic responses in plant tissue culture.

A. Working Principle of LED

The LED comprises a semiconductor chip housed within an epoxy or plastic lens, with connecting wires for directing the electrical current. The chip is a small (approximately 1 mm2 in size) semiconductor wafer that has been impregnated with specific impurities or dopants (n types and p

types). n-type, i.e., elements having a high number of valence electrons, and p-type, i.e., elements having a high number of empty slots or "holes" in the valence shell. The p-type- and n-type-doped semiconductor crystals are fused together to form a "p–n heterojunction." As the electric current moves across the diode from the p-side to the n-side, electrons from the n-side cross over to the p-side. These electrons now fall into the vacant spaces in the orbitals of the p-type dopant resulting in "electron-hole pairing."

As the energy of the newly acquired orbital is lower than the energy possessed by the electron, the excess energy is liberated as electromagnetic radiation having a specific wavelength or color. This wavelength corresponds to the difference in valence shell energies of the p and n dopants. The phenomenon can be mathematically expressed as DE = (hc)/k (DE = change in energy of an electron, h = Planck's constant, c = velocity of light, k = wavelength of light). By virtue of its constituent dopants, an LED is capable of emitting light at a fixed wavelength only.

The application of red and blue monochromatic LEDs alone or in combinations has been reported for plant morphogenesis both in vivo and in vitro over the decades [34,35,36,37]. However, such LED lighting suffers from the waveband mismatch with the photosynthetic action spectrum and the high fabrication cost of the complicated circuit. Such LEDs are called trichromatic or tetrachromatic depending upon the combination of monochromatic LEDs used. White LEDs made by red, green, and blue LED clusters have a tunable spectral output controlled by the drive current through individual red, green, and blue LED units [38]. Phosphor-coated blue and UV-LEDs are the preferred source of white light owing to their common availability at low cost. However, the initial phosphor-coated LED models suffered from significant energy losses at the phosphor due to low energy conversion efficiency [39]. Approaches are being made to develop high-efficacy white LEDs using a hybrid model which includes colored phosphors along with monochromatic LEDs. A decrease in total internal reflection within the chip and device encapsulation with multicolor-emitting phosphors could enhance the luminous efficiency [40]. Recently, Chen et al. [41] proposed the potential of Eu+-doped fluorophosphate in fabricating white LEDs for application in plant growth.

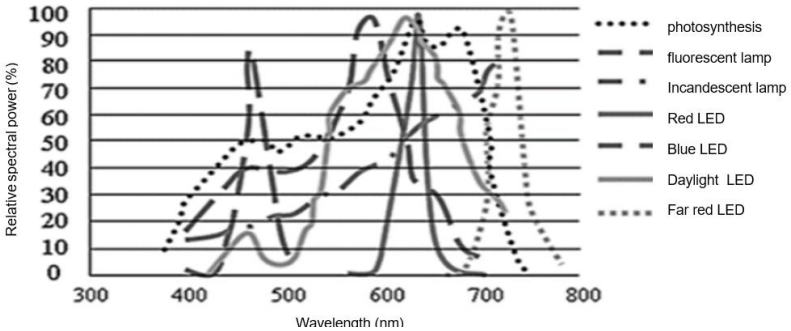

Figure 4. Characteristic of the photosynthesis and the artifical light sources[42]

B. Features of LED

Lamp features such as spectral quality, luminous efficacy, power requirement, life span, heat emission, robustness, and ease of disposal is some features of Lamp. They are discussed in the below for assessing the performance of each lighting system.

Plants absorb radiation mostly in the 400-700 nm visible range and convert CO_2 uptake and water into oxygen and glucose. The amount of absorption in each wavelength depends on the cellular structure of the plant and may differ from species to species somewhat.

Another important parameter is Daily Light Integral which is defined as the total number of photons impinging per square meter in one day. DLI is measured in units of mol/m².d and each plant has a specific requirement of DLI for its growth. Values ranging between 6-18 mol/m²/d are common depending on the particular plant.

There is a relationship between PPFD and DLI which is given by:

DLI=PPFD x light hours per day x (3600/1000,000).

You can see from this formula that there is a trade-off between PPFD and number of light hours required to achieve a certain DLI value. If there is a certain amount of natural lighting available for a

green-house, it has to be subtracted from the original DLI value for proper artificial lighting fixture calculations. Taking into account the DLI, PPFD and number of light hours per day, you can calculate the total number of fixtures required in a green-house to illuminate the crops.
In Greenhouse, Vegetative Growth (Leafy Greens/Herbs)is minimum 17 mol/m²/d
Flowering Crops (Peppers/Tomatoes): 20-40 mol/m²/d
In Indoors, for microgreens it is 6-12 mol/m²/d and for Vegetative Growth (Leafy Greens/Herbs) is 12-17 mol/m²/d. For flowering Crops it is 15-40 mol/m²/d [51]
We know that for plant growth availability of a proper light environment is pivotal. Incident spectrum and photon flux density (PFD) are two major factors that govern plant development in response to the lighting conditions. Plants essentially utilize the infrared, red, and blue portions of the incident spectrum for conducting photosynthesis and regulating numerous developmental and adaptive processes. Chlorophylls absorb photons and utilize the energy for photosynthesis [43].The main absorption peaks of chlorophyll are located in the red (625–675 nm) and blue regions (425– 475 nm). Carotenoids, the auxiliary photoreceptors of chlorophyll, absorb light mainly in the blue region. Photomorphogenic responses including germination, phototropism, leaf expansion, flowering, stomatal development, chloroplast migration, and shade avoidance are regulated by three types of photoreceptors, viz. phytochromes, cryptochromes, and phototropins[44,45,46].Interconvertible forms of Pr and Pfr in the red at 660 nm and in the far-red at 730 nm, respectively, constitute the phytochrome photoreceptor system. Phytochrome-mediated photomorphogenic responses are critically regulated by the sensing of R/FR ratio [47].The pigments absorbing blue light include both cryptochromes (cry1, cry2) and phototropins (phot1, phot2).
Cashmore et al. reported [48] that the cryptochrome system controls several aspects of morphological responses, such as germination, leaf expansion, stem elongation, and stomatal opening. It also regulates the circadian rhythm in flowering plants.
Phototropins are involved in the regulation of pigment content and the positioning of photosynthetic organelles in order to optimize the harvesting of light and to prevent photo inhibition[49].
Insolation contains all the regions of the visible spectrum along with radiations in the infrared and UV regions. Intensity of solar radiations is relatively higher in the blue-yellow (460– 580 nm) range. Like sunlight, all conventional electric lamps, viz. Incandescent lamps, fluorescent lambs, and high-intensity discharge lamps, are broad-spectrum light sources. The Incandescent lamps have a continuous emission spectrum having high proportions of photons in the infrared and red ranges, the PFD gradually reducing toward blue. Due to the presence of phosphor coating, white fluorescent lambs also have a continuous visible spectrum with peaks near 400–450 nm (violet-blue), 540– 560 nm (green-yellow), and 620–630 nm (orange-red) that results in a balanced white color rendition. High-pressure mercury lamps employing phosphor coatings also feature a similar emission spectrum but with sharper peaks than fluorescent lambs. Spectral emission of high-pressure sodium lamps exhibits peaks in the 560–610 nm (yellow-orange) region which imbues these lamps with a predominantly yellow light output. Metal-halide lamps emit a continuous visible light spectrum with several peaks distributed evenly across the entire spectrum. Fluorescent lambs, high-pressure mercury lamps, and metal-halide lamps are capable of delivering bright white light and are hence also referred to as "daylight lamps."
LEDs are essentially monochromatic light sources. They have a specific emission wavelength this feature is determined by the constituent elements of the LED chip. A wide variety of light spectra can be obtained from LED-based luminaries by simply embedding specific LEDs for the desired wavelengths. All conventional artificial light sources have significant emissions in regions of the visible spectrum that plants simply do not require. Since electrical lamps produce light at the expense of electrical energy, delivering wavelengths of light that are not utilized by the plants becomes impractical. Also they are not economic. With LEDs, it is possible to produce artificial light with selected peak wavelength emission that closely matches the absorption peak of a known important photoreceptor. Furthermore, the designs of Incandescent lamps and gas-based electrical lamps do not allow the regulation of operating light intensity. Intensity of emission from LED lamps can be easily regulated by altering the electrical current. Thus, it is possible to construct LED panels with specific

peak emission that are utilized by plants, having intensity control for adjusting the PFD most suited for the plants being raised. In this way, customized LED luminaries would allow a versatile control of radiation intensity and spectrum (Fig. 5).

Efficient conversion of electrical energy to light energy is an important factor. It used in the selection of the light source for indoor plant cultivation. The luminous efficacy of artificial light sources is a measure of luminous flux produced by the lamp per watt of electricity consumed (lm/W). It must be noted that luminous efficacy takes into consideration only the spectral output in visible range. Thus, lamps emitting significant amounts of radiations in the infrared and ultraviolet regions tend to have lower luminous efficacies compared to others. Power requirement of a lamp refers to the wattage supply required for operating the lamp. The lower the power requirement, the cheaper and easier it is to run any electrical lamp.

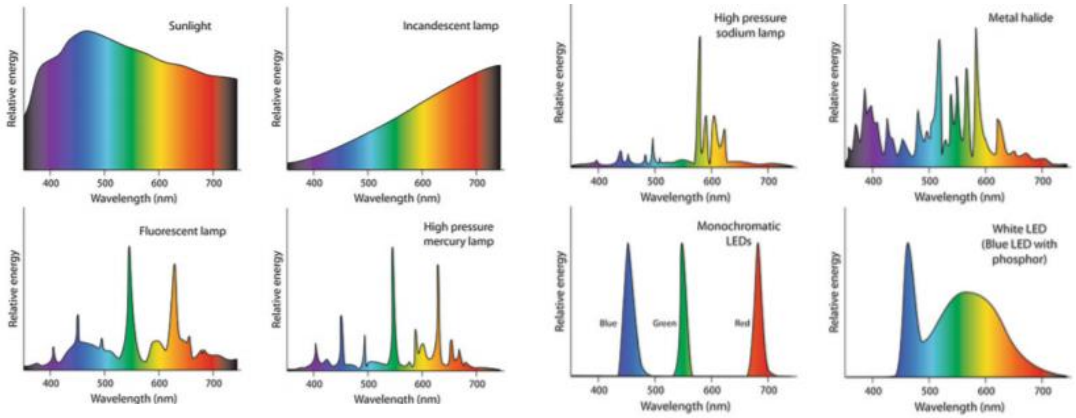

Figure 5. Spectral outputs of the various light lamps[18]

Among all artificial light sources, high-pressure sodium HPS and metal-halide lamps have the highest luminous efficacies. However, if we consider the lumens utilized by plants, the value gets reduced significantly since only the blue and red regions must be considered for plant use. The useful luminous output of even the most power-efficient electrical lamps may be considered to be quite low for plant growth. Although the luminous efficacies of conventional light sources have improved significantly since their initial development, the values attained plateau in the range of 80–125 lm/W. LEDs with luminous efficacy of 80–150 lm/W are already available in the market. Combinations of monochromatic LEDs can also be used to produce specific spectra that may be completely utilized by the plants, thus making the useful luminous output equivalent to the total luminous output. Further, due to rapid advancements in LED lighting technology, it is expected that LEDs with an efficacy of >200 lm/W will be developed within the next few years. The power requirement of a typical LED is 10–100 times less than most conventional lamps, thus making LED lamps highly cost-effective. Since LEDs consume less electricity, application of this technology shall also reduce the pressure on fossil fuel reserves used for generating electricity.

Dissipation of heat from the lamp is undesirable for indoor farming as well as for in vitro propagation from various aspects. Artificial light sources generating a lot of heat tend to raise the ambient temperature, a situation which may affect the quality of crops and the process of morphogenesis during in vitro culture. Additionally, this increases the load on the cooling system used for maintaining the temperature, leading to an increment in the electricity consumption. Furthermore, such light sources need to be placed at a safe distance from the crops/cultures as direct exposure to the heat may prove to be fatal. In vertical farming models where the crops are grown in tiers, using light sources having lower surface temperatures allows the placing of crops closer to the light source, thus giving more space for constructing more tiers and obtaining a higher yield per volume of the farming space. This notion is also applicable for in vitro culture. Dissipation of heat to the surroundings during any form of energy conversion has been considered as a loss of energy from the system. Since light

sources having cool operating temperatures lose lesser energy to the surroundings in the form of heat, they are able to convert electrical energy to light energy more efficiently.
Inelastic collisions of electrons occurring in Incandescent lamps and gas discharge lamps liberate a lot of heat energy, a condition absent in LEDs. LEDs also generate heat due to their intrinsic resistance at the p-n junction. However, the heat generated is negligible as compared to that in the conventional lamps. Furthermore, incorporation of heat sinks in modern high-power LED designs allows the LED to keep on operating at cool temperatures even while conducting significantly higher electrical currents. They have a cool surface temperature and are safer for growing plants as they practically do not emanate any heat as compared to the Incandescent lamps and gas discharge lamps [50].
The overall operating cost is influenced by the lifetime of the luminaire. Because frequent replacement of a large number of lamps on a commercial scale involves a huge capital input on a regular basis. Because of the extremely high operating temperatures conventional lamps gradually wear out. LED components do not wear out easily and that extended its life span by several thousand hours from within owing to the low working temperature. As the IL and gas discharge lamp illumination units grow old, precipitations on the inner surface tend to make the lamp dim. Thus, despite the lamp functioning optimally, the luminosity produced by it gets reduced. LEDs are solid-state light sources that do not contain any vapors or gases nor involve vaporization of elements, hence eliminating the chances of dimming due to precipitations.
All conventional artificial light sources, by virtue of their design, emit light in all directions. The use of reflective coatings in fixtures reduces the loss of light within the fixture. However, the luminous flux or the total useful light obtained in the desired direction becomes significantly lower than the total light produced by the lamp. An artificial light source with directionality of light emission can be used to provide greater luminous flux to the plants with significantly lower fixture losses. An LED contains a reflective cavity housed within the epoxy cover that concentrates all the photons in a single direction. Furthermore, half-isotropic spatial pattern of LEDs makes them directional emitters. LEDs with a small viewing angle and the use of secondary optics such as collimator lenses can improve the luminous efficacy by directing the light toward the plant canopy.
One factor that increases the desirability of the lamps is their small size and robustness. Small lighting units occupy a small volume, allowing more space for growing products, especially in vertical farms. Further, lamps made of durable materials are easy to handle and thus more user friendly. Artificial light sources devoid of hazardous materials such as mercury are preferable from the point of view of disposal. Incandescent lamps and gas discharge lamps are made up of different types of glass filled with various gases. Users have to exercise caution while handling such lamps. gas discharge lamps contain mercury which is highly toxic when released in the environment, making the disposal of spent gas discharge lamps a matter of concern. High-intensity discharge lamps are under high pressure at the operating level, making them unsafe where there is a production error. They are often large Luminaires for such lamp make them uneconomical in terms of space. On the contrary, LEDs are small, solid-state lamps housed within epoxy or plastic lens. LEDs are not only more robust and easy to handle, but also occupy a very small portion of the space being utilized for growing plants. If we evaluate LEDs in terms of plant growth and development compared to traditional electrical light sources, the advantages can be listed as choice of the peak emission for customized plant growth and development, Versatile control of the flux emission and the light spectrum, High luminous efficacy, Small size and directional light emission, Long life expectancy, Negligible heat emission, Does not get dim with age, Economical in terms of space and power (wattage) requirement, Plastic body, hence more robust and easy to handle, and Easy to dispose without any environmental hazards.

IV. RESULTS

Incandescent lamps, fluorescent lambs and the different high-intensity discharge lamps, have been employed in agriculture. Advancements in lighting technology have allowed the implementation of

electrical lamps for controlled environment agriculture and growing plants. High-power requirement and relatively short life span of these lamps made such crop production systems highly uneconomical. Although the various conventional electrical lamps used for agricultural lighting have the capacity to boost the qualitative and quantitative yield of the plants, they all suffer from certain limitations. Energy conservation is one of the major concerns in controlled environment, using traditional lamps, especially in northern latitudes. Continuously LED technologies have been developed. This advancements in the LED technology over time including packaging, current drop, phosphor coatings, intelligent control of light distribution, intensity and spectral quality along with the reduction in prices will make LED-based illumination system a smart choice for novel open as well as closed plant production systems.Emergence of solid-state lighting has not only offers the energy-efficient interior agriculture but has also opened up new frontiers for studying plant response to a specific wavelength and radiation quantity. LEDs have been adopted as a new source of artificial lighting to promote photosynthesis, regulate photomorphogenesis and improve the nutritional quality of leafy vegetables.
It is now possible to grow strawberries in the middle of winter thanks to LED technology indoors. Thanks to the LEDs that can be adjusted at the desired wavelength, the way of growing agricultural products with the desired characteristics is opened. For people who want to do winter farming, they prefer hydroponics (indoor farming) and buy some high-tech hydroponic pots illuminated by full-spectrum growth lights, and some even design their own systems. Plants are grown five times faster and naturally with systems with ideal climate created with LED lighting and water tanks. In other words, agricultural products develop rapidly and save energy. In addition to these, LED products are more durable than other broad-spectrum lighting products, thus saving on fixed costs.
Although some experts say that LED has benefits in agriculture, it should not be forgotten that the effect of LED technology on human health and nature is not known yet and it may lead to some risky situations. On the other hand, daylight is a must for vitality life. Another question is whether agricultural products grown with LED have the same taste and quality as those grown with daylight.
As a result, plant / greenhouse lighting with LED light sources will contribute to agricultural production and economy with many advantages. In addition to energy savings, as with any project, it will provide additional monetary savings with reduced maintenance costs and long lamp replacement times provided by the long life advantage.

REFERENCES

[1] Annoymous,"FAO. How to fees the world in 2050",http://www.fao.org/fileadmin/templates/wsfs/docs/expert_paper/How_to_feed_the_in_2050pdf. 2009

[2] Annonymous"Dikey tarım nedir",http://www.dikeytarim.com/dikey_tarim_nedir. 2015

[3] K.J. McCree, "The Action Spectrum, Absorption and Quantum Yield of Photosynthesis in Crop Plants", Agricultural Meteorology 9, 1972, p:191-216

[4] C.J.Bern, D.I.Olson, "Electricity for Agricultural Applications", Book, Willey, 2002, 235 p.

[5] A. Eriş,"Bahçe Bitkileri Fizyolojisi", Uludağ Üniversitesi Ziraat Fakültesi Yayınları:11, Ders Kitabı: 152, 2007, Bursa.

[6] H.H.Kim, G.D.Goins, R.M.Wheeler andJ.C.Sager, " Green-light supplementation for enhanced lettuce growth under red- and blue-light-emitting diodes",*HortScience* 39, 2004, p: 1617-1622.

[7] K.Ohasi-Kaneko, M.Takase, N.Kon, K.Fujiwara andK.Kurata,"Effect of light quality on growth and vegetable quality in leaf lettuce, spinach and komatsuna" Environ. Cont. Biol. 45, 2007, p: 189-198.

[8] Z.C.Yang, C.Kubota, P.L.Chia andM.Kacira,"Effect of end-of-day far-red light from a movable LED fixture on squash rootstock hypocotyl elongation",*Scientia Horticulturae* 136, 2012, p: 81-86.

[9] X.G.Zhu, S.P.Long andD.R.Ort, "What is the maximum efficiency with which photosynthesis can convert solar energy into biomass?",*Current Opinion in Biotechnology*. 19(2), 2008, p: 153-159.

[10] C.Andic, "Tarımsal Ekoloji", Ataturk Universitesi Ziraat Fakultesi Yayinlari: 106, Ders Notlari, 1993, Erzurum.

[11] H.Padem andH.Ozdamar, " Sebze buyume ve gelişiminde fotoreseptorler",*Derim* 9(2), 2002, p: 1-8.

[12] D.W.Lee, B.Krishnapilay, M.Mansor, H.Mohamad andS.K.Yap, " Irradiance and spectral quality affect Asiantropical rain forest tree seedling development",*Ecology* 77, 1996, p: 568-580.

[13] D.W.Lee, S.F.Oberbauer, P.Johnson, B.Krishnapilay, M.Mansor, H.Mohamad andS.K.Yap, " Effects of irradiance and spectral quality on leaf structure and function in seedlings of two Southeast Asian Hopea (Dipterocarpaceae) species",*American Journal of Botany* 87, 2000, p: 447-455.

[14] J.F.Stuefer andH.Huber, " Differential effects of light quantity and spectral light quality on growth, morphology and development of two stoloniferous Potentilla species",*Oecologia* 117, 1998, p: 1- 8.

[15] J.B.Fisher, U.Posluszny andD.W.Lee, " Shade promotes thorn development in a tropical liana, Artabotrys hexapetalus (Annonaceae)",*International Journal of Plant Sciences* 163, 2002, p: 295- 300.

[16] M.P.Croster, W.W.Witt andL.A.Spomer, " Neutral density shading and far-red radiation influence black nightshade (Solanum nigrum) and eastern black nightshade (*Solanum ptycanthum*) growth",*Weed Science* 51, 2003, p: 208–213.

[17] T.M. Griffith andS.E.Sultan, " Shade tolerance plasticity in response to neutral vs. green shade cues in Polygonum species of contrasting ecological breadth",*New Phytologist* 166, 2005, p: 141- 148.

[18] S.Dutta Gupta and A.Agarwal,"Artificial Lighting System for Plant Growth and development: Chronological Avancement, working principles and Comparative Assesment", Light Emitting Diodes for Agriculture, Chapter 1, Editor S. Dutta gupta, Springer, 2017, 334p

[19] S. Kitsinelis,"Light sources: technologies and applications" CRC Press, 2011, Florida

[20] R.S.Simpson, "Lighting control—technology and applications", Focal Press, 2003, Oxford

[21] M.S.Shur andA.Žukauskas," Solid-state lighting: toward superior illumination", Proc Inst Electr Electron Eng 93(10), 2005, p:1691–1703

[22] T.J.Blom, M.J.Tsujita andG.L.Roberts," Far-red at end of day and reduced irradiance affect plant height of easter and asiatic hybrid lilies",*HortScience* 30, 1995, p: 1009-1012.

[23] P.L.Chia andC.Kubota, "End-of-day far-red light quality and dose requirements for tomato rootstock hypocotyl elongation",*HortScience* 45, 2010, p: 1501-1506.

[24] P.Pinho andL.Halonen, " Agricultural and horticultural lighting", In: Karlicek R, Sun CC, Zissis G, Ma R (eds) Handbook of advanced lighting technology. Springer, Switzerland, 2010, pp 1–14

[25] H.J.Round, "Discovery of electroluminescence blue light emission from silicon carbide", Electron World 19, 1907, p:309

[26] M.Johkan, K.Shoji, F.Goto, S.Hahida andT.Yoshihara, "Effect of green light wavelength and intensity on photomorphogenesis and photosynthesis in *Lactuca sativa",Environmental and Experimental Botany* 75, 2012, p:128-133.

[27] N.S.Johansen, A.S.Eriksen andL.Mortensen, " Light quality influences trap catches of Frankliniella occidentalis (Pergande) and Trialeurodes vaporariorum (Westwood)", Integrated control in protected crops, temperate climate *IOBC/wprs Bulletin* 68,2011, p: 89-92.

[28] Anonymous, " Dijital Teknik", S:102. Available:http://www.neoneon.com.tr/uploads/basinda/510b 9ae5824653d8.pdf, 2012.

[29] N.C.Yorio, G.D.Goins, H.R.Kagie, R.M.Wheeler andJ.C.Sager, "Improving spinach, radish and lettuce growth under red light-emitting diodes (LEDs) with blue light supplementation",*HortScience* 36(2), 2001, p:380-383.

[30] A.Teke, O. Haddur andH.I.Mutlu, " LED teknolojileri, Bölüm 1: Çeşitleri ve sürücü devreleri, *Yeni Enerji, Yenilenebilir Enerji Teknolojileri Dergisi* 24, 2011, p: 48-54.

[31] A. Teke, O. Haddur and H.I. Mutlu, " LED teknolojileri, Bölüm 2: LED'lerin kullanım alanları ve bazı özel uygulamaları, *Yeni Enerji, Yenilenebilir Enerji Teknolojileri Dergisi* 25, 2011, p: 50- 54.

[32] E.F.Schubert, "Light-emitting diodes", Cambridge University Press,2003, UK

[33] G.Tamulaitis, P.Duchovskis, Z.Bliznikas, K.Breive, R.Ulinskaite, A.Brazaityte, A.Novickovas andA.Zukauskas, " High-power light-emitting diode based facility for plant cultivation", J Phys D Appl Phys 38, 2005, p:3182–3187

[34] H.H.Kim, R.M.Wheeler, J.C.Sager, N.C.Yorio andG.D.Goins," Light-emitting diodes as an illumination source for plants: a review of research at Kennedy Space Center, " Habitat (Elmsford) 10, 2005, p:71–78

[35] G.Massa, H.Kim, R.M.Wheeler andC.A.Mitchell, " Plant productivity in response to LED lighting", HortScience 43, 2008, p:1951–1956

[36] S.Dutta Gupta andB.Jatothu, " Fundamentals and applications of light emitting-diodes (LEDs) in vitro plant growth and morphogenesis", Plant Biotechnol Rep 7, 2013, p:211–220

[37] A.Agarwal andS.Dutta Gupta, ") Impact of light emitting-diodes (LEDs) and its potential on plant growth and development in controlled-environment plant production system", Curr Biotechnol 5, 2016, p:28–43

[38] G.He andL.Zheng, " Color temperature tunable white-light light-emitting diode clusters with high color rendering index. Appl Opt 49(24), 2010, p:4670–4676

[39] Bourget C.M. (2008) An introduction to light-emitting diodes. HortScience 43(7):1944–1946

[40] P.M.Pattison, J.Y.Tsao andM.R.Krames, " Light-emitting diode technology status and directions: opportunities for horticultural lighting. Acta Hortic 1134,2016, p:413–426

[41] J.Chen, N.Zhang, C.Guo, F.Pan, X.Zhou, H.Suo, X.Zhao andE.M.Goldys, "Site-dependent luminescence and thermal stability of Eu2+ doped fluorophosphate toward white LEDs for plant growth", ACS Appl Mater Interfaces 8, 2016 , p:20856–20864

[42] N.Caglayan, and C.Ertekin, " Sebze Üretiminde İlave LED Aydınlatma Uygulamaları (Applications of Supplemental LED Lighting in Vegetable Production)", Journal of Agricultural Machinery Science, Vol.12(1), 2016, p:27-35.

[43] J.M.Anderson, W.S.Chow andY.I.Park, " The grand design of photosynthesis: acclimation of the photosynthetic apparatus to environmental cues", Photosynth Res 46, 1990, p:129–139

[44] H.Smith , "Physiological and ecological function within the phytochrome family", Annu Rev Plant Biol 46, 1995, p:289–315

[45] A.Sancar, " Structure and function of DNA photolyase and cryptochrome blue-light photoreceptors. Chem Rev 103(6), 2003, p:2203–2238

[46] W.R.Briggs andJ.M.Christie, " Phototropins 1 and 2: versatile plant blue light receptors", Trends Plant Sci 7(5), 2002, p:204–210

[47] T.Shinomura, K.Uchida andM.Furuya, " Elementary processes of photoperception by phytochrome A for high-irradiance response of hypocotyl elongation in Arabidopsis", Plant Physiol 122(1), 2000, p:147–156

[48] A.R.Cashmore, J.A.Jarillo, Y.J.Wu andD.Liu, " Cryptochromes: blue light receptors for plants and animals", Science 284(5415), 1999, p:760–765

[49] E.P.Spalding, K.M.Folta, " Illuminating topics in plant photobiology. Plant, Cell Environ 28, 2005, p:39–53

[50] C.A.Mitchell, A.J.Both, C.M.Bourget, J.F.Burr, C.Kubota, R.G.Lopez, R.C.Morrow andE.S.Runkle, " LEDs: the future of greenhouse lighting! Chron Hortic 52, 2012, p:6–10

[51] Annonymous, " Typical-ppfd-dli-values-per-crop", https://www.horti-growlight.com/typical-ppfd-dli-values-per-crop. 2019

[52] Anonymous, " What-wavelengths-colors-do",https://www.horti-growlight.com. 2019

International Journal of Innovation Engineering and Science Research
(ISSN: 2581-4591)
www.ijiesr.com

Using Nano-SiO_2 to improve the Mechanical and abrasion Properties of High-Volume Fly Ash Concrete Subjected to Elevated Temperatures

Sherif A. Khafaga

Building Materials Research and Quality Control Institute, Housing & Building National Research Center, HBRC, Cairo, Egypt

ABSTRACT

Fly ash (FA) disposal resultant from coal-fired electrical power-stations combustion is one of the main-environmental challenges. The disposal of FA is accompanying with leaching of heavy metal and immense threat of pollution. To eliminate these problems, FA with high-volume (HVFA) can be incorporated into concrete as a part of cementitious material. In this work, cement was partially replaced with FA at ratio of 60%, by weight, to obtain HVFA-concrete (F60). Because the early strength of HVFA concrete is low, F60 was improved by incorporation of 2% (F60n2) and 5% (F60n5) nano-SiO_2 (NS) as a partially replacement of FA, by weight. Mechanical strength and modulus of elasticity were measured. The compressive strength and abrasion resistance before and after subjected to 200-800 ^{o} C for 2 h were investigated. The results showed an improvement in the HVFA concrete properties with the inclusion of NS particles. HVFA concrete showed better performance than the control at elevated temperatures. This better performance increased with the incorporation of NS particles.

Keywords: High-volume fly ash, recycling, mechanical properties, Abrasion resistance, Nano silica, high temperature.

I. Introduction

Concrete is a major material used in construction field because concrete is a cheap material which has an acceptable durability. But cement production has a negative effect on the environmental. So, many countries trend to limit cement industry. This negative effect led to searching about using cementitious materials (SCMs) as a partially replacement of cement especially in a large amount. Fly ash is one of the chosen materials used as a partially replacement of cement in the concrete by a typical ratios of approximately 20–25%. Currant researches incorporated HVFA in concrete aiming to get rid of FA and limiting pollution occurs by cement industry. Generally, if 50% or more of PC is replaced by FA, the concrete is termed as HVFA concrete [1]. Because the early strength of HVFA concrete is low, using mineral additives like Nano silica, silica fume, rice husk ash to improve the mechanical properties of HFVA concrete are recommended [2,3].

Many researchers studied the effect of HVFA on the mechanical properties of concrete compared with those of normal concrete. Rashad [4] presented an overview of the previous studies carried out on the use of high-volume Class F FA as a partially replacement of cement. They found that the reduction in the compressive strength of concrete at age of 28 days was between 38-43%, when cement was partially replaced by 50% FA [1,5,6]. While, the reduction in compressive strength was between 26-41% when 60% of FA was incorporated [7-9]. Also it was observed that using 70% fly ash deceased the compressive strength by around 49-67% [10-12]. The main conclusion obtained from the previous studies that the reduction in the compressive strength increased with increasing in FA content. In the same manner, a lot of studies reported a reduction in the flexural strength, splitting

tensile strength, and modulus of elasticity for concrete at age of 28 days with the inclusion of HVFA as cement replacement. This reduction increased with increasing FA content [13-17].

A lot of approaches have been conducted to enhance the strength at early ages of HVFA matrices. These approaches include adding other cementitious materials such as silica fume (SF) and MK, including ultra-fine FA, adding nano particles, including fibers and including chemical activators. Special curing conditions such as steam curing and high temperature curing also can be used [4]. In this regards, Musa et al. [18], studied the mechanical properties and the performance of HVFA concrete containing NS (53.78 % FA + 1.22% NS) as a cement replacement. The main conclusion found by this study is that the addition of NS increased the compressive strength, splitting tensile strength, flexural strength, modulus of elasticity, and abrasion resistance of HVFA rolled-compacted concrete (RCC) pavement. Also Min Liu, et, al. [19] studied the effect of adding 1-4% NS on the early strength of mortar containing 50% FA as replacement of cement under the effect of steam curing. It was found that NS largely and steam curing increased the 9 h strength of HVFA mortar. The more NS added the higher strength increase rate was obtained. Shikh, et al., [20] studied the effects of incorporated 2 % NS 10% micro silica (MS) and their combined on the bond behavior of steel and polypropylene (PP) fibers in HVFA mortar containing 40, 50 and 60% FA as a cement replacement, by weight. The main conclusions from the results indicated that maximum pull-out force of both steel and PP fibers decreased with increasing FA content at both 7 and 28 days. The addition of 2% NS and 10% MS showed almost similar improvement in the maximum pull-out force of steel and PP fibers at both ages. Rashad, prepared HVFA concrete by partially replacing cement with 70% FA. Then FA was partially replaced with 10% and 20% SF, by weight, [21], 10% and 20% slag, by weight, [22] or SF coupled with slag [23]. The specimens were exposed to elevated temperatures in the range of 400-1000 ^{o}C for 2 h. The results indicated a higher relative strength of all HVFA concrete types. The incorporation of slag showed a negative effect on HVFA concrete before and after different heating. The incorporation of SF exhibited a good fire performance up to 600 °C. The incorporation of 10% SF + 10% slag exhibited a good fire performance followed by the 5% SF + 5% slag up to 600°C. For all mixes, severe degradation in residual strength was observed at 800 and 1,000°C. Rahel Kh. et al, [24], investigated the fire resistance of HVFA mortars with NS addition, in this study, cement was partially replaced by HVFA combined with colloidal NS to produce high strength mortars with high residual strength after exposure to high temperatures of 400 °C and 700 °C. The results indicated that, high strength mortars that have equivalent residual strength after exposure to 700 ^{o}C in comparison with that of the control cement mortar specimens before exposure to high temperature can be produced by replacing cement with HVFA and using colloidal NS

This study focuses on the effect of using Nano silica to improve the mechanical properties of HVFA concrete exposed to elevated temperatures. To produce HVFA concrete, cement was partially replaced with 60% Class F FA. Because the early strength of HVFA concrete is low, FA was partially replaced with 2% and 5% NS. Flexural strength, tensile splitting strength and modulus of elasticity. In addition, compressive strength and abrasion resistance before and after exposure to 400, 600 and 800 ^{o}C for 2 h were investigated. This study could add violable data for HVFA concrete system.

II. Excremental details

2.1 Materials

The cement used in this investigation was CEM I 42.5 N complies with Egyptian Standard specifications E.S.S No. 4756-1. Its specific gravity and Blaine surface area was 3.15 and 300 m^2/kg, respectively. The properties of used coarse aggregate (crushed stone – with nominal maximum size of 10 mm) and fine aggregate (silica sand) in this experimental work comply with E.S.S No. 1109. Potable water was used for all mixes. The FA was obtained from disposal waste resulting from the combustion of pulverized coal in the coal-fired furnaces. It complies with the requirements of BS3892: Part and classified as a low calcium Class F FA in ASTM-C618. Its specific gravity and Blaine surface area FA was 2.4 and 400 m^2/kg. The NS is a synthetic product with spherical particles (size 8-18 nm). Its average Blaine surface area was 240000 m2/kg. These particles were supplied from Sigma-Aldrich (Germany). Fig. 1 shows TEM morphology of NS. Figs. 2, and 3 shows XRD pattern of NS, FA respectively. Strong broad peak of NS was centered on around 22◦ 2θ, which indicates the amorphous characteristic of SiO2. The chemical composition of cement, FA and NS was determined by X-ray fluorescence (XRF) spectrometry analysis and listed in Table 1. High-range water reducer (HRWR) has a sulphonated naphthalene base was used with a fixed dosage of 2.0% from the total cementitious materials weight to accomplish high followability.

Table 1 Chemical composition of PC, FA and NS

Oxide (%)	PC	FA	NS
CaO	63.47	2.35	0.01
SiO_2	20.18	59.05	98.6
Al_2O_3	4.83	23.3	0.01
MgO	2.47	1.85	-
Fe_2O_3	3.16	4.84	0.01
SO_3	3.26	0.65	0.46
K_2O	0.52	1.82	0.045
Na_2O	0.16	0.91	0.21
TiO_2	0.3	1.03	-
MnO	0.22	0	-
P_2O_5	0.09	0.73	-
L.O.I.	1.34	3.47	0.65

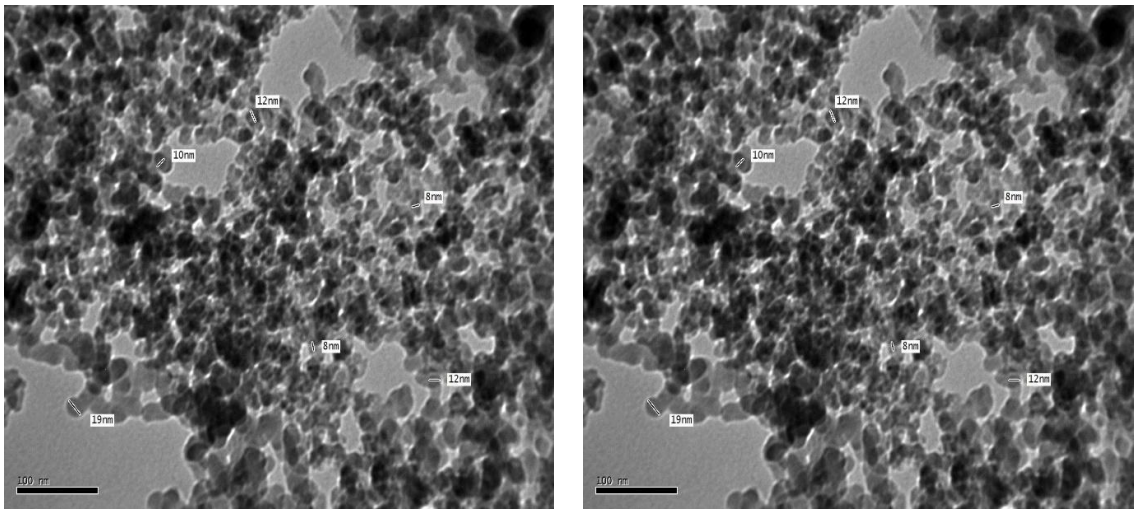

Fig. 1: TEM Micrograph of NS

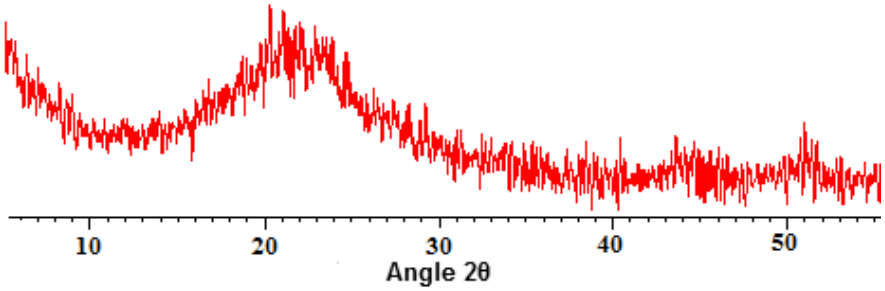

Fig. 2: XRD Pattern of NS

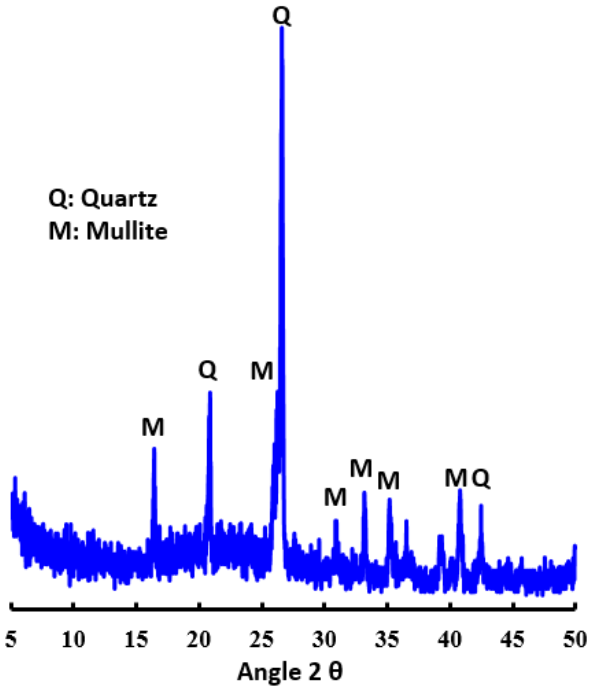

Fig. 3: XRD Pattern of FA

2.2 Mixture proportions

Four concrete mixtures were cast. All concrete mixtures were proportioned for constant effective w/b ratio of 0.4 and total cementitious content of 400 kg/m^3. The first mixture was made of only PC as the main binder material. This mixture was designated as (F0) and used as a control. In the second mixture, PC was partially replaced with FA at level of 60%, by weight. This mixture was designated as (F60). In the third and fourth mixtures, FA was partially replaced with NS at levels of 2% and 5%, by weight. These mixtures were designated as F60n2 and F60n5, respectively. The mixture proportions are summarized in Table 2.

Table 2 Concrete mixture proportions

Mixture	Ingredient /m^3					
Designation	PC (kg)	FA (kg)	NS (kg)	CA/Sand[1]	W/b	HRWR (liter)
F0	400	0	0	1.8	0.4	8
F60	160	240	0	1.8	0.4	8
F60n2	160	235.2	4.8	1.8	0.4	8
F60n5	160	228	12	1.8	0.4	8

[1] Coarse aggregate to fine aggregate ratio by weight

2.3 Methods

The mixing process was kept constant to supply the same homogeneity and uniformity for all mixtures. It started by mixing all of powders/aggregates for 3 min using pan mixer. NS (if any), mixing water and HRWR were mixed together with helping of ultrasonic mixer for a period of 5 min. The sonicated mixture was added to the powders/aggregates and mixed for 6 min. until the mixture became homogenous. The fresh concretes were cast into cubes of 100 mm side long moulds comply with BS 1881 (for compressive strength tests), cylinders of 150 × 300 mm comply with ASTM C469-02 (for modulus of elasticity tests), cylinders of 150 × 300 mm comply with ASTM C496/C496M-17 (for splitting tensile strength tests), prisms of 100 × 100 × 500 mm comply with ASTM C78 (for flexural strength tests) and samples with dimensions of 71 × 71 × 30 mm comply with ES: 269-2/2003 (for abrasion resistance tests). After casting, the moulds were vibrated for 1 min to remove air bubbles. The specimens were demolded after 24 h form casting and cured in water till the age of testing.

After curing, four specimens were tested in splitting tensile strength, flexural strength, modulus of elasticity and abrasion resistance at age of 28 days and the average was determined. For compressive strength tests, the similar number of specimens were tested at ages of 7, 28, 90 and 180 days. At age of 28 days, some compressive strength and abrasion resistance specimens were dried at 100 ± 2 ^{o}C for 24 h, then transferred to a symmetrical electrical furnace to be exposed to 400, 600 and 800 ^{o}C at a rate of 6.67 ^{o}C/min and held at each peak temperature for 2 h. After finishing, the specimens were then left to cool inside the furnace so as to avoid temperature shock. The specimens were then brought out from the furnace and weighed then tested in compression and abrasion to determine the residual compressive strength and abrasion resistance.

III. Results and discussion

3.1 Initial compressive strength

The compressive strength of the studied concrete mixtures at ages 7, 28, 90, and 180 days are presented in Fig. 4. There were reductions were (73.3, 59.1, 54.3, and 47.9) % for concrete specimens tested at age 7, 28, 90, and180 days respectively. These reductions were obtained which was attributed to the slow pozzolanic reaction of FA (low-calcium) and the dominant dilution effect, especially during the early ages, with only a few parts of the FA participating in the reaction. This effect is reduced with time.

Fig. 4 shows the compressive strength results starting from 7 days up to 180 days for all mixtures. As expected, partially replacing cement with 60% FA significantly reduces the compressive strength. The incorporation of 60% FA reduces the compressive strength by 73.3, 59.1, 54.3, and 47.9% at ages of 7, 28, 90 and 180 days, respectively. The higher reduction in the compressive strength is observed at early age. As the hydration time increases as the compressive strength gap between F0 and F60 decreases. The huge reduction in the early age compressive strength could be relevant to the slow pozzolanic reaction of low-calcium FA, of which a few parts of the FA participating the reaction and the dominant dilution effect [21]. To overcome this problem, FA was partially replaced with 2% and 5% NS. As can be seen from Fig. 4, the incorporation of only 2% NS can effectively enhance the 7, 28, 90 and 180 days compressive strength by 25.8%, 42.6%, 33.2% and 23.8%, respectively. Increasing the dosage of NS to reach 5% leading to more improvement in the compressive strength at all ages, but the highest improvement was noted at early age. The incorporation of 5% NS increases the 7, 28, 90 and 180 day compressive strength by 92.2%, 79.1%, 67.5% and 52.5%, respectively. More than one factor can attribute the improvement of compressive strength of concrete specimens containing NS. The first one is the faster pozzolanic reaction of NS with free lime produced in the hydration reaction of cement. Due to extremely high surface area and small particle size, the NS can react more quickly with free lime in the hydration reaction than FA. It can act as a nucleation site, accelerates the dissolution of C_3S and reacts with CH to form supplementary CSH gel. The second one called seeding effect, of which the ultra-fine particles of NS can act as seeds to hasten the cement hydration. The third one called the packing effect, of which NS can act as a filler which filled the pores among the microstructure of the concrete, due to their nano-size particles, resulting in immobilization of the free water and a more dense system **[**25],[26]**.**

Higher content of NS particles could have no significant effect on the compressive strength due to the agglomeration of the particles in wet mix. Nanoparticles, due to their small size, have high inter-particle van der Waal's forces causing the nanoparticles to agglomerate [3, 27-29]. Hence stored nanoparticles will form agglomerates hundreds of times larger than the primary nanoparticle causing them to lose the desirable surface area to volume ratio. Due to its higher van der Waal's forces, the nanoparticles agglomerate more than other pozzolans e.g. SF, metakaolin, etc.

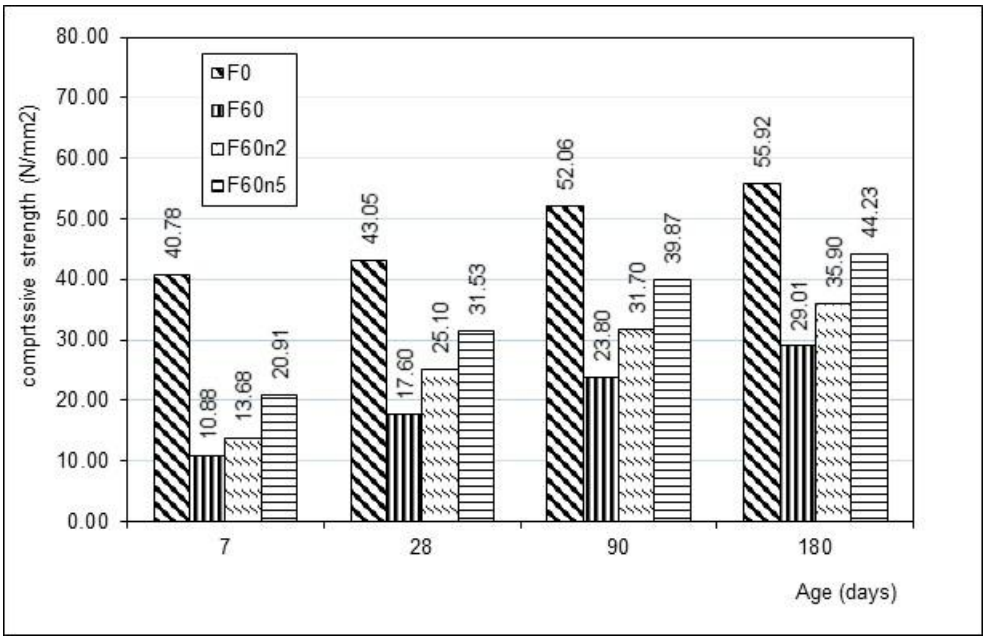

Fig. 4 Compressive strength of different concrete types at different ages

3.2 Flexural strength, splitting tensile strength and modulus of elasticity

Figs. 5-7 shows the flexural strength, splitting tensile strength and modulus of elasticity, respectively, test results for all mixtures at age of 28 days. As can be observed, the incorporation of 60% FA (F60) leads to 37.5% and 41.4% reduction in the flexural strength and splitting tensile strength, respectively. The obtained results are in agreement and follow the same trend of the results of compressive strength. The negative effect of FA is attributed to its lower early strength development resulted in its lower modulus of rupture. Also, because of lower pozzolanic reactivity of FA at early ages, which causes a weak cementitious matrix, thereby reducing the splitting tensile strength. Incorporating 2% NS results in an improvement in both flexural strength and splitting tensile strength by 19.4%, and 14.9% respectively. As the content of NS increased from 2% to 5%, more enhancement was obtained.

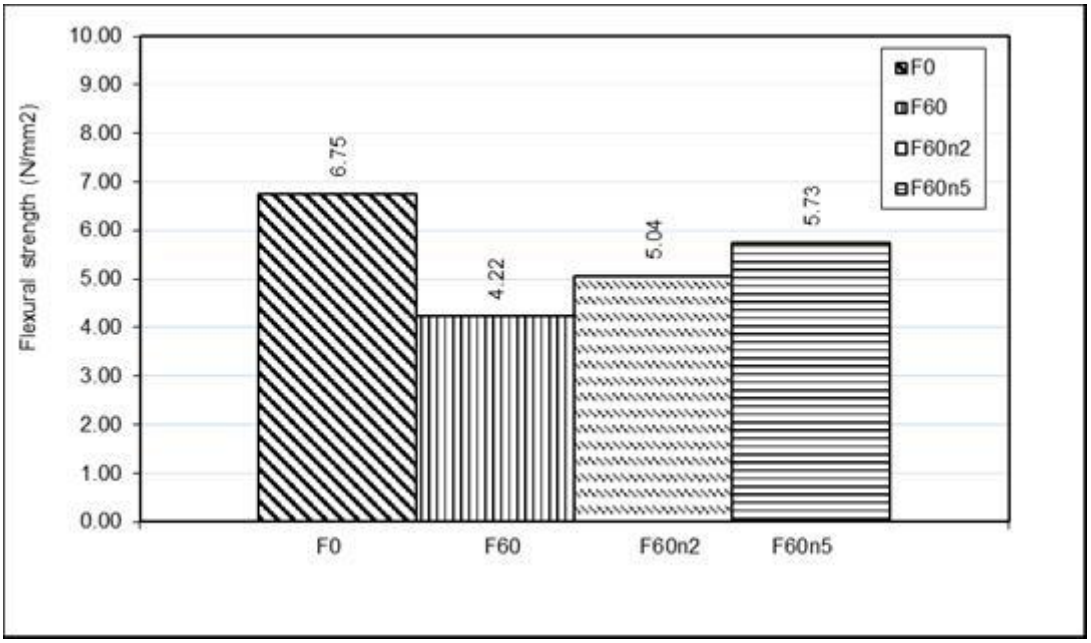

Fig. 5 Flexural strength of different concrete types at age of 28 days

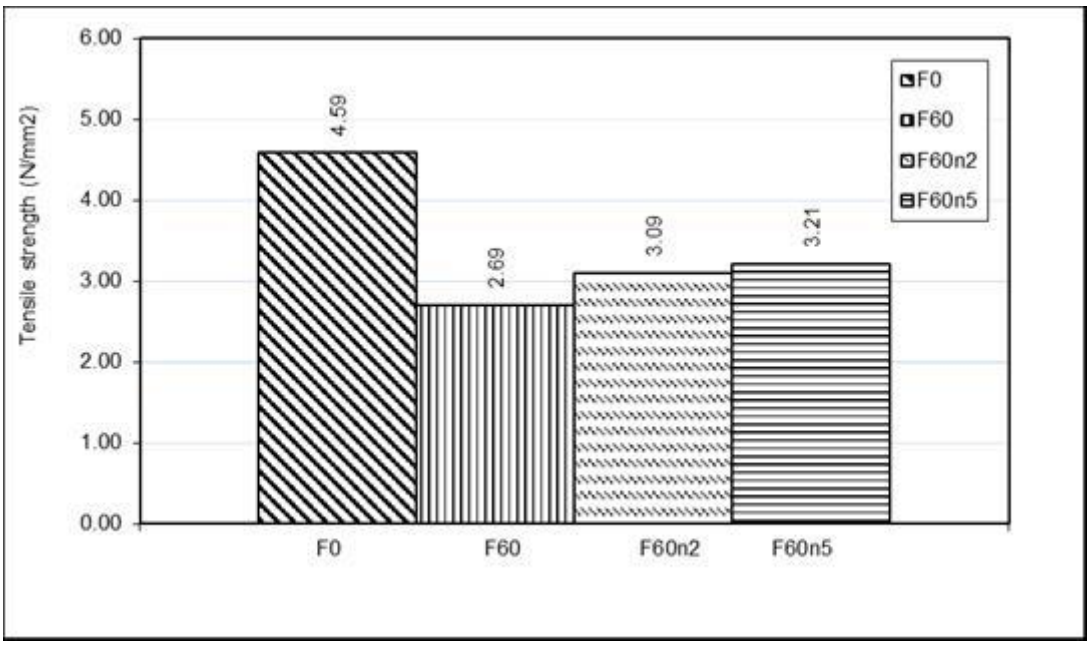

Fig. 6: Splitting tensile strength of different concrete types at age of 28 days

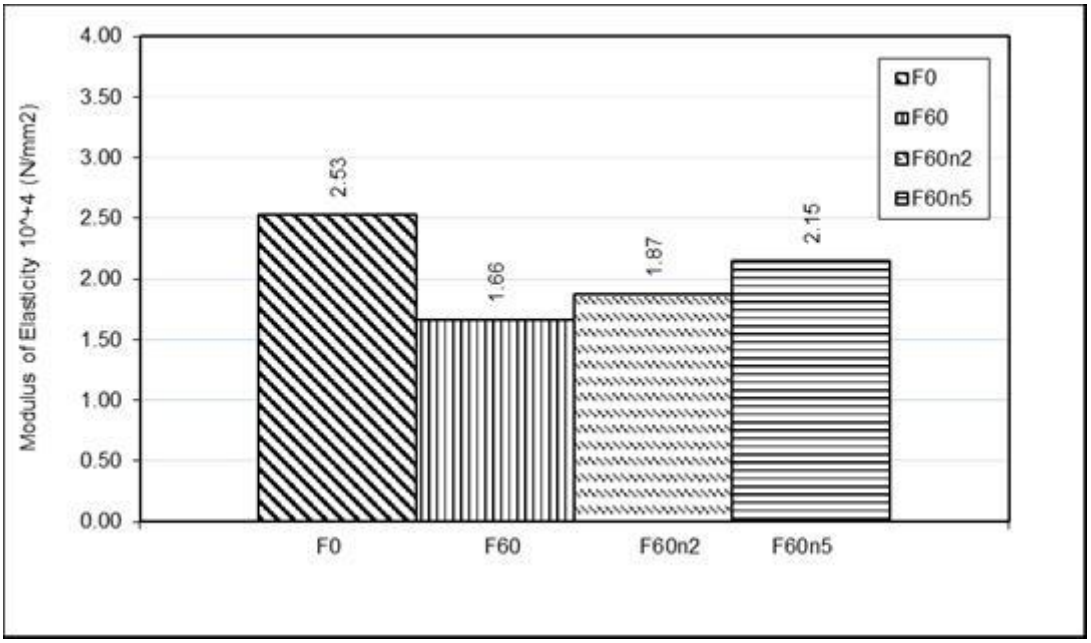

Fig. 7 Modulus of elasticity of different concrete types at age of 28 days

The results of static modulus of elasticity (MOE) at age of 28 days are shown in Fig. 7 which indicates that the MOE of F60 concrete reduces by 34.4% when compared with those of the control (F0). This is due to the same reason mentioned before (i.e slow pozzolanic reactivity of FA). On the other hand, the addition of NS increases the MOE of HVFA concrete. At 28 days, the MOE of F60n2 and F60n5 are greater than that of F60 by 12.65% and 29.52%, respectively. The increase in MOE with the addition of NS to HVFA concrete can be attributed to the pore filling ability as well as the pozzolanic reaction of NS. This increases the compressive strength which subsequently increases the MOE.

3.3 Residual compressive strength after exposure to elevated temperatures

The behavior of concrete mixtures without FA, incorporated HVFA and those incorporated HVFA coupled NS exposed to different high elevated temperatures were investigated by measuring the compressive strength after heating (i.e residual compressive strength). The test results for compressive strength are shown in Fig. 8 which shows the effect of HVFA and using NS on the residual compressive strength The results show that the compressive strength of the PC concrete (F0) approximately did not affected when the specimens exposed to 400 °C, in which the relative compressive strength is 98.49% referred to its control at room temperature. The slight reduction in the compressive strength at 400 °C may be due to the evaporated water and hydrates. On the other hand, all HVFA concrete specimens show a significant increase in the strength after exposed to 400 °C. The compressive strength of F60 concrete at 400 °C increases compared with its reference at room temperature and its relative strength reaches as high as 243.30%. When partially replacing FA with 2% and 5% NS (F60n2, F50n5), an increase in the residual compressive strength was obtained. The residual compressive strength of reaches 50.25 MPa for F60n2 and 60.56 MPa for F60n5. Comparing these compressive strength values with their counterparts, it can be noted that the relative strength reaches 200.2% for F60n2 and 192.1% for F60n5. The main conclusion of this part of the results are that all HVFA concrete types performed better than the PC concrete at 400 °C. They showed rapid gain in their compressive strength. The F60n5 concrete exhibited the highest residual compressive strength followed by F60n2. On the other hand, the F60 concrete exhibited the highest relative strength followed by F60n2 and F60n5. The relative strength of all types of HVFA concretes was higher than that of the PC concrete by about 2.47 to 1.95 times.

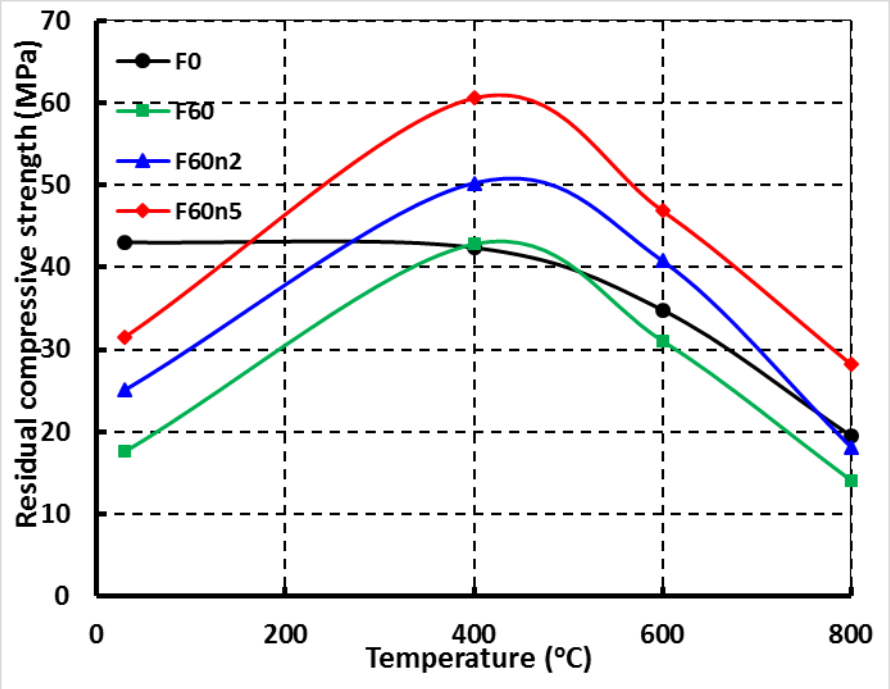

Fig. 8 Effect of elevated temperatures on the compressive strength of different concrete types

With increasing temperature to 600 °C, the compressive strength decreases due to weakling the bond between the aggregate and the cement paste, of which the aggregates expanded, while the paste lost its water. Anyhow, for F0 concrete, the loss of strength becomes more significant at 600 °C compared to that at 400 °C. The retained strength is 80.83% of the 28 days compressive strength. This degradation of strength, also, could be caused by the coarsening of the porestructure of the hardened cement paste [21]. On the other hand, the residual compressive strength values of all HVFA concrete types are still higher than their originals before heating. The residual compressive strength of F60 concrete records 31.05 MPa, which is still higher than its original by about 76.42%. The recorded highest residual compressive strength is 46.86 MPa for F60n5 followed by 40.78 MPa for F60n2. These two values of residual compressive strength are still higher than their originals by 48.6% and 62.7%, respectively. The main features of this part of the results are that even though exposure to 600 °C, the compressive strength of HVFA concrete mixes was still more than their originals. The relative strength of all types of HVFA concretes was higher than that of the PC concrete by about 2.44 to 2.06 times.

Exposure to 800 °C results in a significant decrease in compressive strength for all specimens, which is mainly attributable to the excessive build-up of vapor pressure; this pressure produces large cracks in the specimens. Additionally, the binder products in cement paste dehydrate at this temperature and cause a reduction in strength. However, specimens containing 5% NS shows a higher residual strength. The residual compressive strength for specimens containing 5% NS is comparable to the compressive strength of the unheated specimen, most likely due to the filler effect of the NS and the higher calcium silicate hydrate content of specimens containing both NS and FA,.

3.4 Abrasion resistance after exposure to elevated temperatures

The weight loss, which is inversely proportional to the abrasion resistance, was used to evaluate the abrasion resistance of different types of concrete before and after exposure to elevated temperatures. Therefore, a greater percentage loss implies a lower abrasion resistance, and vice versa. The results of the weight loss tested at room temperature and after exposure to 400, 600 and 800 °C are shown in Fig. 9. The loss increases with incorporation 60% FA as a cement replacement, as can be seen where of which the loss value of F60 is higher than that of F0 by about 157.9%. This could be attributed to the lower pozzolanic reactivity of FA resulted in slower strength development, poor bonding between cement paste and aggregates, and subsequent decreased abrasion

resistance. Another contributing factor is a reduction in the compressive strength, of which the abrasion resistance of concrete is directly proportional to its compressive strength. The addition of 2% and 5% NS increases the abrasion resistance of HVFA concrete by decreasing its weight loss by about 24% and 43.9%, respectively. Increasing abrasion resistance with the addition of NS could be attributed to the increased pozzolanic reaction, which led to increased strength, and increased abrasion resistance.

The weight loss of all concrete types after exposure to elevated temperatures is presented in Fig. 9. As can be seen, weight loss of F0 shows marginal change when the specimens exposed to 400 °C, in which the relative weight loss is 103.55% referred to its control at room temperature. This slightly reduction in the weight strength (increase in weight loss) at 400 °C is compatible with deceasing its compressive strength. On the other hand, all HVFA concrete specimens show a significant increase in the strength after exposed to 400 °C. The weight loss for F60 at 400 °C decreases compared with its reference loss at room temperature by about 52.23%. Also, using 2% and 5% NS (F60n2, F50n5) lead to an increase in the abrasion strength by decreasing the weight loss by 48.9% for F60n2 and 54.7% for F60n5 compared with its reference loss at room temperature. The main conclusion of this part of the results are that all HVFA concrete types performed better than the PC concrete at 400 °C. They showed rapid gain in their abrasion strength. The F60n5 concrete exhibited the lowest weight loss followed by F60n2.

With increasing temperature to 600 °C, the abrasion strength decreases due to weakling the bond between the aggregates and the cement paste, of which the aggregates expanded, while the paste lost its water. Anyhow, for F0 concrete, the weight loss becomes more significant at 600 °C compared to that at 400 °C. The weight loss of F60 concrete is still lower than its original by about 54.33%. F60n5 exhibits the lowest weight loss followed by F60n2. These two values of weight loss are still lower than their originals by 54% and 70.9%, respectively. The main features of this part of the results are that even though exposure to 600 °C, the abrasion strength of HVFA concrete mixes was still higher than their originals. Finally, exposure specimens to 800 °C resulted in a significant decrease in abrasion strength, which is mainly attributable to the excessive build-up of vapor pressure. However, specimens containing 5% NS shows the highest abrasion resistance lowest weight loss). The main contributing factor is a reduction in the compressive strength, as the abrasion resistance of concrete is directly proportional to its compressive strength.

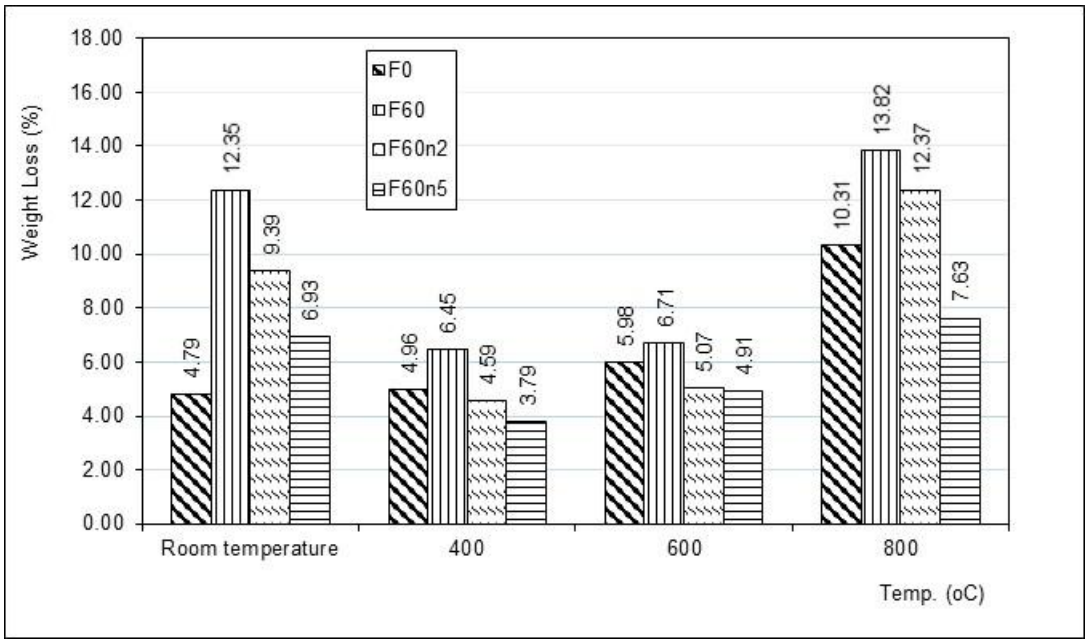

Fig. 9 Effect of elevated temperatures on the weight loss of different concrete types

Conclusions

In this article, the effects of incorporation of HVFA with/without NS on the mechanical strength as well as compressive strength and abrasion resistance before and after exposure to elevated temperatures were studied. The main conclusions of this investigation can be summarized as follows:

1. Using HVFA in the matrix sharply decreased its mechanical strength and abrasion resistance especially at early ages.
2. The addition of 2% NS increased the compressive strength, splitting tensile strength, flexural strength, modulus of elasticity, and abrasion resistance of HVFA concrete, this is due to increasing hydration products.
3. The addition of 5% NS resulted in increasing the compressive strength, splitting tensile strength, flexural strength, and abrasion strength.
4. All HVFA concrete mixes showed a significant increase in the compressive strength, and abrasion resistance after exposure to 400 °C, The incorporation of 2% and 5% NS led to more enhancement of both compressive strength and abrasion resistance at this degree.
5. Even though exposure to 600 °C, the compressive strength of HVFA concrete specimens was still higher than their originals. The relative strength of all types of HVFA concretes was higher than that of the PC concrete by about 2.44 to 2.06 times.
6. With increasing temperature to 600 °C, the abrasion strength decreased due to weakling the bond between the aggregates and the cement paste, of which the aggregates expanded, while the paste lost its water.
7. Exposure specimens to 800 °C resulted in a significant decrease in compressive strength and abrasion resistance for the specimens, which is mainly attributable to the excessive build-up of vapor pressure. However, specimens containing 5% NS showed the highest residual strength. The residual compressive strength for specimens containing 5% NS was comparable to the compressive strength of the unheated control specimen.

References

[1.] Siddique R. Performance characteristics of high-volume class F fly ash concrete. Cem Concr Res 2004; 34(3):487–93.

[2.] Naik TR, Singh SS, Hossain MM. Permeability of concrete containing large amounts of fly ash. Cem Concr Res 1994;24(5):913–22.

[3.] F.U.A. Shaikh ⇑, S.W.M. Supit, P.K. Sarker. A study on the effect of nano silica on compressive strength of high volume fly ash mortars and concretes. Materials and Design 60 (2014) 433–442

[4.] Rashad Alaa M .A brief on high-volume Class F fly ash as cement replacement – A guide for Civil Engineer. International Journal of Sustainable Built Environment (2015) 4, 278–306

[5.] Wei, Xiaosheng, Zhu, Hongping, Li, Guowei, Zhang, Changqing, Xiao, Lianzhen, 2007. Properties of high volume fly ash concrete compensated by metakaolin or silica fume. J. Wuhan Univ. Technol. Mater Sci. Ed. 22 (4), 725–732.

[6.] Sahmaran, Mustafa, Yaman, I. Ozgur, 2007. Hybrid fiber reinforced selfcompacting concrete with a high-volume coarse fly ash. Constr. Build. Mater. 21, 150–156.

[7.] El-Chabib, Hassan, Ibrahim, Ahmed, 2013. The performance of high strength flow able concrete made with binary, ternary, or quaternary binder in hot climate. Constr. Build. Mater. 47, 245–253.

[8.] Kumar, Binod, Tike, G.K., Nanda, P.K., 2007. Evaluation of properties of high-volume fly-ash concrete for pavements. J. Mater. Civil Eng. 19 (10), 906–911.

[9.] Siddique, Rafat, 2004a. Performance characteristics of high-volume Class fly ash concrete. Cem. Concr. Res. 34, 487–493.

[10.] Laplante, P., Aı¨tcin, P.C., 1991. Vezina, Abrasion resistance of concrete. J. Mater. Civil Eng. 3 (1), 19–30.

[11.] Rashad, Alaa M., 2014. A comprehensive overview about the influence of different admixtures and additives on the properties of alkali-activated fly ash. Mater. Des. 53, 1005–1025.

[12.] Mukherjee, S., Mandal, S., Adhikari, U.B., 2013. Comparative study on physical and mechanical properties of high slump and zero slump high volume fly ash concrete (HVFAC). Global NEST J. 15 (4), 578–584.

[13.] John, Jino, Ashok, M., 2014. Strength study on high volume fly ash concrete. Int. J. Adv. Struct. Geotech. Eng. 3 (2), 1680171.

[14.] Dura`n-Herrera, A., Jua`rez, C.A., Valdez, P., Bentz, D.P., 2011. Evaluation of sustainable high-volume fly ash concretes. Cement Concr. Compos. 33, 39–45.

[15.] Saravanakumar, P., Dhinakaran, G., 2013. Strength characteristics of high-volume fly ash-based recycled aggregate concrete. J. Mater. Civil Eng. 25 (8), 1127–1133.

[16.] Yoon, Seyoon, Monteiro, Paulo J.M., Macphee, Donal E., Glasser, Fredrik P., Imbabi, Mohammed Salah-Eldin, 2014. Statistical evaluation of the mechanical properties of high-volume class F fly ash concretes. Constr. Build. Mater. 54, 432–442.

[17.] K ayali, Obada, Ahmed, M. Sharfuddin, 2013. Assessment of high volume replacement fly ash concrete – concept of performance index. Constr. Build. Mater. 39, 71–76.

[18.] Musa Adamu, Bashar S. Mohammed, Mohd Shahir Liew. Mechanical properties and performance of high volume fly ash roller compacted concrete containing crumb rubber and nano silica. Construction and Building Materials 171 (2018) 521–538

[19.] Min Liu, Hongbo Tan, Xingyang He. Effects of nano-SiO2 on early strength and microstructure of steam-cured high volume fly ash cement system. Construction and Building Materials 194 (2019) 350–359

[20.] F.U.A. Shaikh, Y. Shafaei, P.K. Sarker. Effect of nano and micro-silica on bond behavior of steel and polypropylene fibers in high volume fly ash mortar. Construction and Building Materials 115 (2016) 690–698

[21.] Rashad Alaa M.. An exploratory study on high-volume fly ash concrete incorporating silica fume subjected to thermal loads. Journal of Cleaner Production 87 (2015) 735e744

[22.] Rashad Alaa M. An investigation of high-volume fly ash concrete blended with slag subjected to elevated temperatures. Journal of Cleaner Production 93 (2015) 47e55

[23.] Rashad Alaa M. Potential Use of Silica Fume Coupled with Slag in HVFA Concrete Exposed to Elevated Temperatures. ascelibrary.org by New York University on 04/28/15. Copyright ASCE.

[24.] Rahel Kh. Ibrahim, R. Hamid, M.R. Ta ha. Fire resistance of high-volume fly ash mortars with nano silica addition. Construction and Building Materials 36 (2012) 779–786

[25.] Gerrit, L. and Dietmar, S., "Controlling cement hydrationwith nanoparticles", Cem. Concr. Compos. 57, 2015, 64–67.

[26.] Rashad Alaa M., El-Nouhy Hanan A. and Zeedan Sayieda R., "An investigation on HVS paste modified with nano-SiO2 imperiled to elevated temperature"

[27.] Quercia G, Husken G, Brouwers HJH. Water demand of amorphous nano silica and its impact on the workability of cement paste. Cem Concr Res 262012;42 : 344–57.

[28.] Quercia G, Spiesz P, Husken G, Brouwers J. Effects of amorphous nano-silica additions on mechanical and durability performance of SCC mixtures. Proc. International congress on durability of concrete; 2012.

[29.] Senff L, Hotza D, Repette WL, Ferreira VM, Labrincha JA. Influence of added Nano silica and/or silica fume on fresh and hardened properties of mortars and cement pastes. Adv. Appl Ceram 2009; 108(7):418-28.

[30.] Musa Adamu, Bashar S. Mohammed, Mohd Shahir Liew. Mechanical properties and performance of high volume fly ash roller compacted concrete containing crumb rubber and nano silica. Construction and Building Materials 171 (2018) 521–538